

**THE LIN28B/LET-7 AXIS REGULATES DEVELOPMENTAL
TIMING IN THE MAMMALIAN COCHLEAR EPITHELIUM**

By

Erin Jennifer Golden

A dissertation submitted to Johns Hopkins University in conformity with the
requirements for the degree of Doctor of Philosophy

Baltimore, Maryland

May 2015

ABSTRACT

Proper tissue development requires strict coordination of proliferation, growth and differentiation. This is particularly true for the auditory sensory epithelium, where deviations from the normal spatial and temporal pattern of auditory progenitor cell (prosensory cell) proliferation and differentiation result in abnormal cellular organization and thus auditory dysfunction. The molecular mechanisms involved in the timing and coordination of auditory prosensory proliferation and differentiation are poorly understood. Here we identify the RNA-binding protein LIN28B as a critical regulator of developmental timing in the murine cochlea. We show that *Lin28b* and its opposing *let-7* miRNAs are differentially expressed in the auditory sensory lineage, with *Lin28b* being highly expressed in undifferentiated prosensory cells and *let-7* miRNAs being highly expressed in their progeny – hair cells (HCs) and supporting cells (SCs). Using recently developed transgenic mouse models for LIN28B and *let-7g*, we demonstrate that prolonged LIN28B expression delays prosensory cell cycle withdrawal and differentiation, resulting in HC and SC patterning and maturation defects. Surprisingly, *let-7g* overexpression, although capable of inducing premature prosensory cell cycle exit, failed to induce premature HC differentiation, suggesting that LIN28B's functional role in the timing of differentiation utilizes *let-7* independent mechanisms. Lastly, we demonstrate that overexpressing LIN28B or *let-7g* in the postnatal cochlea alters the capacity for HC production in response to Notch inhibition; LIN28B has a positive effect on SC plasticity, while *let-7* antagonizes the capacity for SC trans-differentiation.

Thesis Advisor: Angelika Doetzlhofer, Ph.D.

Thesis Reader: Mollie K. Meffert, M.D., Ph.D

ACKNOWLEDGEMENTS

It is hard to put in to words how thankful I am to everyone who has helped me along this journey. I am extremely lucky to have so much love and support in my life and without it - without all of you - I would be nowhere.

I would first like to thank my advisor, Angelika, who has been a fantastic mentor and friend to me. It is pretty special to be someone's first graduate student, and I am glad I could be yours. Throughout my time in the lab, your door has always been open and you have always been ready and enthusiastic to help troubleshoot my latest experiment or celebrate my most recent finding. Under your guidance I learned to conceptualize meaningful scientific questions and developed the analytical skills to interpret and contextualize my results. Most importantly, with your support, I built the confidence to work as an independent research scientist. I will always be thankful for your careful guidance and endless patience and I will attempt to emulate your scientific passion and intellectual prowess throughout my career. I am hopeful that we will finally go on that long discussed lab ski trip next time you are out in Colorado!

I would next like to thank Randy Reed for his role in my scientific training. Randy, you have created a fantastic resource with the Center for Sensory Biology, which was a wonderfully supportive place to complete my Ph.D. The passion you convey for training the next generation of scientists is inspiring and the breadth of knowledge you possess, while intimidating, is just plain impressive. I will miss hearing your morning greeting of "Hel-lo" sing-songing through the lab and your ability to fix just about anything – from Keurig coffee machines to the 780 LSM – you are the original lifehacker.

I would also like to thank my lab mates, past and present. Ana, Dean, Jen, Elena, Meenakshi, Lale, Soumya, Matt, and Yi-Feng – you helped make the lab a more fun, and certainly more interesting (I'm looking at you Dean), place to work. Thank you for all of the support with experiments, companionship during walks to the mouse room, and conversations – scientific and otherwise. Likewise, I would like to thank our neighbors in the Center for Sensory Biology: Renee, Heather, Tanu, Marquis, Chris, Sonia, Darya, Chun-Chieh, Leena, and Liz. I will miss you all a lot!

I must also thank the Meffert lab, especially Claudia, Alex, Anca, Alvin, Dan, and Megha for all of the protocols, reagents, and technical support. A special thank you to Mollie as well for always acting as my cheerleader. Whether it be your poignant questions during thesis committee meetings or sage advice during personal crises, I've always felt like you've had my best interests at heart, and I will forever be thankful for that.

I am so lucky to have gotten to be a graduate student in the Solomon H. Snyder Department of Neuroscience. Oh my what a place! I am certain that there is not a more fun and collaborative environment in which to complete your Ph.D. I will miss the people, happy hours, and annual retreat immensely (okay, and the world-class science), and will always speak fondly of my time here. I would especially like to thank Shan Sockanathan, Seth Blackshaw, David Ginty, Paul Fuchs, Dwight Bergles, our fantastic department administrators Rita Ragan & Beth Wood-Roig, and my rotation advisors Mike Caterina, Jay Baraban, and Akira Sawa.

Finally I must thank my family and friends for being there, always.

First to my fellow Neuroscience graduate students, especially Claudia, Robbie, and Alex - you will be the hardest part of Baltimore to leave behind.

To Paige, Emily, Riva, and Meredith, no matter how far away we live from each other, I know I can always count on you to be there when needed. Thank you for offering a sounding board for my frustrations, of which there were many, and for being ready with a pep talk, joke, or the latest celebrity gossip when I needed to regroup.

To my parents, thank you for your unwavering support and confidence. Thank you for instilling in me a love for learning and for enabling me to explore my passions. Thank you for every sacrifice you ever made on my behalf. Thank you for showing me the world. Thank you for my no-longer annoying, and just plain awesome little brother Eli (and his even cooler wife Michelle). Thank you for believing in me. Thank you for spoiling me. Thank you for always being there. Thank you, thank you, thank you, thank you, thank you...I love you.

Thank you to the incredibly strong female role models in my life. Mom, Grandma Marlene, and Grandma Sylvia, you inspired me to follow in your footsteps, and because of you never once did it occur to me that being a woman was something that could ever hold me back.

Finally, thank you to my husband. Spencer, you are the most kind, supportive, and patient man I know and I am so fortunate to get to love you. I feel like this degree is almost as much yours as it is mine, and there is no one else I would want to share it with. Thank you.

TABLE OF CONTENTS

Abstract.....	ii
Acknowledgments.....	iii
Table of Contents.....	vi
List of Figures and Tables.....	viii
Chapter 1 Introduction to the mammalian auditory system.....	1
The auditory system: structure and organization.....	4
Developmental timing of the auditory sensory epithelium.....	5
Heterochronic genes and developmental timing.....	9
The <i>Lin28b/let-7</i> axis.....	10
Figures and Legends.....	14
Chapter 2 Lin28b regulates developmental timing within the mammalian cochlear epithelium through both <i>let-7</i> dependent and independent mechanisms.....	22
Introduction.....	23
Results.....	25
Discussion.....	35
Materials and Methods.....	41
Protocol 1: Total RNA Extraction.....	43
Protocol 2: SybrGreen RT-qPCR.....	45
Protocol 3: Taqman RT-qPCR.....	46

Protocol 4: Western Blotting.....	48
Protocol 5: mRNA <i>ISH</i> Probe Production.....	53
Protocol 6: mRNA <i>In Situ</i> Hybridization.....	52
Protocol 7: miRNA <i>In Situ</i> Hybridization.....	56
Figures and Legends.....	63
Chapter 3 Manipulation of the Lin28b/<i>let-7</i> axis modulates the capacity for supporting cell-to-hair cell conversion.....	82
Introduction.....	83
Results.....	86
Discussion.....	88
Materials and Methods.....	90
Figures and Legends.....	91
Appendix A Identification of LIN28B's mRNA targets in the differentiating cochlear epithelium.....	95
References.....	102
Curriculum Vitae.....	112

LIST OF TABLES AND FIGURES

Chapter 1	Introduction to the mammalian auditory system	
Figure 1.1	Anatomy of the mammalian auditory system.....	15
Figure 1.2	Schematic of prosensory cell cycle withdrawal and the onset of hair cell differentiation.....	16
Figure 1.3	Lin28b acts through let-7 dependent and independent mechanisms to regulate developmental timing.....	18
Figure 1.4	Hypothesized role of the Lin28b/ <i>let-7</i> axis in the developing cochlear Epithelium.....	20
Chapter 2	Lin28b regulates developmental timing within the mammalian cochlear epithelium through both <i>let-7</i> dependent and independent mechanisms	
Figure 2.1	Multiple Heterochronic genes are expressed in the developing cochlear epithelium and are rapidly downregulated during differentiation.....	63
Figure 2.2	Let-7 miRNAs are upregulated in the differentiating cochlea.....	65
Figure 2.3	<i>LIN28B</i> overexpression in the embryonic cochlea.....	67
Figure 2.4	<i>LIN28B</i> overexpression delays auditory HC differentiation.....	69
Figure 2.5	Acute <i>LIN28B</i> overexpression delays auditory HC differentiation.....	71
Figure 2.6	<i>LIN28B</i> overexpression delays progenitor cell cycle withdrawal and causes mis-patterning of the auditory sensory epithelium.....	74
Figure 2.7	<i>LIN28B</i> overexpression delays progenitor cell cycle withdrawal and causes mis-patterning of the auditory sensory epithelium.....	76

Figure 2.8	<i>Let-7</i> overexpression accelerates progenitor cell cycle withdrawal.....	78
Figure 2.9	<i>Let-7</i> overexpression does not accelerate progenitor differentiation.....	80
Chapter 3	Manipulation of the <i>Lin28b/let-7</i> axis modulates the capacity for supporting cell-to-hair cell conversion	
Figure 3.1	<i>LIN28B</i> re-expression promotes supporting cell conversion in the absence of Notch signaling.....	91
Figure 3.2	<i>Let-7</i> overexpression antagonizes supporting cell conversion in the absence of Notch signaling.....	93
Appendix A	Identification of <i>LIN28B</i>'s mRNA targets in the differentiating cochlear epithelium	
Table A.1	Transcripts upregulated by more than 3 standard deviations.....	99
Table A.2	Transcripts downregulated by more than 3 standard deviations.....	99
Table A.3	Gene pathway categories and functional annotations.....	100
Figure A.1	qRT-PCR validation of the <i>iLIN28B</i> microarray.....	101

Chapter 1

Introduction to the mammalian auditory system

“If you wish to make an apple pie from scratch, you must first invent the universe.”

– Carl Sagan

The ability to sense and react to the environment is essential for living organisms to survive. Animals have developed a range of mechanisms for sensory perception, the capacity of which differ between species, and in humans include the sense of vision, hearing, taste, olfaction, and touch. These senses allow us to perceive everything from the safety of our surroundings (is an imminent threat present?) to the nuances of our culture – including art, music, and gourmet food. Each of the five major senses are mediated by a dedicated sensory organ that processes environmental stimuli into neural code. The mechanism used by sensory tissues to convert information from the outside world into signals understood by the brain has long been of interest to the scientific community. More recent areas of study focus on the molecular and genetic mechanisms that underlie development of these sensory tissues. While the specific genes and molecules involved in these processes may vary between tissues, the overarching questions remain the same – How is sensory cell fate specified? How are functional circuits between the sensory organ and brain assembled? How can a mature sensory tissue regenerate/repair itself? Study of the sensory organs has revealed many insights into how cohesive biological systems are formed and maintained.

Spoken language is one of the fundamental abilities separating humans from non-human species. While many animals use sound to communicate, humans are thought to

be unique in the complexity of information that is shared through speech. Tragically, despite our dependence on aural communication, hearing loss remains the most prevalent neurosensory disorder. It is estimated that over 10% of the US population suffers from some form of hearing difficulty, including nearly half of adults over the age of 65 (NIDCD: <http://www.nidcd.nih.gov/health/statistics/pages/quick.aspx>). Hearing aids and cochlear implants are able to provide at least partial hearing restoration, but lack in their ability to fully recapitulate “normal” sound perception. Instead, it is widely agreed that “the world’s best hearing aid” will utilize molecular and genetic mechanisms to guide regeneration of the specialized cells whose loss causes hearing impairment (Groves, 2010; Kopecky and Fritzscht, 2012; Puligilla and Kelley, 2009). Before therapies targeting gene expression can be developed, however, the molecular mechanisms that underlie the generation of these sensory cells must first be understood. In recent years scientists have identified several factors involved in this process, but much remains to be uncovered.

In this dissertation, I describe my thesis work characterizing the role of the *Lin28b/let-7* microRNA (miRNA) axis in guiding the development of the mammalian auditory sensory organ, the cochlea. Our findings indicate that the RNA-binding protein Lin28b coordinates the precise timing of key developmental processes – progenitor cell terminal mitosis and the onset of differentiation – through two distinct mechanisms. Additionally, we show that shifting the expression of *Lin28b* or *let-7* in the postnatal cochlea can significantly alter the capacity for supporting cell conversion, revealing this axis as a promising target for future hair cell regeneration therapies.

The auditory system: structure and organization

The mammalian auditory system is a multifaceted structure that converts sound wave-induced vibrations of the atmosphere into neural code. From the pinna to the inner ear, each component of this system has evolved to aid in this transduction (Fig. 1.1 A). The outer ear pinna serves to collect incoming sound waves and direct them into the auditory canal. This results in vibration of the tympanic membrane (ear drum) and movement of the 3 middle ear ossicle bones. The third middle ear bone, the stapes, is coupled to the outer membrane of the fluid-filled cochlear duct (the oval window). Movement of the stapes causes fluid movement within the cochlear duct displacing the basilar membrane that houses the auditory sensory epithelium. The auditory sensory epithelium contains the mechanosensory hair cells (HCs) critical for sound perception (Fig. 1.1 B, C). There are two types of HCs; inner hair cells (IHCs) are the primary sensory receptor cells, while outer hair cells (OHCs) act as cochlear amplifiers, mediating the sensitivity of the auditory epithelium. Vibration of the auditory epithelium causes deflection of stereocilia bundles located on the apical surface of the HCs (Fig. 1.1 B). This deflection opens mechanically activated ion channels, leading to HC depolarization and neurotransmitter release. Neurotransmitter release from IHCs stimulates the afferent auditory neurons that comprise the statoacoustic nerve and mediate communication between the inner ear and the brain. Thus, the auditory system is able to seamlessly translate environmental stimuli into neural code.

Stereotyped organization of the auditory sensory epithelium is essential for proper sound transduction, and deviations in its distinct cytoarchitecture lead to sensorineural hearing loss. HCs are precisely arranged such that a single row of IHCs and three rows of

OHCs run along the entire length of the cochlear duct (Fig. 1.1 B, C). The physical characteristics of the basilar membrane (i.e. thickness, rigidity) differ along the cochlear duct causing the auditory epithelium to be frequency tuned. Low frequency, low-energy sound waves are only able to vibrate the wider, more flexible apical (distal) end of the cochlea, stimulating HCs in this region; while high frequency, high-energy sound waves can vibrate the stiffer and narrower basal (proximal) end of the cochlea. This phenomenon is known as tonotopy and results in a frequency map that begins with HC stimulation in the auditory periphery and is maintained throughout the central auditory processing centers in the brain.

Lying below and intercalating the HC layer are the supporting cells (SCs; Fig. 1.1 C). These glial-like cells are responsible for maintaining both the structure and homeostasis of the auditory epithelium. At least 4 different subtypes of SCs exist in the cochlea including the phalangeal cells (i), which flank the IHCs and mark the border of the greater epithelial ridge on the medial side; the inner and outer pillar cells (p), which form the walls of a fluid-filled tunnel that separates the IHC and OHC domains; the Deiter's cells (d), which surround the OHCs, separating them from one another; and finally the Hensen's cells (h), which are found lateral to the 3rd row of OHCs and mark the start of the lesser epithelial ridge. Together, HCs and SCs comprise the auditory sensory epithelium.

Developmental timing of the auditory sensory epithelium

Formation of the auditory epithelium requires strict coordination of proliferation, cell cycle exit, and differentiation. Each of these steps must occur in the correct order and

at precisely the right time in order to achieve proper epithelial patterning. Even slight shifts in timing can have catastrophic effects on sensory cell formation and arrangement, leading to impaired auditory transduction. HCs and SCs differentiate from a common pool of progenitor cells within the embryonic cochlear duct, and over the past several decades key regulators of their differentiation have begun to be identified. Still, the molecular mechanisms that time and coordinate cochlear development remain poorly understood.

The entire inner ear, including the auditory (cochlear) and vestibular organs and their innervating neurons, arises from the otic placode, which forms as an ectodermal thickening near the hindbrain at embryonic day 8.5 (E8.5) in mice. This placode invaginates to form the spherical, fluid-filled otocyst (E9.5), which continues to morph and elongate so that a rudimentary cochlear duct can be identified by E12.5 (Kelley, 2006; Ohyama et al., 2007). Running along the length of this developing cochlear duct is a specified prosensory patch that contains all of the progenitor cells from which the cochlear HCs and SCs will differentiate. This prosensory progenitor cell pool is defined by expression of the high mobility group (HMG)-box transcription factor *Sox2* (Fig. 1.2), which is required for both prosensory domain specification and subsequent HC differentiation (Dabdoub et al., 2008; Kiernan et al., 2005b).

The prosensory progenitor population is highly proliferative until E12.5, when progenitor cells in the cochlear apex begin to undergo terminal mitosis (Ruben, 1967). This cell cycle withdrawal (CCW) is mediated by expression of the cyclin-dependent kinase inhibitor *p27^{kip1}*, which is upregulated in an apical-to-basal wave of expression over the following two days (Fig. 1.2) (Chen and Segil, 1999b; Lee et al., 2006). At

E14.5, soon after the basal progenitors have exited the cell cycle, HC differentiation begins in the mid-basal portion of the cochlea. This process is mediated by expression of the bHLH transcription factor *Atoh1*, which is both necessary (Bermingham et al., 1999a) and sufficient (Zheng and Gao, 2000) for the differentiation of HCs. Strikingly, differentiation proceeds in the opposite direction from progenitor CCW, progressing from base-to-apex (Fig. 1.2). Due to these opposing waves of CCW and differentiation, post-mitotic prosensory progenitor cells are held in an undifferentiated state for vastly differing lengths of time depending on their basal-to-apical location. Basal progenitors differentiate within hours of exiting the cell cycle, while the most apical progenitors remain post-mitotic and undifferentiated for several days.

This temporal separation between CCW and differentiation in the cochlear epithelium is in stark contrast to other neuronal structures, such as the retina and cortex, where these two processes are intimately linked (Cepko, 2014; Costa and Muller, 2014; Livesey and Cepko, 2001; McConnell and Kaznowski, 1991). Indeed, *Atoh1* and *p27^{kip1}* loss-of-function studies confirm that these processes are largely uncoupled within the developing cochlear epithelium. CCW occurs normally in *Atoh1* null mice (Chen et al., 2002a), and the onset of differentiation is unaffected by the absence of *p27^{kip1}* expression (Chen and Segil, 1999b). This specific temporal coordination is thought to assure the precise morphogenic patterning of the cochlear epithelium that is critical to its proper functioning. For instance, as a result of prolonged proliferation, supernumerary HCs and SCs are prevalent throughout the auditory epithelium of *p27^{kip1}* null mice, leading to severe hearing impairments (Chen and Segil, 1999b).

Recently, two signaling pathways have been shown to play a role in regulating the temporal separation between CCW and differentiation in the cochlea. The insulin-like growth factor (Igf) signaling cascade acts via the phosphatidylinositol 3-kinase (PI3K)/Akt pathway to coordinate the timing of developmental events occurring after prosensory cell terminal mitosis (Okano et al., 2011). In mice lacking the Igf1 receptor (*Igf1r*^{-/-}), prosensory domain formation and *p27^{kip1}* expression proceed normally; however, the onset of *Atoh1* expression is significantly delayed, leading to defects in HC and SC formation/maturation and subsequent irregularities in cellular patterning. Strikingly, while *Igf1r* knockout does not alter the timing of CCW, the authors observed a significant decrease in the rate of progenitor cell proliferation, resulting in significantly shorter cochlear ducts.

The morphogen Sonic Hedgehog (Shh) also plays an instructive role in timing cochlear development. Results from several recent studies suggest that *Shh*, expressed by the developing spiral ganglion, promotes cochlear outgrowth and inhibits HC differentiation. As the cochlear duct develops and elongates, *Shh* is downregulated in a basal-to-apical gradient, so that its expression is limited to the apical portion of the spiral ganglion by E14.5 (Bok et al., 2013; Driver et al., 2008; Liu et al., 2010). This shift in *Shh* expression corresponds to the stages during which prosensory cells transition from proliferative progenitors to differentiating HCs and SCs. Disruption of Shh signaling, either genetically (Bok et al., 2013; Tateya et al., 2013) or pharmacologically (Benito-Gonzalez and Doetzlhofer, 2014), causes precocious HC differentiation, and in extreme cases even reverses the basal-to-apical gradient of HC differentiation, effectively eliminating the delay between CCW and the onset of differentiation (Bok et al., 2013). In

these experiments, premature progenitor CCW was also observed, suggesting a broad role for Shh in coordinating this developmental transition. The mechanisms by which Shh regulates CCW are not known; however, recent evidence from our own lab, suggests that Shh acts via the HES-related transcriptional repressors, Hey1 and Hey2, to inhibit Atoh1 expression and time the onset of HC differentiation (Benito-Gonzalez and Doetzlhofer, 2014).

Heterochronic genes and developmental timing

Due to their morphological complexity and the frequent overlap of developmental events, vertebrates, as a whole, are not the ideal model in which to study developmental timing (Moss, 2007). Instead, simpler model organisms, such as the roundworm *Caenorhabditis (C.) elegans*, have traditionally been used to study heterochrony. Because of its organismal simplicity and stereotyped differentiation, the lineages of individual blast (precursor) cells can be easily followed in developing larvae, making *C. elegans* an ideal system for identifying genes whose mutation disrupts the normal progression of development. These so-called “heterochronic genes” can be broadly characterized into two classes; those whose mutation results in a “precocious” phenotype or the skipping of developmental events; and those whose mutation results in a “retarded” phenotype, or the repetition of developmental events (Ambros and Horvitz, 1984; Moss, 2007). Using phenotypic and molecular analysis of *C. elegans* larvae, an entire network of heterochronic genes has been characterized. In general, two families of heterochronic microRNAs (miRNA) act to regulate the expression of multiple heterochronic protein coding genes, which include transcription factors, RNA-binding proteins, and ubiquitin

ligases, among others. Together, these “precocious” and “retarded” heterochronic genes comprise bistable switches whose shift in expression mediate developmental stage progression (Nimmo and Slack, 2009). Many of the heterochronic genes are evolutionarily conserved, and study of their mammalian homologs has revealed their broad role in regulating stem cell development, organismal growth, and tumorigenesis as well (Huang, 2012; Nimmo and Slack, 2009; Shyh-Chang and Daley, 2013).

The striking temporal separation of CCW and differentiation in the developing auditory epithelium makes the mammalian cochlea an ideal system for the study of vertebrate heterochrony. As described above, this system is especially sensitive to changes in developmental progression and even slight shifts in timing can result in substantial disruptions to its stereotyped epithelial morphology. Intriguingly, we recently found that cochlear prosensory cells express several heterochronic genes and miRNAs, leading us to hypothesize that this evolutionarily conserved pathway plays an essential role in coordinating the timing of prosensory cell differentiation.

The *Lin28b/let-7* axis

Perhaps the best-characterized heterochronic relationship involves the *let-7* family of miRNAs and the RNA-binding protein LIN28. In developing *C. elegans*, *lin28* mutation results in a “precocious” phenotype – accelerated differentiation of larval stem cells (Ambros and Horvitz, 1984). Subsequent studies in a range of organisms and model systems have revealed this highly conserved RNA-binding protein to be a critical regulator of stemness, organismal growth, metabolism, tumorigenesis and tissue repair (Nimmo and Slack, 2009; Shyh-Chang and Daley, 2013). In mammals there are two

homologs of the *C. elegans lin28* gene, *Lin28a* and *Lin28b*, which share 77% identity at the protein level (Guo et al., 2006). Both LIN28A and LIN28B proteins contain two types of RNA-binding motifs: a cold shock domain (CSD) and a pair of retroviral-type CCHC zinc knuckles (Moss and Tang, 2003), which mediates their pleiotropic role in development and disease (Huang, 2012). LIN28A/B were initially thought to enhance pluripotency primarily by inhibiting biogenesis of the *let-7* family of miRNAs; however, growing evidence suggests that they can directly target and regulate the translation of select protein-coding mRNAs as well (Fig. 1.3).

The miRNA *let-7* was also first identified in a screen for *C. elegans* heterochronic genes. Mutation of *let-7* leads to a “retarded” phenotype, resulting in delayed larval stem cell differentiation (Reinhart et al., 2000). Fortuitously, *let-7* and *lin-4* (another heterochronic gene) were the first ever identified miRNAs. Their discovery has subsequently led to a “small RNA revolution”, and the realization that all eukaryotes produce short RNA sequences (miRNAs, piRNAs, siRNAs) that act as key regulators of gene expression (Nimmo and Slack, 2009).

In general, miRNAs modulate gene expression by inhibiting the translation and/or promoting the degradation of their target mRNAs. In particular, *let-7* miRNAs regulate differentiation by targeting many cell cycle and growth-associated genes (Nimmo and Slack, 2009; Rehfeld et al., 2015). In the absence of LIN28A/B expression, *let-7* miRNA transcripts undergo two processing steps to generate a mature *let-7* miRNA. The RNA polymerase II transcribed primary *let-7* transcript (pri-*let-7*) is cleaved by the Drosha/DGCR8 microprocessor complex, generating a ~70 nucleotide precursor *let-7* miRNA hairpin (pre-*let-7*). This pre-*let-7* is then transported to the cytoplasm where it is

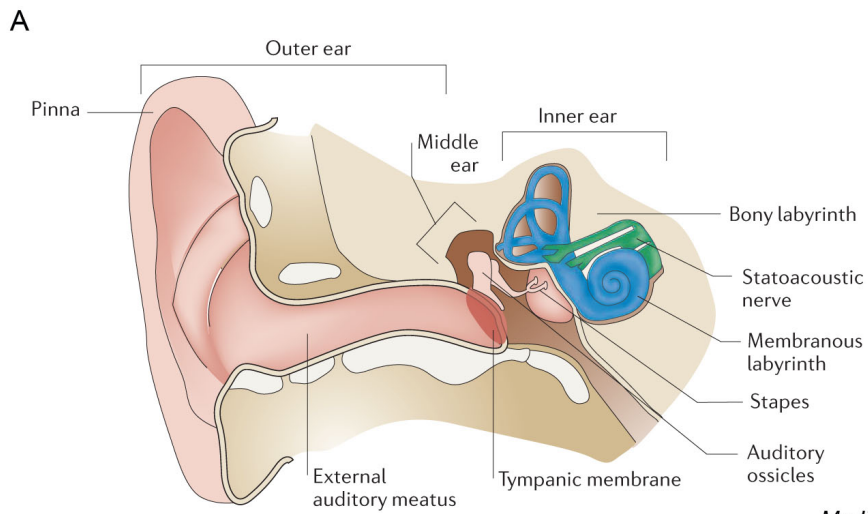
further processed by the RNase Dicer, to generate a mature ~22 nucleotide miRNA duplex. One strand of this duplex is incorporated into the Argonaute-containing miRNA-induced silencing complex (miRISC), which targets and represses the expression of mRNAs that possess sequences (typically within the 3' untranslated region) complementary to the mature *let-7* miRNA. Many of these mRNAs include regulators of growth and proliferation (e.g. *Hmga2*, *Igf2bps*, *Myc*, *Ras*, *Ccnd1*), and their repression by *let-7* promotes terminal differentiation.

LIN28A/B is able to promote growth and proliferation, in part, by inhibiting the biogenesis of the *let-7* miRNAs. When LIN28A/B are expressed, these proteins recognize and bind a specific GGAG motif in the terminal loop of pri- and pre-*let-7* transcripts, preventing their processing by the RNases Drosha and Dicer, respectively (Huang, 2012; Nimmo and Slack, 2009; Rehfeld et al., 2015). Importantly, *let-7* miRNAs are able to modulate the expression of *Lin28a/b* as well, since these genes possess multiple *let-7* binding sites within the 3'UTRs of their mRNAs. Thus, a double negative feedback loop exists between *Lin28a/b* and the *let-7* family of miRNAs that acts to regulate the capacity for growth/self-renewal versus differentiation (Fig. 1.3) (Rybak et al., 2008).

There is emerging evidence for a critical role of the *Lin28/let-7* axis in controlling developmental timing and differentiation during neurogenesis (Rehfeld et al., 2015), and recent experiments in retinal explants provide compelling evidence that *Lin28b* and its opposing miRNAs, *let-7*, *mir-9*, and *mir-125*, regulate the developmental timing of retinal neurogenesis (La Torre et al., 2013). Given these findings, we hypothesized that the *Lin28b/let-7* axis plays an essential role in regulating the transition of cochlear prosensory cells from proliferative progenitors to differentiated sensory cells (Fig. 1.4).

Using recently developed iLIN28B and iLet-7g transgenic mouse lines (Zhu et al., 2011b), we found that *Lin28b* functions as a developmental timer in the murine cochlea through both *let-7* dependent and independent mechanisms. Furthermore, we found that by altering the expression of the *Lin28b/let-7* axis in the postnatal cochlea, we could modify the capacity for SCs to trans-differentiate into HCs in the absence of Notch signaling. Our findings suggest that this axis plays a key role in driving prosensory cell differentiation and maintaining SC plasticity.

Figure 1.1: Anatomy of the mammalian auditory system. (A) Overview of the human auditory system. The outer ear is comprised of the pinna and ear canal and is bounded on its medial end by the tympanic membrane. The middle ear is an air-filled space containing the three auditory ossicles. The third ossicle, the stapes, is couple to the outer membrane of the fluid-filled cochlear duct, the oval window. **(B, C)** Running along the length of the cochlear duct is the auditory epithelium. **(B)** A top down view of the auditory epithelium shows the stereocilia bundles (Phalloidin+, grey) that are found on the apical hair cell surface. One row of inner hair cells (ihc) and three rows of outer hair cells (ohc) run the entire length of the cochlear duct. **(C)** A cross-section through the auditory epithelium reveals the multiple supporting cell subtypes (SOX2/P27+, blue and green) that surround the inner and outer hair cells (MYO6+, white). Abbreviations: i – phalangeal cell, p – pillar cell, d – Deiter’s cell, h – Hensen’s cell.



Modified from Kelley, 2006

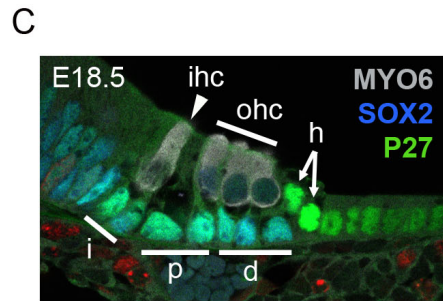
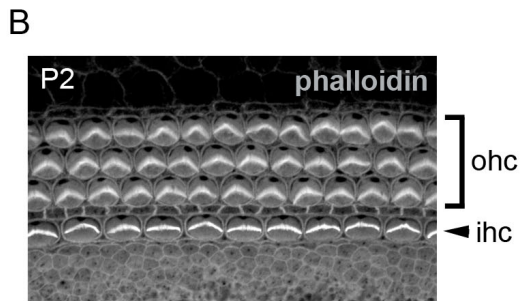


Figure 1.2: Schematic of prosensory cell cycle withdrawal and the onset of hair cell differentiation. Hair cells and supporting cells differentiate from a common pool of prosensory progenitor cells that is defined by expression of the transcription factor Sox2 (left panel, green). By E13.5, about half of these prosensory cells have withdrawn from the cell cycle, driven by the expression of the cyclin-dependent kinase inhibitor p27 (center panel, red). At E14.5, hair cell differentiation begins in the mid-basal cochlea, when the transcription factor Atoh1 begins to be expressed (right panel, green).

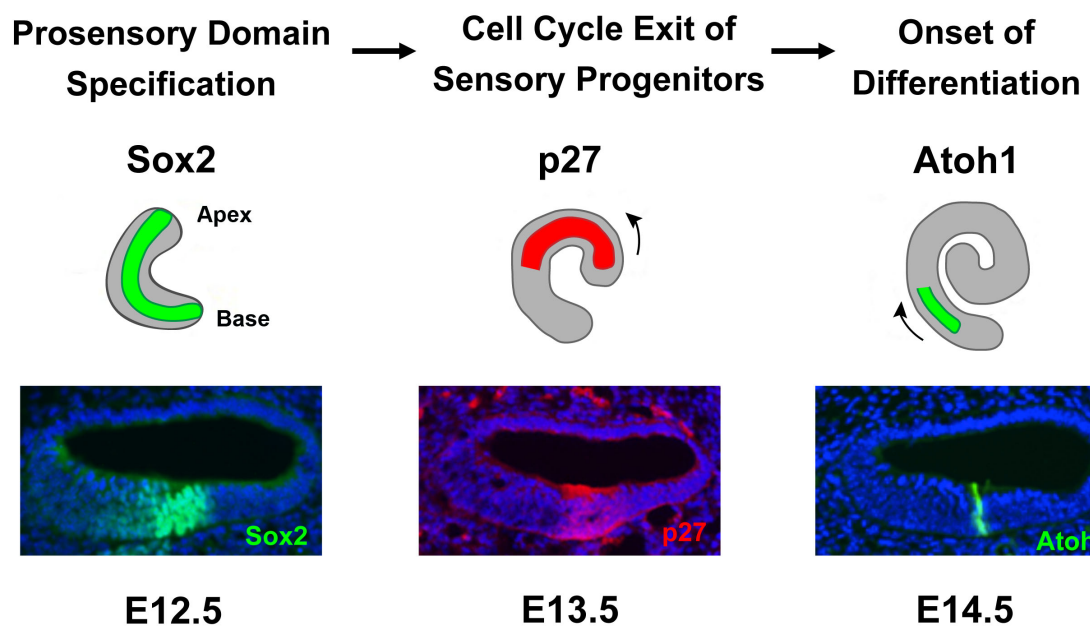


Figure 1.3: Lin28b acts through let-7 dependent and independent mechanisms to regulate developmental timing. The *Lin28* genes share a mutually antagonistic relationship with the *let-7* family of miRNAs. In the absence of *Lin28a/b* expression, the *let-7* miRNAs downregulate the expression of multiple growth and proliferation associated genes, including *Lin28a/b*. When LIN28A/B is expressed, these proteins inhibit the biogenesis of mature *let-7* transcript, relieving the repressing of these growth-related genes. LIN28A/B can also directly target certain mRNA transcripts and enhance their expression by promoting mRNA translation.

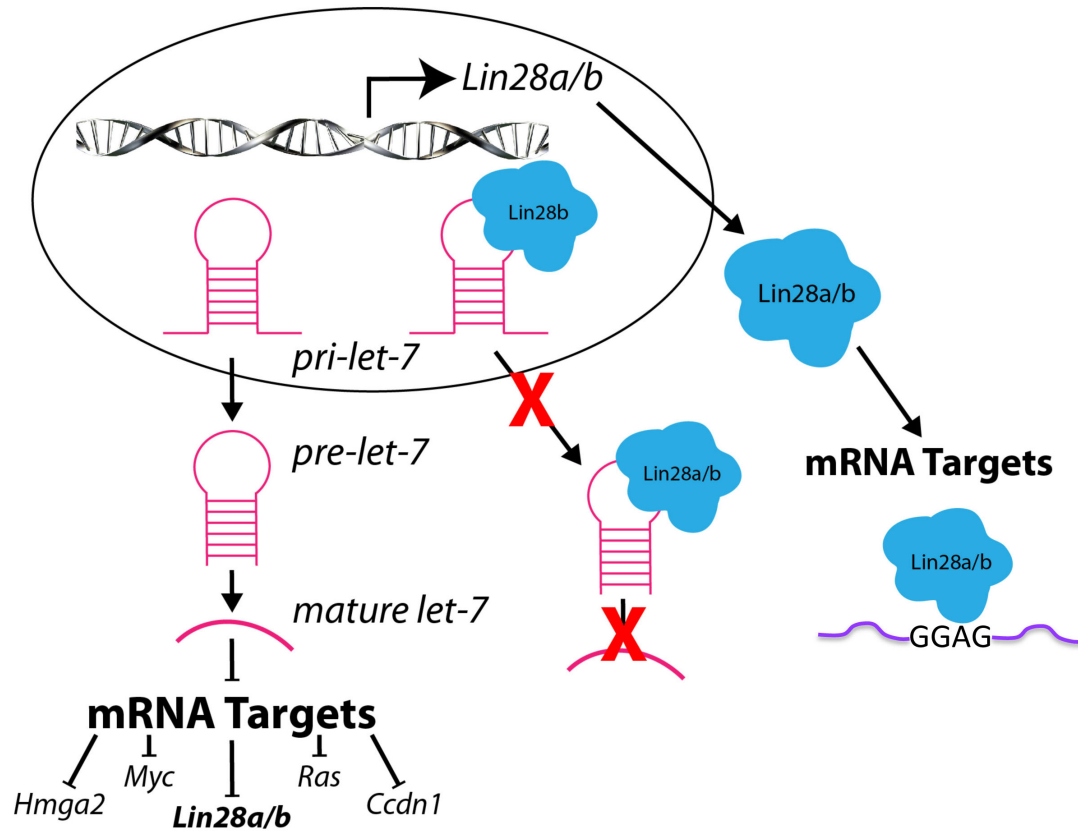
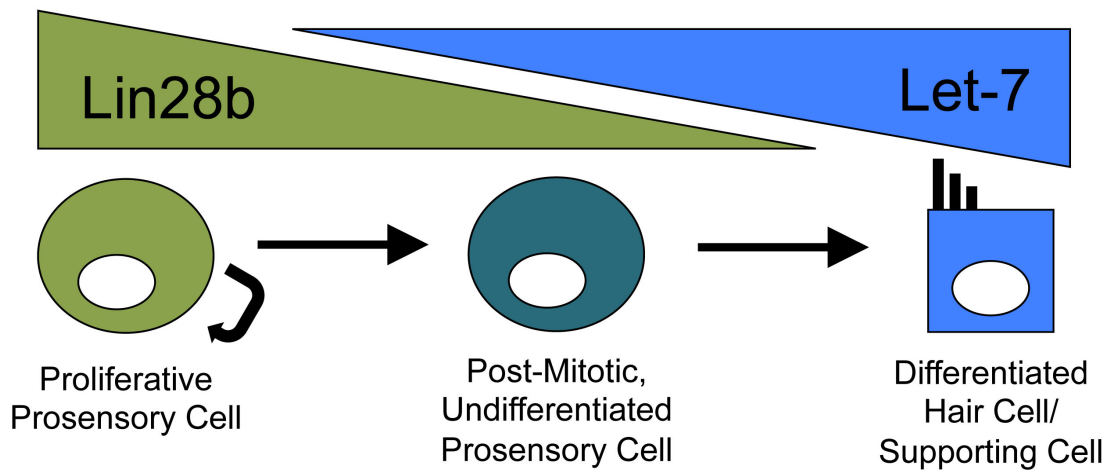


Figure 1.4: Hypothesized role of the *Lin28b/let-7* axis in the developing cochlear epithelium. Based on *Lin28b*'s proven role in promoting proliferation and stemness in other systems and its expression in undifferentiated cochlear prosensory cells, we hypothesized that *Lin28b* acts to maintain these cells in an undifferentiated state. Furthermore, we expected that *Lin28*'s downregulation and *let-7*'s upregulation would regulate the timing of prosensory cell cycle withdrawal and subsequent differentiation.



Chapter 2

Lin28b regulates developmental timing within the mammalian cochlear epithelium through both *let-7* dependent and independent mechanisms

INTRODUCTION

Over the past several years, key regulators of cochlear prosensory cell proliferation and differentiation have been identified (Raft and Groves, 2014; Schimmang and Pirvola, 2013). For instance, P27/Kip1 (CDKN1B), a cyclin-dependent kinase inhibitor, controls prosensory cell cycle withdrawal (Chen and Segil, 1999a), whereas ATOH1, a bHLH transcriptional activator, controls HC and SC differentiation (Bermingham et al., 1999b; Woods et al., 2004). *Atoh1* and *p27/Kip1* loss-of-function studies indicate that prosensory cell cycle exit and differentiation occur independently from each other (Chen et al., 2002b; Chen and Segil, 1999a); however, the molecular mechanisms coordinating the timing of these processes remain unknown.

Using microarray-based transcriptional profiling we recently identified *Lin28b* mRNA to be highly expressed in prosensory cells. *Lin28 genes* encode for evolutionarily highly conserved RNA binding proteins (Moss and Tang, 2003) known to regulate larval developmental timing (heterochrony) in *C. elegans* (Ambros and Horvitz, 1984). In humans and mice *Lin28a* and its homolog *Lin28b* are critical regulators of stemness, organismal growth, metabolism, tumorigenesis and tissue repair (Shyh-Chang and Daley, 2013). LIN28A and LIN28B proteins promote a stem cell/progenitor-like state through two distinct mechanisms. First, LIN28 proteins bind to and stabilize mRNAs encoding for cell cycle regulators and growth stimulating genes, leading to increases in their protein abundance (Graf et al., 2013; Hafner et al., 2013; Poleskaya et al., 2007; Xu et al., 2009). Second, LIN28 proteins block *let-7* microRNA (miRNA) biogenesis (Heo et al., 2008; Newman et al., 2008; Rybak et al., 2008; Viswanathan et al., 2008). Mature miRNAs are small non-coding RNAs that interact with their targets by partial base

pairing with complementary sequences commonly found within the 3' untranslated region (3' UTR) of the target mRNA. In the majority of cases, miRNA binding inhibits translation and/or destabilizes the target mRNA (Shenoy and Blelloch, 2014). Similar to *lin-28*, *let-7* was initially identified in *C. elegans* as a heterochronic gene (Ambros and Horvitz, 1984; Reinhart et al., 2000). *Let-7* miRNAs inhibit stem cell/ progenitor cell proliferation and promote differentiation by targeting cell cycle and growth-associated genes (Johnson et al., 2005; Lee and Dutta, 2007; Lin et al., 2007). The *Lin28* genes possess multiple *let-7* binding sites in their 3'UTR and are subject to negative regulation by *let-7* miRNAs, establishing a double negative feedback loop (Rybak et al., 2008). There is emerging evidence for a critical role of the *Lin28/let-7* axis in controlling self-renewal, lineage commitment and differentiation during neurogenesis (Rehfeld et al., 2014). For instance, experiments in retinal explants provide compelling evidence that *Lin28b* and its antagonistic miRNAs, *let-7*, *mir-9*, and *mir-125*, regulate the developmental timing of retinal neurogenesis (La Torre et al., 2013). Here, utilizing recently developed *iLIN28B* and *ilet-7g* transgenic mouse lines (Zhu et al., 2011a), we show that *Lin28b* functions as a developmental timer in the murine cochlea through both *let-7* dependent and independent mechanisms.

RESULTS

***Lin28b* and *let-7* miRNAs are differentially expressed in the auditory sensory lineage.**

To characterize the spatial and temporal expression pattern of the *Lin28b/let-7 axis* during cochlear differentiation, a series of RNA in situ hybridization (ISH) and qPCR experiments were performed. In addition to *Lin28b*, we characterized the expression of the high mobility group transcription factor *Hmga2*, which has been shown to promote organismal growth and stemness in other systems (Nishino et al., 2008; Zhou et al., 1995). Similar to *Lin28b*, both human and murine *Hmga2* harbor *let-7* binding sites in their 3'UTRs and are negatively regulated by the *let-7* miRNAs (Lee and Dutta, 2007; Lin et al., 2007; Mayr et al., 2007; Schulman et al., 2008). In the mammalian cochlea, prosensory differentiation follows a steep basal-to-apical gradient, whereby mid-basally located HCs differentiate prior to more apically located HCs. Our analysis revealed that both *Lin28b* and *Hmga2* transcripts are expressed in prosensory progenitor cells but are rapidly down-regulated in a basal-to-apical fashion upon the onset of HCs differentiation (Fig. 2.1 A-I'). At E13.0, *Lin28b* and *Hmga2* were co-expressed with *Sox2* in prosensory cells (Fig. 2.1 A-C) (Kiernan et al., 2005c). At E14.5, following the onset of *Atoh1* expression in nascent HCs, *Lin28b* and *Hmga2* transcript expression was reduced in the differentiating cochlear base and mid turn (Fig. 2.1 D-F). At the peak of HC differentiation (E16.5), *Lin28b* and *Hmga2* expression was only maintained in the most apical segment of the cochlear duct, which had not yet differentiated (Fig. 2.1 G-I').

Quantification by qPCR and western blot revealed that this more than 4-fold down-regulation in *Lin28b* transcript expression (Fig. 2.1 J, K) correlated with a nearly 5-fold reduction in LIN28B protein levels between E13 and E16 (Fig. 2.1 L, M). In

addition to *Lin28b* and *Hmga2*, we quantified the expression of the *Lin28b* paralog *Lin28a* as well as *Lin41*. *Lin41* encodes for an E3 ubiquitin ligase-like protein that, similar to *Lin28b*, shares a mutually antagonistic relationship with the *let-7* miRNAs and has been shown to regulate progenitor differentiation in other systems (Ecsedi and Grosshans, 2013). Like *Lin28b* and *Hmga2*, *Lin28a* and *Lin41* were rapidly downregulated in the differentiating cochlear epithelium (Fig. 2.1 J, K); however, the expression of each of these genes was significantly lower than that of *Lin28b*, - approximately 225x and 45x lower at E13.5, respectively (Fig. 2.1K).

The dramatic decline in LIN28B levels in the differentiating cochlea strongly correlated with a rise in *let-7* miRNA expression. The murine *let-7* family is comprised of nine mature *let-7* miRNA species (*let-7a*, *let-7b*, *let-7c*, *let-7d*, *let-7e*, *let-7f*, *let-7g*, *let-7i* and *mir-98*) (Thornton and Gregory, 2012). Our qPCR analysis revealed that eight out of nine *let-7* miRNA species were expressed in the early postnatal auditory sensory epithelium and that with the exception of *let-7i*, showed a rapid rise in mature *let-7* transcript expression with the advancement of cochlear differentiation and maturation (Fig. 2.2 G, H). Our analysis also revealed a steady increase in the levels of *mir-125b* during cochlear differentiation (Fig. 2.2 G, H). *Mir-125b* and *mir-125a*, vertebrate homolog's of the *C. elegans* heterochronic gene *lin-4* (Lagos-Quintana et al., 2002), are critical regulators of *Lin28a/b* expression (Wu and Belasco, 2005). ISH-based analysis using locked nucleic acid (LNA) probes revealed high expression of *let-7f* and *let-7c* in early postnatal cochlear and vestibular HCs and cells of the cochlear and vestibular ganglion. In contrast to *mir-183*, whose expression was confined to HCs and spiral ganglion cells (Sacheli et al., 2009; Weston et al., 2006), *let-7f* and *let-7c* were also

expressed in SCs and non-sensory epithelial cells of the greater epithelial ridge (Fig. 2.2 A-F). In summary, our expression analysis revealed reciprocal expression of *Lin28b* and mature *let-7* miRNAs in the developing cochlea, with *Lin28b* being highly expressed in undifferentiated prosensory cells, and mature *let-7* miRNA species being highly expressed in terminally differentiated HCs and SCs.

***LIN28B* overexpression delays prosensory cell differentiation.**

Based on the opposing expression pattern of *Lin28b* and *let-7* miRNAs in the differentiating murine cochlea, and the known heterochronic function of this axis in *C. elegans* larval development (Ambros and Horvitz, 1984), we hypothesized that *Lin28b* might be functioning as an intrinsic regulator of developmental timing in the mammalian cochlea. In order to address the function of the *Lin28b/let-7* axis in the murine cochlea, we made use of the *iLIN28B* transgenic mouse line (Zhu et al., 2011a). In this mouse line, a flag-tagged human *LIN28B* transgene is under the control of a tetracycline-responsive promoter element (*TRE*). When combined with a ubiquitous (*Rosa26*) or inner ear-specific (*Pax2*) reverse tetracycline transactivator (*rtTA*) transgene, doxycycline (dox) administration resulted in robust *LIN28B* overexpression within the developing cochlear duct (Fig. 2.3 A-E). In addition, due to *Lin28b*'s inhibitory function on *let-7* miRNA biogenesis, *LIN28B* overexpression resulted in more than an 80% reduction in mature *let-7* miRNA expression within the developing cochleae of *iLIN28B* transgenic embryos (Fig. 2.3 F).

To determine if *LIN28B* overexpression might inhibit or delay prosensory cell differentiation, HC-specific *Atoh1/nEGFP* reporter expression was used to monitor HC

differentiation in E13.0 *LIN28B* overexpressing (*Rosa26-M2 rtTA tg/+; iLIN28B tg/+; Atoh1/nEGFP tg/+*) and non-transgenic littermate control (*Rosa26-M2 rtTA tg/+; Atoh1/nEGFP tg/+*) cochlear explants over three days (Fig. 2.4 A-J). HC differentiation follows a steep basal-to-apical gradient and a less steep medial-to-lateral gradient, causing basally located HCs to differentiate prior to more apically located HCs and medial IHCs to differentiate prior to more lateral OHCs (Chen et al., 2002b; Sher, 1971). After 16 hours *in vitro* (HIV), a stripe of GFP+ IHCs was visible in the cochlear base of control explants (Fig. 2.4 B, J). In contrast, *LIN28B* overexpressing cochlear explants remained undifferentiated after 16 HIV (Fig. 2.4 C, J). 16 hours later (32 HIV), IHCs in *LIN28B* overexpressing cochlear cultures became apparent (Fig. 2.4 E, J) and over the next 32 hours, HC differentiation progressed at a similar rate in control and *LIN28B* overexpressing cultures (Fig. 2.4 J). Consistent with the observed delay in HC differentiation *in vitro*, both IHC and OHC differentiation was less advanced in acutely isolated E15.5 *LIN28B* overexpressing cochlear tissue compared to control (Fig. 2.4 T).

To rule out that the observed delay in cochlear HC differentiation was due to a more general developmental delay, an inner ear-specific overexpression approach was employed (Fig. 2.3 C-E) and the basal-to-apical extent of HC differentiation was analyzed using the HC-specific protein myosin VI (MYO6)(Avraham et al., 1995). Our analysis revealed that similar to global overexpression, selective, inner ear-specific *LIN28B* overexpression delayed auditory HC differentiation. In E15.5 non-transgenic control animals (*Pax2-Cre tg/+; rtTA tg/+*) MYO6+ IHCs were present throughout nearly the entire length of the cochlear duct (Fig. 2.4 L, N, P, U) and MYO6+ OHCs were already evident in the cochlear base (Fig. 2.4 L, N, U). In contrast, cochlear tissue

from *Pax2-iLIN28B* transgenic littermates (*Pax2-Cre tg/+; rtTA tg/+; iLIN28B tg/+*) contained no MYO6+ OHCs yet (Fig. 2.4 M, O, U) and MYO6+ IHCs were not found as far apically as in control cochlear tissue (Fig. 2.4 M, O, Q, U).

To determine the time window of this *LIN28B*-driven differentiation delay, we next acutely overexpressed *LIN28B*. Timed mated females were put on dox feed beginning at E12.5 and cochlear explant cultures were obtained 12 hours later, at E13.0 (Fig. 2.5 B). Overexpression of the *iLIN28B* construct takes approximately 24 hours (Fig. 2.5 A), indicating that *LIN28B* was still being upregulated when these cultures were begun. Because of this, *LIN28B* overexpression was not yet adequate to delay the onset of HC differentiation in the cochlear base; however, a significant delay in apical HC differentiation was observed after 48 hours (Fig. 2.5 C). This observation was recapitulated with lentiviral-mediated overexpression of murine *Lin28b* as well (Fig. 2.5 D-H).

***LIN28B* overexpression results in a delay in prosensory cell cycle exit.**

We next assayed the effects of *LIN28B* overexpression on prosensory cell proliferation. *Lin28b* functions as an oncogene in many tumors (Molenaar et al., 2012; Urbach et al., 2014; Viswanathan et al., 2009); however, little is known about *Lin28b*'s role in controlling cell proliferation during normal development. In the mammalian cochlea, prosensory cells withdraw from the cell cycle in a striking apical-to-basal gradient. Murine prosensory cells exit the cell cycle within a 48-hour time window, with apical prosensory cells exiting the cell cycle as early as E12.5 and the most basal progenitors exiting as late as E14.5 (Lee et al., 2006; Ruben, 1967). To determine

whether higher than normal LIN28B protein levels might delay prosensory cell cycle exit, a series of EdU pulse chase experiments were performed and EdU incorporation in differentiated HCs and SCs was analyzed at E18.5. Cytoplasmic myosin VII a (MYO7A) staining was used to identify HCs and nuclear p27/Kip1 and SOX2 staining were used to identify SCs (Chen and Segil, 1999a; Hasson et al., 1997). In the first set of experiments timed mated dams received a single injection of EdU at E13.5, the peak of cell cycle withdrawal. These experiments revealed that at stage E13.5 basally located HC and SC precursors in both control and *LIN28B* over-expressing cochlea were actively dividing and incorporated EdU at a similar rate (Fig. 2.6 A-D, N). However, whereas in control cochlear tissue HC and SC precursors located further apically had largely withdrawn from the cell cycle, in the *LIN28B* over-expressing cochleae HC and SC precursors continued to proliferate and incorporate EdU at a significantly higher rate than controls (Fig. 2.6 E-L, N). To determine whether the altered pattern of HC and SC precursor proliferation was due to a delay in the initial onset of cell cycle withdrawal, a single injection of EdU was administered at E12.5 and EdU incorporation in apically located HCs was analyzed at E18.5. Our analysis revealed that at E12.5 the majority of apical prosensory cells were actively cycling in *LIN28B* overexpressing cochleae, whereas in control cochleae, prosensory cells had started to withdraw from the cell cycle (Fig. 2.6 M). Consistent with a shift in timing rather than a permanent derailment of prosensory cell cycle withdrawal, EdU injections for three consecutive days beginning at E14.5, only labeled basally located HCs in *LIN28B* overexpressing cochleae. No EdU labeled cells were observed within the auditory sensory epithelium further apically, indicating that once post-mitotic, HC and SC precursors permanently withdrew from the cell cycle in the

LIN28B overexpressing cochlea (Fig. 2.6 O-Q). Furthermore, no proliferation was detected in either control or *iLIN28B* sensory epithelia at E15.5 (Fig. 2.7 A, B).

At E18.5, HC differentiation and patterning is largely complete in the murine cochlea. In non-transgenic littermate control cochleae, the typical stereotyped pattern of one row of IHCs and three rows of OHCs (Fig. 2.6 A, E, I, P) resting on a single layer of SCs (Fig. 2.6 C, G, K, P) was observed throughout the length of the cochlear duct. In contrast, the stereotyped organization of HCs and SCs was disrupted in the cochlear base of E18.5 *Pax2-iLIN28B* transgenic embryos. Ectopic IHCs were frequently observed in the basal segment of the *LIN28B* overexpressing cochleae (Control = 1.6 ± 0.5 ectopic IHCs per 1mm, *iLIN28B* = 14.7 ± 4.6 ectopic IHCs per 1mm, $n = 5$ animals/group, $p = 0.045$; Fig. 2.6 B; Fig. 2.7 F). In addition, OHCs were frequently missing, resulting in patches of sensory epithelium containing only two rows of OHCs (Control = 0.7 ± 0.7 missing OHCs per 1mm, *iLIN28B* = 34 ± 9 missing OHCs per 1 mm, $n = 5$ animals/group, $p = 0.02$; Fig. 2.6 B; Fig. 2.7 G). These HC patterning defects were mostly confined to the cochlear base; cellular patterning of the auditory sensory epithelium in more apical segments of the *LIN28B* overexpressing cochleae was largely normal (Fig. 2.6 F, J; Fig. 2.7 F, G). Interestingly, despite prolonged proliferation of both HC and SC precursors, only the number of SCs was increased in the *iLIN28B* cochleae (Fig. 2.6 R; Fig. 2.7 D, E). SCs were more densely packed, and in contrast to the single SC layer in control cochleae (Fig. 2.6 C, G, K, P), SCs were frequently found stacked on top of each other within *LIN28B* overexpressing cochleae (Fig. 2.6 D, H, L, Q). In addition to the observed cellular patterning defects, maturation of HCs and SCs was delayed in *iLIN28B* cochleae as evidenced by delayed down-regulation of the prosensory marker SOX2 in

HCs (Fig. 2.6 P, Q) and delayed up-regulation of the SC-specific marker S100 (Fig. 2.7 H, I).

What is the molecular basis of the *LIN28B*-mediated delay in prosensory cell cycle withdrawal and differentiation? One possible mechanism is that the up-regulation of *let-7* target genes due to lower than normal *let-7* levels alters the timing of prosensory proliferation and differentiation. Recent studies have revealed a critical role for the *let-7* targets *Igf2bp1* (*Imp1*), *Hmga2* and *Lin41* (*Trim71*) in neuronal stem cell/ progenitor cell maintenance (Nishino et al., 2008; Nishino et al., 2013; Schulman et al., 2008). Our analysis of *let-7* target gene expression revealed that *LIN28B* overexpression significantly increased transcript levels of *Igf2bp1*, *Lin41* and *Hmga2* (Fig. 2.6 S). Furthermore, *LIN28B* overexpression significantly increased the expression of the *let-7* targets *N-Myc* (*Mycn*) and *Cyclin D1* (*Ccnd1*) (Buechner et al., 2011; Zhao et al., 2010), which have been shown to positively regulate prosensory cell proliferation in the murine cochlea and vestibular organs (Dominguez-Frutos et al., 2011; Kopecky et al., 2011b; Laine et al., 2010) (Fig. 2.6 S).

***Let-7* overexpression results in premature progenitor cell cycle exit but does not cause precocious differentiation.**

To test whether *LIN28B* regulates prosensory proliferation and differentiation via a *let-7*-dependent mechanism, we made use of transgenic mice that express a *Lin28a/b*-resistant form of *let-7g* under the control of a tetracycline response element (Fig. 2.8 A) (Zhu et al., 2011a). When combined with either a ubiquitous or inner ear-specific *rtTA*, dox administration induced a more than 15 fold increase in *let-7g* miRNA expression

within the developing cochlear duct (Fig. 2.8 B). *Let-7g* overexpression significantly reduced *Hmga2* mRNA (Fig. 2.8 D; Fig. 2.9 E, F) and LIN28B protein levels (Fig. 2.8 C, D). To determine whether higher than normal *let-7* levels might cause precocious prosensory cell cycle withdrawal, dox-fed timed-mated dams received a single injection of EdU at E13.5 and EdU incorporation within *Pax2-ilet-7* transgenic and control embryos was analyzed 24 hours later (Fig. 2.8 F). Our EdU incorporation analysis revealed a dramatic decrease in the number of proliferating SOX2+ prosensory cells within *ilet-7* transgenic cochleae (Fig. 2.8 G-I). In *let-7g* overexpressing cochleae less than 5% of basally located prosensory cells incorporated EdU compared to more than 30% in control (Fig. 2.8 I). In addition, global (*Rosa26-ilet-7*) as well as inner ear specific (*Pax2-ilet-7*) *let-7* overexpression caused defects in cochlear outgrowth, and at E18.5 *let-7* overexpressing cochleae were 40% shorter than controls (Fig. 2.9 C, K). Likely due to the premature prosensory cell cycle withdrawal, both IHC and OHC density, as well as total HC number was significantly reduced (Fig. 2.9 L, M). Moreover, the 3rd row of OHCs was frequently missing in the *ilet-7* cochleae (Fig. 2.9 I, J, N). Surprisingly, the timing of HC differentiation appeared to be unaffected by *let-7* overexpression. At E14.5, both *Rosa26-ilet-7* cochleae and non-transgenic littermate control cochleae had a similar extent of HC differentiation along the length of the cochlear duct. *Atoh1/nEGFP* positive IHCs were observed only within the basal half of the cochlear duct; the apical half remained undifferentiated (Fig. 2.9 A-D). Similarly, no difference in HC-specific *Atoh1* mRNA expression was observed in E14.5 *Pax2-ilet-7* transgenic cochlear tissue compared to non-transgenic littermate controls (Fig. 2.9 G, H). In summary, our analysis suggests that the *Lin28b/let-7* circuit controls the timing of prosensory cell cycle

withdrawal in the developing cochlea. However, in contrast to *LIN28B* overexpression, *let-7g* overexpression had little effect on the timing of HC differentiation, suggesting that *Lin28b* utilizes a distinct, *let-7*-independent mechanism in regulating the timing of HC differentiation. Alternatively, it is possible that *let-7* overexpression alone is insufficient to induce HC differentiation and that additional signaling factors are necessary to mediate this effect.

DISCUSSION

Regulation of *Lin28b/let-7* expression in the developing cochlea

The differentiating inner ear cochlea expresses hundreds of miRNA species and RNA binding proteins, indicating that post-transcriptional regulation is likely to play an important role in controlling the dynamics of cochlear development. Here we have demonstrated that the RNA-binding protein LIN28B is a critical component of a timing mechanism that regulates both prosensory cell cycle withdrawal and differentiation in the murine cochlea. We have found that the evolutionary conserved LIN28B/*let-7* circuit is active in the developing cochlear epithelium. *Lin28b* is specifically expressed in prosensory progenitors and is rapidly down-regulated upon differentiation, whereas levels of mature *let-7* miRNAs rise during prosensory differentiation and are highly expressed in early postnatal HCs and SCs. LIN28B inhibits mature *let-7* miRNA processing, and likely serves a critical role in *let-7*'s post-transcriptional regulation within the developing cochlea. Despite the mutually antagonistic relationship between *Lin28b* and the *let-7s*; however, it is unlikely that the initial down-regulation of *Lin28b* is mediated by the *let-7s*, since these miRNAs are only upregulated after *Lin28b* down-regulation. Instead, we hypothesize that *mir-125b* mediates *Lin28b*'s down-regulation. Similar to the *let-7* miRNAs, *mir-125b* targets the expression of *Lin28b*; however, unlike the *let-7* miRNAs, *Lin28b* and *mir-125b* do not share a mutually antagonistic relationship, and LIN28B is unable to regulate *mir-125b*'s expression (Rybak et al., 2008; Wu and Belasco, 2005; Wulczyn et al., 2007). Here we show that *mir-125b* is highly expressed in the undifferentiated (E13) cochlear epithelium and continues to be upregulated during differentiation. Previous studies have found that *mir-125* starts to be expressed prior to

let-7 miRNAs in the embryonic mouse (Schulman et al., 2005), indicating that this regulatory mechanism, that is highly prevalent during *C. elegans* development, is likely to be evolutionarily conserved (Nimmo and Slack, 2009). Further experiments are needed to determine the effects of *mir-125b* gain or loss of function on cochlear epithelial development.

Lin28b acts through a *let-7* dependent mechanism to time prosensory cell cycle withdrawal but not differentiation

The regulatory functions of the RNA binding protein LIN28B and its opposing *let-7* miRNAs have been extensively studied in stem cells, tumor models and adult tissues; however, little is known about their function during embryonic development. Here we provide evidence that the LIN28B/*let-7* circuit is critical for the proper timing of prosensory cell cycle exit in the murine cochlea. We show that higher than normal LIN28B protein levels delayed the onset of prosensory cell cycle exit, whereas increased *let-7* levels resulted in premature cell cycle exit. The opposing effects of *LIN28B* and *let-7g* overexpression suggest that relative LIN28B/*let-7* levels set the timing of prosensory cell cycle withdrawal in the murine cochlea. Furthermore, our finding that *let-7g* is sufficient to induce premature cell cycle withdrawal, suggests that LIN28B times prosensory cell cycle exit, at least in part, by repressing *let-7* biogenesis. Interestingly, even though both global as well as cochlear-specific *LIN28B* overexpression was sufficient to delay the onset of HC differentiation, similar *let-7g* overexpression strategies failed to induce premature HC differentiation. This is in stark contrast to *let-7*'s differentiation-promoting function in other tissues. For example, overexpression of *let-7*

in neuronal progenitors not only inhibits proliferation, but induces premature neuronal differentiation as well (Nishino et al., 2008; Nishino et al., 2013; Schwamborn et al., 2009; Zhao et al., 2010; Zhao et al., 2013). How can this be explained? In many tissues, including the developing brain, timing of differentiation is tightly linked to timing of progenitor cell cycle exit. However, in the murine cochlea the developmental timing of these processes is largely uncoupled (Chen et al., 2002b; Chen and Segil, 1999a). This difference is illustrated by the divergent behavior of the *let-7* target *Mycn* within different tissue models. Similar to *let-7* overexpression, loss of *Mycn* causes premature prosensory cell cycle withdrawal without altering the timing of HC differentiation within the developing cochlea (Dominguez-Frutos et al., 2011; Kopecky et al., 2011a). In contrast, brain-specific deletion of *Mycn* results in both premature progenitor cell cycle exit and premature neuronal differentiation (Knoepfler et al., 2002). Of course, it is also possible that *let-7g* overexpression and *Mycn* knockdown fail to induce premature HC differentiation due to the absence of critical inductive cues or the presence of inhibitory signals. For instance, we have found that either the inhibition of Shh signaling or the activation of TGF β (activin) signaling is sufficient to induce premature HC differentiation (Benito-Gonzalez and Doeztlhofer, 2014 and unpublished). Further experiments are needed to understand the influence of these signaling pathways on *let-7* function within the developing cochlea.

***Let-7* independent functions of LIN28B**

It is becoming increasingly clear that LIN28 proteins can function in a *let-7* independent manner (Balzer et al., 2010; Nowak et al., 2014) and several recent genome

wide studies have revealed that LIN28A and LIN28B can directly alter the protein abundance of hundreds of their mRNA targets through transcript stabilization and/or modulation of translational efficiency (Cho et al., 2012; Graf et al., 2013; Hafner et al., 2013; Peng et al., 2011; Wilbert et al., 2012). Consistent with an important role in gene regulation, among the top LIN28B targets are RNA binding proteins, transcriptional regulators and RNA splicing factors (Hafner et al., 2013; Wilbert et al., 2012). We find this to be true in the embryonic cochlea as well. Recent microarray experiments comparing the gene expression profiles of iLIN28B versus control cochlea epithelia revealed that a number of genes, including morphogens, morphogen effectors, transcription factors, and RNA binding proteins, were differentially expressed upon LIN28B overexpression in the differentiating (E15.5) cochlear epithelium (Appendix A). While there were a number of *let-7* target genes on this list, there were also many genes that lacked putative *let-7* binding sites as well.

One particularly interesting LIN28B target identified by our microarray was the TGF- β /BMP antagonist *Follistatin* (*Fst*). *Fst* is expressed in an apical-to-basal gradient within the developing cochlear epithelium and has been proposed, along with a cluster of other genes, to help establish apical versus basal identity (Son et al., 2015; Son et al., 2012). We have found *Fst* to be significantly upregulated in iLIN28B cochlear epithelia (Appendix A). Similar to LIN28B overexpression, FST overexpression delays both cell cycle withdrawal and the onset of HC differentiation (A. Benito-Gonzalez, unpublished). We are currently working to determine whether LIN28B directly interacts with *Fst* or if indirect mechanisms mediate its enhanced expression.

We have also begun to try and identify upstream regulators of *Lin28b* expression during cochlear development. One potential candidate is the morphogen Shh, which has previously been shown to play an essential role in timing the onset of HC differentiation (Benito-Gonzalez and Doetzlhofer, 2014; Bok et al., 2013). We, and others, have shown that Shh overexpression inhibits the onset of HC differentiation, while blocking this pathway, for instance with the antagonist cyclopamine, accelerates HC differentiation (Benito-Gonzalez and Doetzlhofer, 2014). Intriguingly, we have observed that exogenous Shh treatment significantly upregulates *Lin28b* and *Hmga2* transcript expression (A. Benito-Gonzalez, unpublished) and we are currently investigating this link between the Shh pathway and the *Lin28b/let-7* axis.

It is widely believed that spiral ganglion-derived Shh is responsible for timing the onset of HC differentiation; however, this morphogen is also expressed by the developing notochord and floor plate, and this earlier expressed source of Shh appears to play an essential role in establishing apical versus basal identity in the developing cochlear duct. Constitutive Shh activity confuses regional identity in the developing cochlear epithelium, expanding the expression domain of apical genes and inhibiting the expression of basal genes. Among these apical genes is *Fst*, and notochord/floor plate derived Shh appears to be essential in establishing the apical-to-basal gradient of *Fst* expression (Son et al., 2015). A direct link between *Fst* and Shh has yet to be established, and we hypothesize that *Lin28b* may mediate this interaction. Similar to *Fst*, there appears to be an apical-to-basal gradient of *Lin28b* expression in the undifferentiated cochlear epithelium, with *Lin28b* expression appearing higher in the cochlear apex than base by *in situ* hybridization. Furthermore, given the similar effects of SHH, LIN28B, and FST

overexpression on HC differentiation, it seems likely that these are components of a common pathway. Experiments confirming this link are ongoing.

In summary, we have demonstrated that the *Lin28b/let-7* miRNA axis is active within the developing cochlea and plays a key role in coordinating the timing of progenitor cell cycle withdrawal and the onset of differentiation. Interestingly, LIN28B appears to act through both *let-7*-dependent and -independent mechanisms in coordinating these processes. Studies investigating the *let-7*-independent function of LIN28B are ongoing.

MATERIALS AND METHODS

Mouse Breeding and Genotyping: All experiments and procedures were approved by the Johns Hopkins University Institutional Animal Care and Use Committees protocol, and all experiments and procedures adhered to National Institutes of Health-approved standards. The *Atoh1/nEGFP* transgenic line was obtained from Jane Johnson (University of Texas Southwestern Medical Center, Dallas) (Lumpkin et al., 2003). The *iLIN28B* and *ilet-7g* transgenic lines were obtained from George Q. Daley (Children's Hospital Boston)(Zhu et al., 2011a). The *Pax2-Cre* line was obtained from Andrew Groves (Baylor College, Houston) (Ohyama and Groves, 2004). The *M2-rtTA* (stock #006965) and *rtTA-EGFP* (stock #005572) lines were purchased from Jackson Laboratories (Bar Harbor, ME). Mice were genotyped by PCR (see table below). Mice of both sexes were used in this study. All mouse lines were maintained on a mixed background of C57BL/6 and CD-1. To induce *iLIN28B* expression, doxycycline (dox) was delivered to time-mated females via ad libitum access to feed containing 2 grams of doxycycline per kilogram feed (Bioserv #F3893) starting at E8.5 and continuing until the embryonic tissue was harvested. To induce *Rosa26-iLet-7* expression, dox treatment was begun at E11.5. To induce *Pax26-iLet-7* expression, dox treatment was begun at E9.5. Embryonic development was considered as E0.5 on the day a mating plug was observed. Littermates expressing only the *M2-rtTA* or *rtTA-EGFP* transgene were used as controls.

Mouse Line	Primer Name	Primer Sequence
Col1A1 (iLIN28B, iLet-7)	ColfirtA	GCA CAG CAT TGC GGA CAT GC
	ColfirtB	CCC TCC ATG TGT GAC CAA GG
	ColfirtC	GCA GAA GCG CGG CCG TCT GG
M2-rtTA	rtTA A	GCG AAG AGT TTG TCC TCA ACC
	rtTA B	AAA GTC GCT CTG AGT TGT TAT
	rtTA C	GGA GCG GGA GAA ATG GAT ATG
rtTA-EGFP	rtTA mutant - F	GAG TTC TCT GCT GCC TCC TG
	rtTA mutant - R	AAG ACC GCG AAG AGT TTG TC
	rtTA wild type - F	CGT GAT CTG CAA CTC CAG TC
	rtTA wild type - R	GGA GCG GGA GAA ATG GAT ATG
Pax2-Cre	Cre - Forward	AAC ATG CTT CAT CGT CGG TCC GGG CTG C
	Cre - Reverse	GAC GGA AAT CCA TCG CTC GAC CAG TTT A
Atoh1/nEGFP	GFP - Forward	CGA AGG CTA CGT CCA GGA GCG CAC CAT
	GFP - Reverse	GCA CGG GGC CGT CGC CGA TGG GGG TGT TCT GC

Tissue isolation: Embryos were removed from timed-mated females and staged using the EMAP eMouse Atlas Project Theiler staging criteria (<http://www.emouseatlas.org>). Inner ears were collected and dissected in HBSS (Life Technologies). To free the cochlear epithelium (E13-E16), the vestibular portion of the inner ear was removed and the remaining cochlear portion was incubated in calcium-magnesium-free PBS (Life Technologies) containing dispase (1mg/ml; Life Technologies) and collagenase (1mg/ml; Worthington) for 8 minutes then placed in DMEM-F12 (Life Technologies) containing 10% FBS for 30 minutes, the cochlear duct was then freed from surrounding mesenchyme by manual dissection with 30-gauge needles. To obtain cochlear sensory epithelia of stages E18 and older, the cochlear capsule and the spiral ganglion were removed prior to dispase/collagenase treatment.

RNA Extraction and Quantitative PCR: Total RNA including mature miRNAs was extracted from cochlea epithelia samples using the miRNeasy Micro Kit (QIAGEN). For mRNA expression analysis, mRNA was reverse transcribed into cDNA using the iScript cDNA synthesis kit (Bio-Rad). SYBR Green based qPCR was performed using Fast SYBR® Green Master Mix reagent (Applied Biosystems, Life Technologies #4385612) and gene-specific primers. For miRNA expression analysis, pre-designed TaqMan Assays (Applied Biosystems, Life Technologies) were used according to manufacturer's instructions for two-step RT-qPCR. qPCR reactions were carried out in triplicate using a StepOne Plus Real-Time PCR System (Applied Biosystems, Life Technologies). Relative gene expression was analyzed using the $\Delta\Delta CT$ method (Schmittgen and Livak, 2008). The ribosomal gene *Rpl19* was used as an endogenous reference gene for SYBR Green-based assays, and the snoRNA *U6* was used as an endogenous reference gene for TaqMan-based miRNA measurements.

Protocol 1: Total RNA Extraction (miRNeasy Micro Kit – Qiagen)

1. Add 700ul QIAzol Lysis Reagent to sample and pipette to homogenize
 - At this step you can freeze at -80°, defrosting can be done in the 37° water bath
2. Incubate at RT for 5 min
3. Add 140ul chloroform and cap securely, shake vigorously for 15sec
4. Incubate at RT for 2-3min
5. Centrifuge for 15min at 12,000xg at 4°

6. Transfer upper aqueous phase (clear liquid at top) to a new tube and add 1.5 volumes (usually ~525ul) of 100% ethanol and mix by pipetting
 - Avoid transferring the interphase, this is where the protein is (can be saved for protein extraction)
7. Pipette up to 700ul of the sample, including and precipitate that may have formed into an RNeasy mini or micro column. Centrifuge at $>8000\times g$ for 15s at room temperature. Discard flow-through.
8. Repeat step 7 until the entire sample is loaded onto the column.
9. Add 350ul of buffer RWT to the column and spin at $>8000\times g$ for 15s. Discard flow through.
10. Combine 10ul of DNase with 70ul of buffer RDD and add all 80ul to the center of column (make sure to pipette directly onto membrane and not onto the sides of the column). Allow column to sit at RT for 15min.
11. Add 350ul of buffer RWT to the column and spin at $>8000\times g$ for 15s. Discard flow through.
12. Pipette 500ul Buffer RPE and spin at $>8000\times g$ for 15s. Discard flow through.
13. Pipette 500ul Buffer RPE and spin at $>8000\times g$ for 2 min. Discard flow through.
14. Can add third wash with either RPE or 80% ethanol if you are concerned with 230/260 ratio (will make sure all extra salts are gone)
15. Place column in a new 2 mL collection tube and centrifuge for 1 min at full speed without the lid to completely dry column membrane.
16. Transfer column to a 1.5 mL collection tube. If using a mini column elute with 30-50ul of RNase-free water. If using a micro column elute with 15ul RNase-free

water. To elute, pipette water directly onto the column membrane (not the walls)
and spin for 1 min at >8000xg

Protocol 2: SybrGreen RT-qPCR

1. cDNA Synthesis (BioRad iScript cDNA Synthesis Kit)

	1x Master Mix
5x iScript RT Buffer	4µl
RNA	x µl (75ng min; 600-800ng ideal; 1µg max)
iScript RT Enzyme	1µl
dH ₂ O	To 20µl

Cycling parameters: 25°C – 5 min; 42°C – 30 min; 85°C – 5 min; 4°C – ∞

2. Dilute primers to 3µM (working mix) by combining 6µl of forward and reverse stock (100µM) with 188µl dH₂O
 - Pipette 2µl primer mix per well
3. Make sample and negative control master mixes

cDNA Mix	1x Master Mix
cDNA	x µl (0.1-0.5µl)
SybrGreen	10µl
dH ₂ O	To 18µl

Negative Control Mix	1x Master Mix
SybrGreen	10µl
dH ₂ O	8µl

- Pipette 18µl

Gene	Forward Primer	Reverse Primer
Atoh1	ATG CAC GGG CTG AAC CA	TCG TTG TTG AAG GAC GGG ATA
Ccnd1	TCC GCA AGC ATG CAC AGA	GGT GGG TTG GAA ATG AAC TTC A
Hmga2	CCC AAA GGC AGC AAA AAC AA	CCA ATG GTC TCT GCT TTC TTC TG
Igf2bp1	GGA GCA GAC CAG GCA AGC TA	GGG CAT GGT TCT CCA GTT GA
Lin28a	TCC AAA GGA GAC AGG TGC TAC A	TTG CAT TCC TTG GCA TGA TG
Lin28b	CAG ACA GGT CAC CCC AAG AAG	TTT TGC TCT CCT ATT GCT GCA A
LIN28B	AAA GGG AAG ACA CTA CAG AAA AGA AAA	GAT GAT CAA GGC CAC CAC AGT
Lin41	AGG TGG CCT CTT TCA CTG TCA	ATC AGG TCA CCT CCC GAA TG
Mycn	TCT AAC AAC AAG GCG GTA ACC A	GCC CAG AGC GGA GGT CTT
Rpl19	GGT CTG GTT GGA TCC CAA TG	CCC GGG AAT GGA CAG TCA

Protocol 3: Taqman RT-qPCR

Step 1: Reverse Transcription

	1x Master Mix
10mM dNTPs with dTTP	1.5 μ l
Reverse Transcriptase (200U/ μ l)	0.25 μ l
M-MLV 5x Buffer	3 μ l
Rnase Inhibitor (40U/ μ l)	0.1 μ l
Nuclease Free H ₂ O	2.15 μ l
Total	7μl

Per Reaction Combine: 7 μ l master mix with 5 μ l RNA (RNA diluted to 2ng/ μ l) and 3 μ l of 5x RT primers (ie: Let7-c, Let7-f, or U6 primers)

Cycling Parameters: 16°C – 30 min; 42°C – 30 min; 85°C – 5 min; 4°C – ∞

Store at -20°C if not using immediately

Step 2: TaqMan qPCR Reaction

Reactions should be run in triplicate with 20µl per reaction

	1x Reaction	3x Reaction
TaqMan small RNA Assay (20x)	1µl	3.6µl
Product from RT reaction	1.33µl	4.80µl
TaqMan Universal PCR Master Mix (2x)	10µl	36µl
Nuclease Free Water	7.67µl	27.6µl
Total	20µl	72µl

Cycling Parameters: 95°C – 10 min; 40 Cycles: 95°C – 15 sec; 60°C – 60 sec

Ordering Information:

M-MLV Reverse Transcriptase (Promega #M1701)

GeneAmp dNTPs (Applied Biosystems #N808-0007)

RNase Inhibitor (NEB #M0307S)

Taqman Universal PCR Master Mix (Applied Biosystems/Roche #4304437)

miRNA	Assay ID (Life Tech)
U6 snRNA	001973
hsa-let-7a	000377
hsa-let-7b	000378
hsa-let-7c	000379
hsa-let-7d	002283
hsa-let-7e	002406
hsa-let-7f	000382
hsa-let-7g	002282
hsa-let-7i	002221
miR-98	000577
miR-125a	002198
miR-125b	000449

Immunoblotting: Cochlear epithelia were placed in lysis buffer (50mM HEPES, 150mM NaCl, 1mM EDTA, 10% glycerol, 1% tritonX-100, 0.2% SDS, pH7.9) supplemented with fresh Complete Protease Inhibitor (Roche). Equal amounts of cochlear lysate were resolved on NuPAGE 4-12% Bis-Tris Gels (Novex, Life Technologies) and transferred to PVDF membrane by electrophoresis. Membranes were blocked in 10% BSA in TBST and immunoblotted: rabbit anti-Lin28b 1:1000 (Cell Signaling #5422), mouse anti- β -actin 1:3000 (Ambion #AM4302), rabbit anti-Flag 1:1000 (Cell Signaling #2368). HRP-conjugated secondary antibodies from Jackson ImmunoResearch were used at a concentration of 1:7500 (goat anti-rabbit IgG #111-035-003; sheep anti-mouse IgG #515-035-003). Signal was revealed using a Western Lightning-ECL kit (Perkin Elmer) according to manufacturer's instructions.

Protocol 4: Western Blotting

Step 1: Tissue Collection

1. Dissect tissue of interest and keep on ice to avoid protein degradation
2. If tissue is not being used that day, snap freeze using liquid nitrogen or dry ice and store at -80°C
3. Prepare Lysis Buffer and supplement with Roche Complete Protease Inhibitor just prior to lysis
 - Lysis Buffer (Meffert Lab Recipe): 50mM HEPES, 150mM NaCl, 1mM EDTA, 10% glycerol, 1% tritonX-100, 0.2% SDS, pH7.9 – store at RT

- 1 Roche Complete Mini Tablet in 2 mL gives 25x stock – aliquot and store in -20°C freezer
4. Lyse tissue in appropriate amount of lysis buffer
 - e.g. 3 embryonic cochlea in 50µl buffer
 5. Homogenize tissue using pipette, needle, or pestle
 6. Rotate sample (end over end) at 4°C for 15 min
 7. Spin sample at 13,000 RPM for 15 min at 4°C and collect supernatant
 - Protein concentration can be determine using Bradford Assay or Coomasi gel
 8. Add NuPage denaturing agent (10x) and NuPage LDS sample dye (4x) to sample
 - Can run up to 20µl of sample per well
 9. If boiling is necessary, heat sample to 85°C for 5 min prior to loading gel

Step 2: Electrophoresis

1. Prepare 800 mL of NuPage MES SDS running buffer from 20x stock
 - Take 200 mL of 1x buffer and add 500µl of antioxidant
2. Snap together gel box and gel. Add running buffer w/ antioxidant to center portion and the remaining running buffer w/o additive to the outer portion
3. Load first well with 10µl of ladder
4. Load up to 20µl of sample per well
5. Run gel at 200V for 40 min

Step 3: Transfer

Transfer Buffer (Reed Lab Recipe)	1 Liter
Tris Base	5.82 g
Glycine	2.93 g
MeOH	200 mL
SDS	0.375 g
dH ₂ O	Up to 1 liter

1. Once gel has finished running, crack case and soak gel in transfer buffer for 20 min with shaking at RT
2. Meanwhile, cut appropriate size piece of PVDF membrane (e.g. 8cm x 8cm) and activate in MeOH for 1 min
 - After activation, soak PVDF membrane in transfer buffer until gel is done soaking (10-15 min)
3. Prepare appropriate size pieces of blotting pad (2) and Watman paper (x2) and wet with transfer buffer
4. Build “transfer sandwich” (bottom to top)
 - 1 piece blotting pad
 - 1 piece Watman paper
 - PVDF membrane
 - Protein gel
 - 1 piece Watman paper
 - 1 piece blotting pad
5. Make sure sandwich is sufficiently wetted with transfer buffer and use falcon tube to role out any bubbles

6. Place sandwich in Semidry Transfer Apparatus (BioRad, belongs to Reed Lab) and run at 15V for 15 min
7. When run is finished carefully take apart sandwich and remove PVDF membrane using forceps

Step 4: Blotting

All steps done with shaking

1. Wash membrane 3x 5 min in TBST at RT
2. Block for 1 hour in 5% BSA in TBST (0.5g BSA in 10mL TBST) at RT
3. Dilute 1° antibody in 10 mL 5% BSA and incubate membrane overnight at 4°C
 - 1° antibody can be saved and reused!
4. Wash membrane 3x 5 min in TBST at RT
5. Dilute HRP conjugated 2° antibody 1:7,500 in TBST and incubate membrane 2hrs at RT
6. Wash membrane 3x 5 min in TBST at RT
7. Develop blot in Western Lightening ECL solution
 - Mix 2 solutions 1:1 (e.g. 2 mL each)
 - Pipette onto membrane and allow to penetrate for 1 min
 - Wrap in saran wrap or other clear plastic and place in developing cassette

In Situ Hybridization and Immunostaining: Embryo heads (E11-E16) or inner ears (E18 and older) were fixed in 4% paraformaldehyde in PBS overnight at 4°C then cryo-protected through sucrose gradient: 10% sucrose 30 minutes at RT, 15% sucrose 1hr at RT, 50:50 30% sucrose:OCT overnight at 4°C. Prior to cryo-sectioning samples were submerged in OCT (Tissue-Tek, Sakura) and flash frozen. 14µM sections were collected on SuperFrost Plus slides (Fisher). pBluescript II (Stratagene) and pGem-T easy (Promega) vectors containing mouse *Atoh1*, *Sox2*, *Lin28b*, and *Hmga2* cDNA were used as templates to synthesize digoxigenin-labeled antisense RNA probes according to the manufacturer's specifications (Roche). Custom-made 5' digoxigenin -labeled locked nucleic acid probes (miRCURY LNA™) from Exiqon were used for *let-7f* and *let-7c* ISH. Probes were detected with the anti-DIG-AP (alkaline phosphatase conjugated) antibody (Roche) and the color reactions were developed using BM Purple AP Substrate (Roche).

Protocol 5: mRNA I *In Situ* Hybridization Probe Production

Step 1: Extract genes from plasmid vector by PCR

	Master Mix
Nuclease Free H ₂ O	76.5µl
10x NEB Buffer	10µl
dNTP (10mM)	2µl
T7 Primer (10µM)	5µl
SP6 or T3 Primer (10µM)	5µl
NEB Taq	0.5µl
Total	100µl

Cycling Parameters: 95°C – 1 min; 35 Cycles: 95° – 30 sec; 55° – 30 sec; 72° – 1 min;
then 72°C – 7 min; 4°C – ∞

Step 2: *In vitro* transcription

	Master Mix
5x transcription buffer	10µl
Linear DNA Template	1-2µg
100mM DTT	2.5µl
RNase Inhibitor (40U/µl)	2.5µl
DIG RNA labeling mix	5µl
T3 or SP6 or T7 RNA polymerase	2.5µl
Nuclease Free H ₂ O	Up to 50µl

1. Incubate 2 hours at 37°C
2. Add 1µl RNase-Free DNase and incubate 30 min at 37°C
3. To precipitate RNA add 100µl TE Buffer, 10µl 4M LiCl, 300µl 100% EtOH to probe, mix, and store at -20°C
4. To use RNA probe: spin at max speed (13000) refrigerated (8°C) for 30 min
5. Re-suspend pellet in 40µl DEPC H₂O or TE Buffer
6. Store at -20°C

Protocol 6: mRNA *In Situ* Hybridization

Day 1 (RNase Free!):

1. 15 min in 100% MeOH at -20°C
2. Rinse in autoclaved H₂O

3. 30 min air dry
4. Bake 20 min at 54°C
5. 10 min in 4% PFA/PBS
6. Rinse in 1x PTw
 - 50 mL 10x PBS
 - 5 mL 10% Tween-20
 - Up to 500 mL autoclaved H₂O
7. 5 min x 2 in PTw
8. ProK solution for 3 min
 - 2.5 mL 1x PBS
 - 12.5 µl ProK
 - Up to 50 mL autoclaved H₂O
9. Rinse in 1x PTw
10. 5 min x 2 in PTw
11. Rinse in autoclaved H₂O
12. 15 min Acetylation (TEA)
 - 1 mL TEA
 - 250 µl acetic anhydride
 - Up to 50 mL autoclaved H₂O
13. Rinse in 1x PTw
14. 5 min x 2 in PTw
15. Rinse in autoclaved H₂O
16. 30 min to 1 h air dry

17. Hybridize in probe O/N at 68°C

- Combine 20 mL Hybridization Buffer with 40µl probe (~1µg/mL)
 - Hybridization Buffer (50 mL)
 - 25 mL Formamide
 - 12.5 mL 20x SSC
 - 0.5 mL 10% Tween-20
 - 0.5 mL 10% CHAPS
 - 0.5 mL 0.5M EDTA
 - 125 µl tRNA (20 mg/mL)
 - 0.005g Heparin
 - Up to 50 mL autoclaved H₂O

Day 2:

1. 10 min in 0.2x SSC at 68°C
2. 25 min in 0.2x SSC at 68°C
3. 25 min in 0.2x SSC at 68°C
4. 5 min TBST at RT x 2
 - 25 mL 10x TBS
 - 25 mL 10% Tween-20
 - 0.1g Levamisole
 - Up to 250 mL autoclaved H₂O
5. Block 1 hour in 10% goat serum in TBST
6. Dilute anti-DIG-AP antibody 1:2000 in blocking buffer and incubate 2 hrs at RT

7. Rinse in TBST
8. 5 min TBST at RT x 3
9. 15 min in NTMT x 2
 - 2 mL 2.5M NaCl
 - 10 mL 100mM Tris (pH 9.5)
 - 250µl 2M MgCl₂
 - 500µl 10% Tween-20
 - Up to 50 mL autoclaved H₂O
10. Develop in BM Purple O/N at RT
11. Rinse in PBS and H₂O to stop reaction and mount in Fluoromount G

Protocol 7: miRNA *In Situ* Hybridization

Step 1: Tissue Preparation

1. **Briefly** fix tissue in 4% PFA in DEPC PBS at RT
 - Postnatal inner ears: 15 min
 - Embryonic heads: 30 min
2. Cryopreserve tissue
 - 10% sucrose 30 min at RT
 - 15% sucrose 1 hour at RT
 - 1:1 30% sucrose:OCT at 4°C O/N
3. Place tissue in fresh OCT in mold, orient, and freeze in liquid nitrogen
4. Collect 14 µm sections at -15-20°C

5. Allow sections to dry 30 min – 3 hours at RT (no longer), use immediately or store at -80°C

- When defrosting sections allow to dry at RT for 30 min

Day 1 (RNase Free!):

1. Bake slides at 52°C 10-30min
2. Fix slides 10 min in 4% DEPC PFA
3. Wash 3x 3 min in DEPC PBS
4. Acetylate 10 min
 - 5 mL triethanolamine (TEA)
 - 1.25 mL acetic anhydride
 - Up to 250 mL DEPC H₂O
5. Wash 1x 5 min in DEPC PBS
6. Proteinase K treatment 10 min at 37°C
 - 250 mL DEPC PBS + 1 µl proK stock (20 mg/mL)
7. Wash 3x 3 min in DEPC PBS
8. Pre-hybridize 1-8 hours at RT in hybridization buffer

Hybridization Buffer	Approx. 18 mL
Formamide	10 mL
20x SSC	5 mL
Yeast tRNA (20 mg/mL stock)	250 µl
Salmon Sperm DNA (10 mg/mL)*	1 mL
10% CHAPS	500 µl
20% Tween-20	100 µl
Autoclaved H ₂ O	1.15 mL

**Deactivate salmon sperm DNA by heating to 95°C for 5 min*

9. Prepare LNA probes

- Dilute LNA miRNA probe to 2pmol/μl stock
 - <https://www.exiqon.com/oligo-tools>
- Add 1.5μl probe to 20μl of hyb. buffer and denature at 80°C for 5 min, then place immediately on ice
- Add 130μl of hyb. buffer to denatured probe and add 150μl diluted probe per slide
- To prevent drying, gently coverslip slides and place in chamber humidified with 5xSSC/50% formamide)

10. Hybridize slides overnight at 52°C

- Hybridization Temperature = Probe T_m - 30°C

Day 2: Low Stringency Washes

Pre-warm solutions in incubator or water bath

1. Float off coverslips in 2x SSC at 50°C
2. Wash 3x 10 min in Buffer B1 at 37°C
 - 20 mL 1M Tris (pH 7.5)
 - 12 mL 2.5M NaCl
 - 218 mL H₂O
3. Equilibrate in Buffer B1 10 min at RT
4. Block 1 hour at RT in Buffer B1 + 10% goat serum
5. Dilute anti-DIG antibody (Roche) 1:2000 in Buffer B1 and incubate O/N at 4°C

Day 2: High Stringency Washes

Pre-warm solutions in incubator or water bath

1. Float off coverslips in 2x SSC at 50°C
2. Wash in HSW for 30 min at 50°C
 - 150 mL formamide
 - 30 mL 20x SSC
 - 120 mL H₂O
6. Wash 3x 10 min in Buffer B1 at 37°C
 - 20 mL 1M Tris (pH 7.5)
 - 12 mL 2.5M NaCl
 - 218 mL H₂O
7. Wash in HSW for 30 min at 50°C
8. Wash in 2x SSC for 15 min at 37°C
9. Equilibrate in Buffer B1 10 min at RT
10. Block 1 hour at RT in Buffer B1 + 10% goat serum
11. Dilute anti-DIG antibody (Roche) 1:2000 in Buffer B1 and incubate O/N at 4°C

Day 3:

1. Wash slides 3x 5 min in Buffer B1 at RT
2. Equilibrate 15 min in Buffer B3
 - 20 mL 1M Tris (pH 9.5)
 - 8 mL 2.5 M NaCl
 - 5 mL 2M MgCl
 - 167 mL H₂O

3. Develop slides at RT in humidified chamber with BM Purple (Roche) for 1 to 4 nights or until sufficient signal is achieved.
4. Rinse in PBS and H₂O to stop reaction and mount in Fluoromount G

5' DIG LNA Probes (Exiqon)

miRNA	Product Number
hsa-let-7a	18000-01
hsa-let-7b	38001-01
hsa-let-7c	38002-01
hsa-let-7f	18005-01
hsa-let-7g	38503-01
hsa-miR-125a-5p	38521-01
hsa-miR-125b	18022-01
hsa-miR-183	38490-01
scramble-miR	99004-01

Immuno-staining was performed according to the manufacture's specifications. Primary antibodies: rabbit anti-myosin VI (1:1000, Proteus #25-6791), rabbit anti-myosin VIIa (1:500, Proteus #25-6790), goat anti-SOX2 (1:500, Santa Cruz #sc-17320), mouse anti-p27/Kip1 (1:200, NeoMarkers/Thermo #MS-256-P1), rabbit anti-S100 (1:500, Abcam #ab868), and rabbit anti-dsRed (1:500 Clontech #632496). Alex Fluor (488, 546, and 633) labeled secondary antibodies were used to visualize staining (1:1000, Molecular Probes/ Life Technologies). Stereocilia were visualized with fluorescently labeled phalloidin (1:500, Molecular Probes/ Life Technologies). For anti-p27/Kip1 immuno-staining, sections underwent antigen retrieval by boiling in 1x Dako Ready-to-Use Target Retrieval Solution (Dako #S1700) in a 95°C water bath for 20 min, followed by a 45 min cooling incubation at RT.

Hair Cell Differentiation Assay: E13.5 undifferentiated *Atoh1/nEGFP* cochlear epithelia, spiral ganglion, and surrounding mesenchyme were cultured on SPI black membranes (SPI Supplies, Structure Probe) in DMEM-F12 (Life Technologies) containing 1x N2 supplement (Life Technologies), 5 ng/mL EGF (Sigma), 2.5 ng/mL FGF (Sigma), 100 U/mL penicillin/streptomycin (Sigma) and 10 μ g/mL doxycycline (Sigma). Cultures were grown in a 5% CO₂/20% O₂ humidified incubator. To monitor HC differentiation, native nuclear GFP expression (*Atoh1/nEGFP*) was imaged every 8-12 hours for three days using fluorescent stereomicroscopy (Leica). Length of the GFP+ HC stripe was quantified using ImageJ64 software (NIH).

Proliferation Assay: EdU (5-ethynyl-2'-deoxyuridine, Life Technologies) was reconstituted in PBS and administered at 50 μ g per gram body weight to time-mated females by intraperitoneal injection. Click-iT Alexa Fluor 546 Kit (Life Technologies) was used to detect incorporated EdU according to the manufacturer's specifications. MYO7A and SOX2 immunostaining labeled HCs and SCs. Cochleae were divided into three equal portions (base, mid, apex) and high-power confocal (Zeiss) z-stack images (4 images per region, representing approximately 700 microns) were taken through the HC and SC layers within each of these regions. The percentage of HCs and SCs that had incorporated EdU was manually quantified within Photoshop and ImageJ.

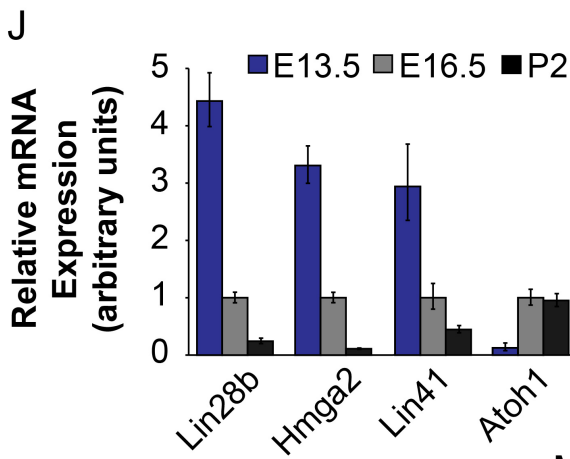
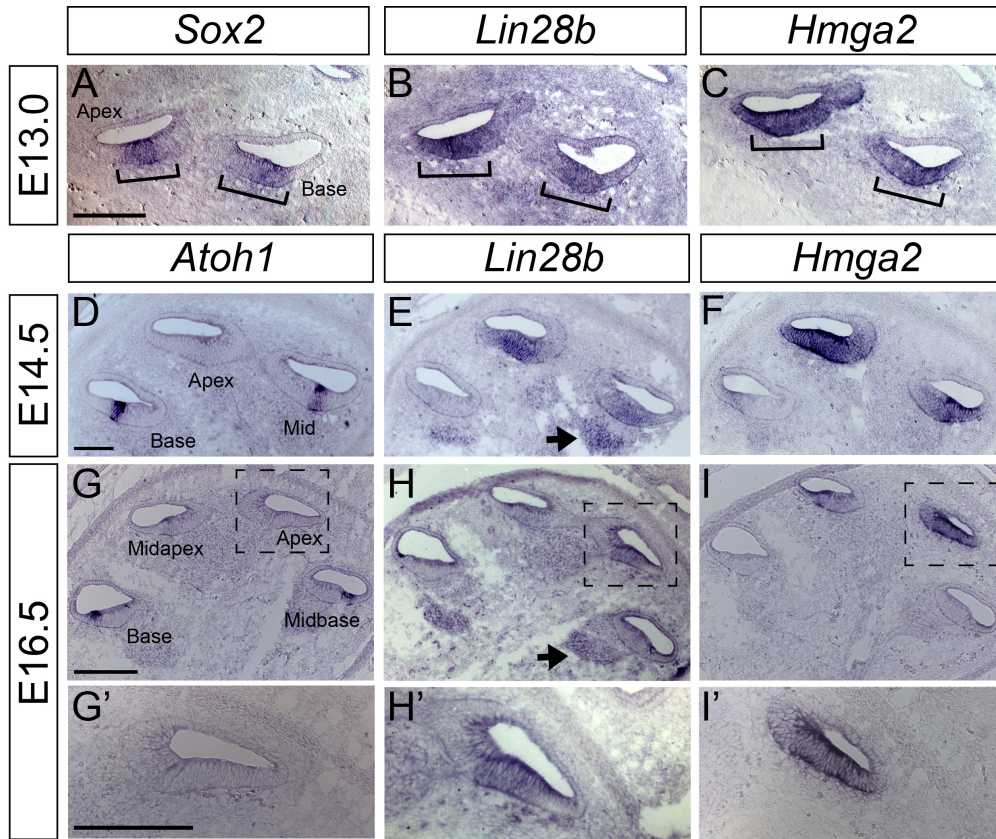
Cochlear Length and Cell Patterning Analysis: Cochlear surface whole mounts were prepared from E18.5 iLIN28B and non-transgenic littermate embryos and immunostained for MYO7A and SOX2. Low power fluorescent images of the HC layer were assembled in Photoshop CS5 (Adobe) and the length of the entire cochlear sensory epithelium was measured in ImageJ64 (NIH). For cell density and patterning analysis,

cochleae were divided into three equal portions (base, mid, apex) and high-power confocal (Zeiss) z-stack images (4 images per region, representing approximately 700 microns) were taken through the HC and SC layers within each of these regions. Images then were manually quantified within Photoshop and ImageJ.

Lentiviral Expression System: Control and experimental constructs (mCherry vs. Lin28bF2AmCherry) were maintained in FUW lentiviral-vector backbone. Multi-step PCR was used to link full-length murine *Lin28b* ORF to a mCherry reporter via a F2A linker sequence (Klump et al., 2001) High titer lentiviral stocks were prepared as previously described (Lois et al., 2002). Undifferentiated *Atoh1/nEGFP* cochlear epithelial explants were incubated in a 1:1 mix of lentivirus and culture media at room temperature for 2-hours prior to plating. Cultures were maintained as described above.

Statistical Analysis: Values are presented as mean \pm standard error (SEM), n = animals per group. All results were confirmed by at least two separate experiments. Two-tailed *Student's* t-tests were used to determine confidence interval. *P*-values ≤ 0.05 were considered significant. *P*-values > 0.05 were considered not significant.

Figure 2.1: Multiple Heterochronic genes are expressed in the developing cochlear epithelium and are rapidly downregulated during differentiation. (A-I') *In situ* hybridization (ISH) based analysis of *Lin28b* and *Hmga2* expression prior to (A-C) and during cochlear differentiation (D-I'). *Sox2* (A) marks prosensory cells, *Atoh1* (D, G, G') marks HCs. Brackets (A-C) indicate the prosensory domain. Arrows (E, H) indicate *Lin28b* expression within the developing spiral ganglion. High power images of the apical turn of G-I are shown in ('). Scale bar, 100 μ m. **(J, K)** RT-qPCR analysis of heterochronic gene expression within the cochlear epithelium prior to (E13.5), during (E16.5), and following (P2) differentiation. *Rpl19* was used as an endogenous reference gene. Data in (J) are mean \pm SEM. **(L, M)** LIN28B protein quantification within the cochlea epithelium at stages acutely surrounding the onset of HC differentiation.



K

Gene	Stage	Δ CT
Lin28b	E13.5	4.14
	E16.5	6.29
	P2	8.34
Lin28a	E13.5	11.97
	E16.5	14.29
	P2	16.45
Hmga2	E13.5	3.42
	E16.5	5.15
	P2	8.32
Lin41	E13.5	9.60
	E16.5	11.16
	P2	12.32
Atoh1	E13.5	10.99
	E16.5	8.01
	P2	8.08

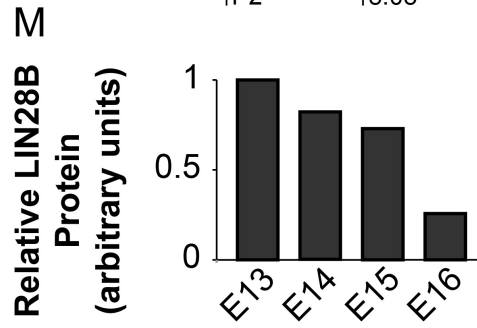
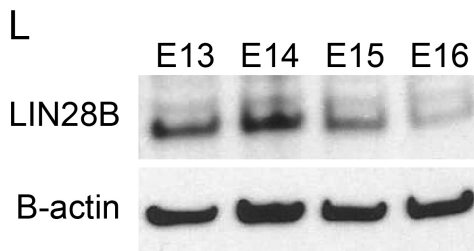
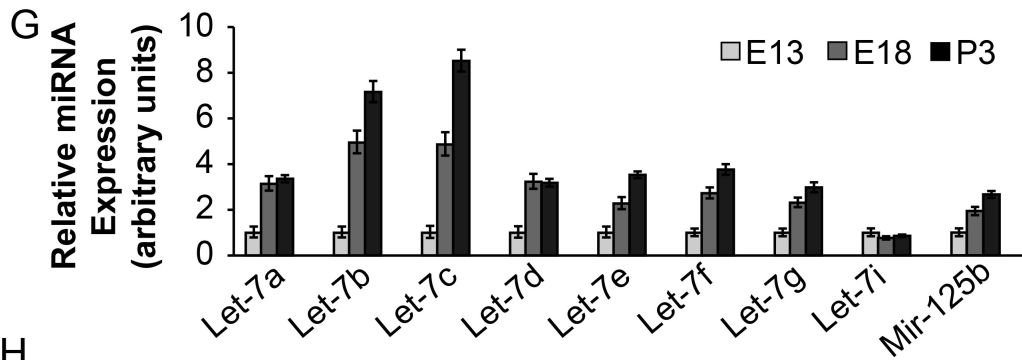
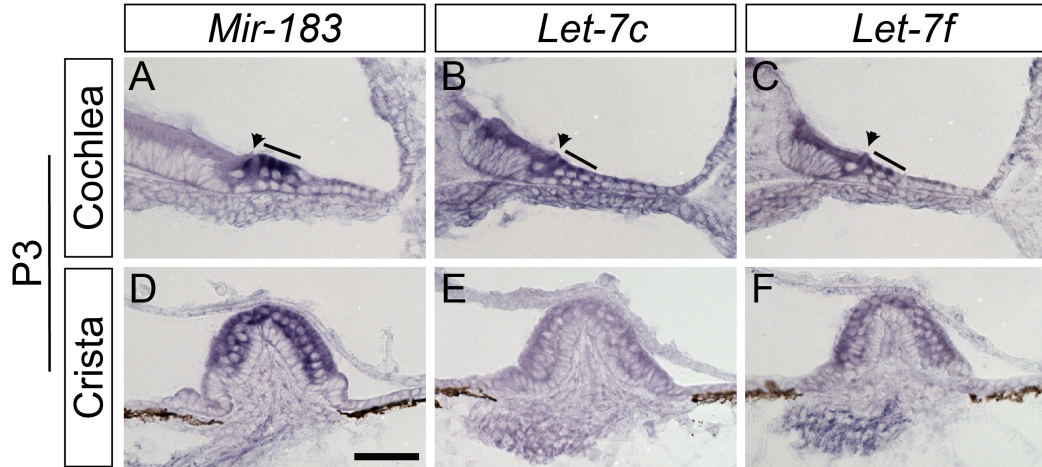


Figure 2.2: Let-7 miRNAs are upregulated in the differentiating cochlea. (A-F) ISH based analysis of *let-7c* and *let-7f* expression within the early postnatal (P3) cochlea (A-C) and vestibular crista (D-F). *Mir-183* (A, D) marks cochlear and vestibular HCs. Arrowheads and lines (A-C) indicate cochlear IHCs and OHCs. Scale bar, 50 μ m. **(G, H)** RT-qPCR analysis of mature *let-7* miRNA expression within the cochlear epithelium prior to (E13), during (E18) and following (P2) differentiation. The snoRNA *U6* was used as an endogenous control. Data in (G) are mean \pm SEM.



H

Gene	Stage	Δ CT	Gene	Stage	Δ CT	Gene	Stage	Δ CT
Let-7a	E13	9.00	Let-7d	E13	10.85	Let-7g	E13	8.725
	E18	7.35		E18	9.155		E18	7.515
	P3	7.25		P3	9.177		P3	7.15
Let-7b	E13	10.00	Let-7e	E13	6.335	Let-7i	E13	9.186
	E18	7.70		E18	5.148		E18	9.565
	P3	7.16		P3	4.515		P3	9.401
Let-7c	E13	8.79	Let-7f	E13	11.35	Mir-125b	E13	3.616
	E18	6.51		E18	9.905		E18	2.661
	P3	5.70		P3	9.442		P3	2.201

Figure 2.3: *LIN28B* overexpression in the embryonic cochlea. (A) The *iLIN28B* transgene, containing flag-tagged human LIN28B ORF driven by the tetracycline inducible promoter and the M2 reverse tetracycline transactivator (rtTA) transgene under control of the ubiquitously expressed *Rosa26* promoter were combined to drive global *LIN28B* expression (*Rosa26-iLIN28B*). **(B)** Doxycycline (dox) was administered to timed mated females by *ad libitum* access to feed containing 2 g dox/kg feed beginning at E8.5. This resulted in robust flag-tagged LIN28B protein overexpression within differentiated (E18) *Rosa26-iLIN28B* inner ears but not non-transgenic littermate controls. **(C-E)** Inner ear-specific overexpression of *LIN28B* was achieved using a trigenic approach. This rtTA line contained a floxed stop cassette between the *Rosa26* promoter and the rtTA. Crossing in *Pax2*-driven CRE recombinase confined *LIN28B* overexpression to the *Pax2*⁺ cells of the cochlear epithelium and spiral ganglion (*Pax2-iLIN28B*). **(D)** Dox administration beginning at E8.5 resulted in human LIN28B overexpression within differentiating (E15.5) *Pax2-iLIN28B* cochlear epithelia but not non-transgenic littermate controls. Endogenous mouse Lin28b protein expression was seen in both transgenic and non-transgenic epithelia. **(E)** ISH based analysis of *LIN28B* expression in E18.5 control and *Pax2-iLIN28B* cochleae. Dox administration was begun at E8.5. Numbers mark the basal (1), mid (2), and apical (3) cochlear turns. Arrow points to *LIN28B* expression within the spiral ganglion. Scale bar, 100 μ m. **(F)** RT-qPCR analysis of mature *let-7* miRNA expression in E14.5 control (grey) and *Pax2-iLIN28B* (red) cochlear epithelia. The snoRNA *U6* was used as an endogenous control. Data are mean \pm SEM (n = 3-5, *p<0.05).

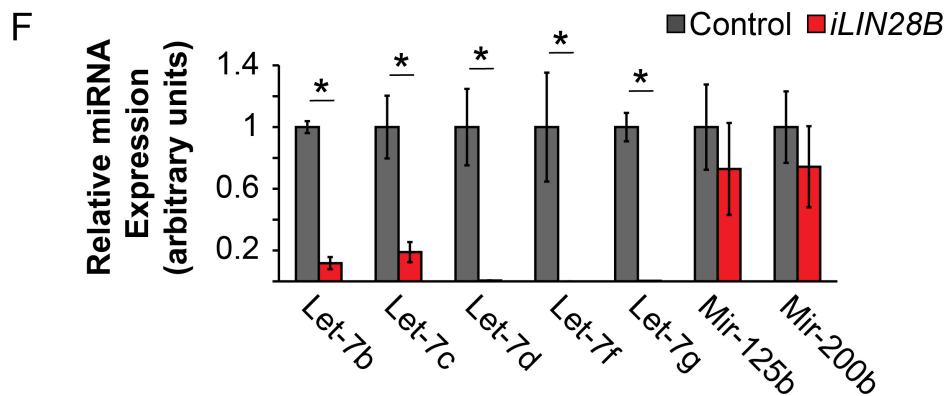
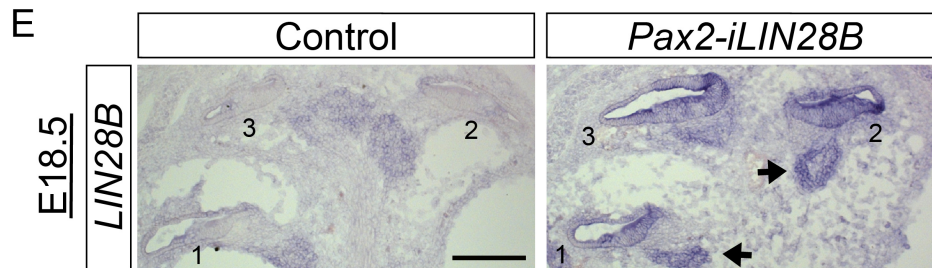
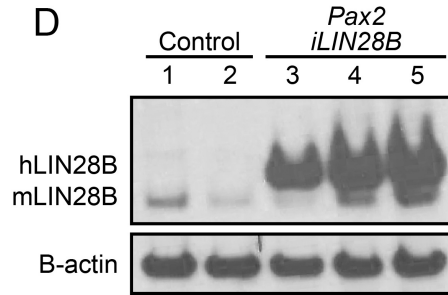
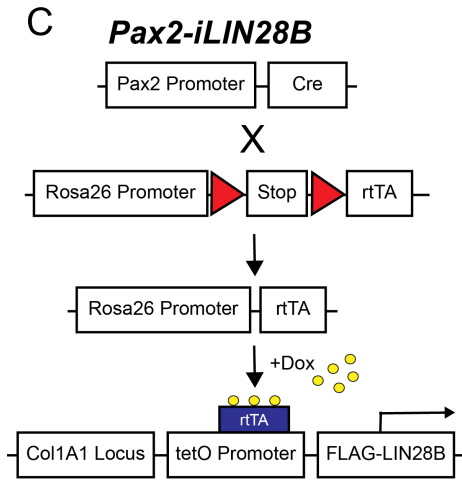
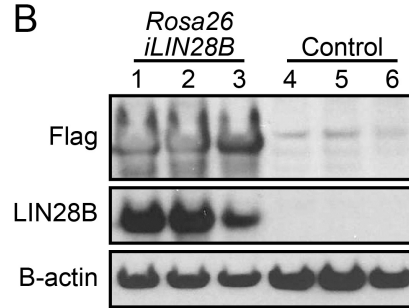
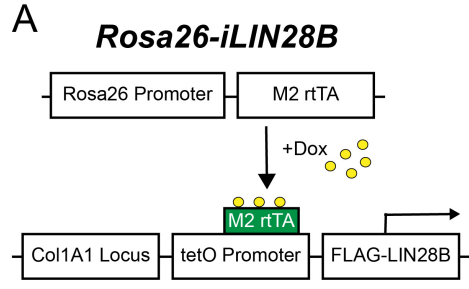


Figure 2.4: *LIN28B* overexpression delays auditory HC differentiation. (A) HC differentiation was monitored in control and *Rosa26-iLIN28B* cochlear explants, stage E13.0, over 3 days. (B-I) *Atoh1/nEGFP* reporter expression (EGFP, green) marks nascent HCs. Asterisks indicate EGFP expression within HCs of the vestibular sacculus. Scale bar, 200 μ m. (J) Length of the EGFP+ HC stripe was used to quantify the extent of HC differentiation in control versus *Rosa26-iLIN28B* cochlear cultures. Data expressed as mean \pm SEM (n = 5 animals per group, *p<0.05). (K) HC differentiation was analyzed in acutely isolated E15.5 *iLIN28b* and control cochlear ducts. (L, M) Low-powered images of E15.5 control and *Pax2-iLIN28B* cochlear ducts labeled with MYO6 (white). Red arrowheads indicate the IHC domain and yellow arrowheads indicate the OHC domain. Scale bar, 200 μ m. (N-S) Cross-sections through the basal, mid, and apical turns of control and *Pax2-iLIN28B* cochleae labeled with MYO6 (red) and p27/Kip1 (green). Scale bar, 50 μ m. (T, U) Analysis of acutely isolated E15.5 cochlear ducts (as demonstrated in L, M) from both the global *Rosa26-iLIN28B* line and inner ear-specific *Pax2-iLIN28B* line compared to their non-transgenic littermates (control). Data expressed as mean \pm SEM (n = 3-7 animals per group, *p<0.05, n.s. – not significant).

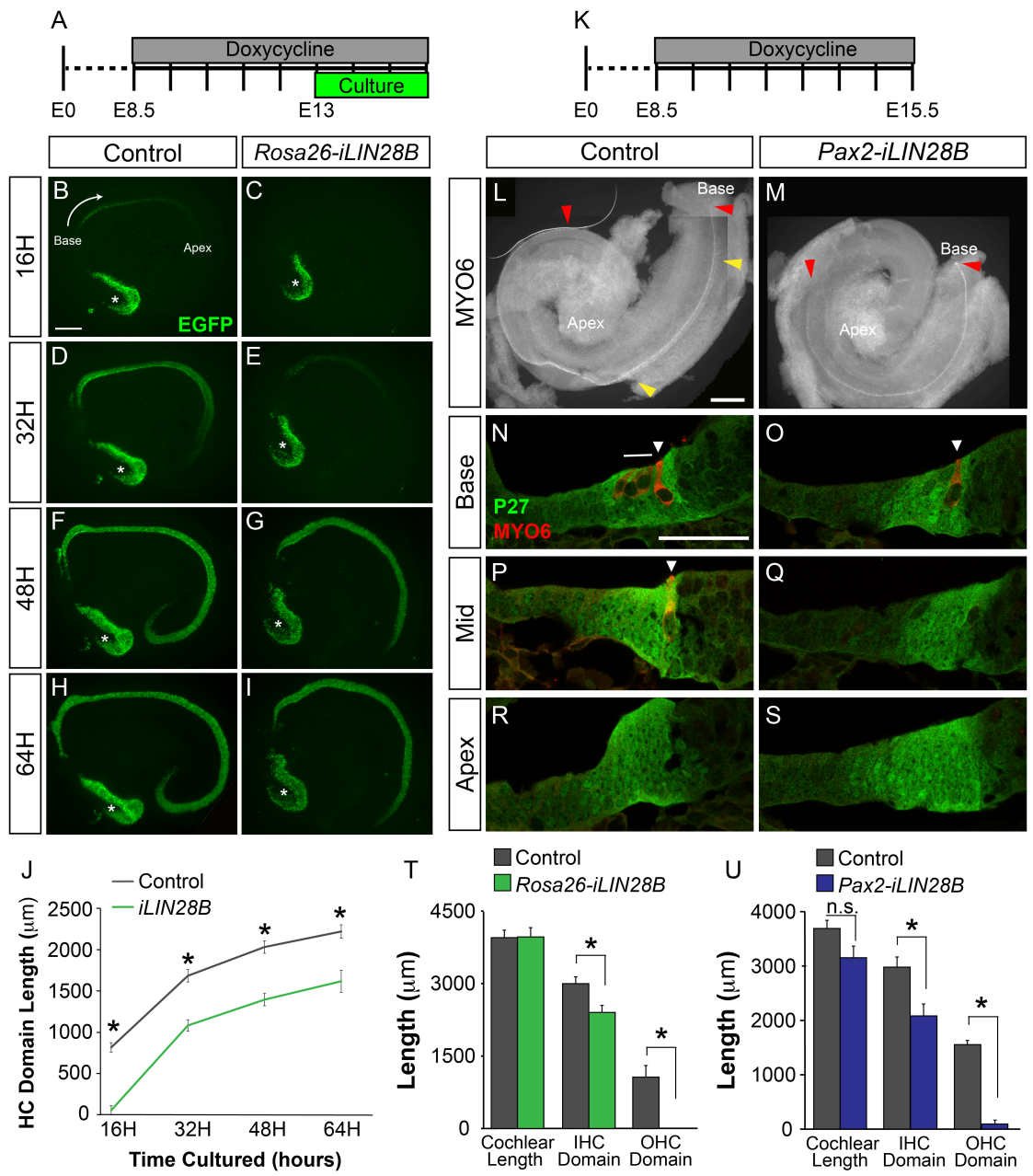


Figure 2.5: Acute LIN28B overexpression delays auditory HC differentiation. (A-C) Acute overexpression of *iLIN28B* slows the progression of HC differentiation. **(A)** LIN28B is overexpressed within the developing cochlea epithelium after 24 hours of dox administration. Dox-containing feed was given to timed-pregnant females beginning at E12.5. E13.5 control and *iLIN28B* cochlea epithelia were collected for analysis 24 hours later. **(B)** To monitor HC differentiation *in vitro*, *LIN28B* overexpression was induced at E12.5 and control and *Rosa26-iLIN28B* cochlear explants were cultured 12 hours later in dox-containing media. HC differentiation was monitored over the following 4 days using HC-specific *Atoh1/nEGFP* (EGFP) reporter expression. **(C)** Length of the EGFP+ HC stripe was used to quantify the extent of HC differentiation in control versus *Rosa26-iLIN28B* cochlear cultures. The grey box indicates the estimated time-point at which *LIN28B* overexpression reached a biologically relevant level. Data expressed as mean \pm SEM (n = 7-13, *p<0.01). **(D-H)** Lentiviral-driven overexpression of murine *Lin28b* delays HC differentiation. **(D)** Schematic of the experimental lentiviral construct, which contained ubiquitin promoter-driven murine *Lin28b* ORF linked to a *mCherry* reporter via an F2A linker sequence. The control lentiviral vector contained only mCherry. **(E)** E13.5 *Atoh1/nEGFP* cochlear explants were infected with either *Lin28b* or *mCherry* (control) lentivirus. HC differentiation (EGFP) and lentiviral driven protein expression (mCherry) were monitored over the following 3 days. **(F)** Western blot analysis of E13.5 cochlea explants infected with *Lin28b* or control lentivirus and cultured for 2 days. Treatment with control virus does not impede the downregulation of LIN28B during HC differentiation. **(G)** When infected with mCherry-containing lentivirus, 60-75% of HCs (MYO6+, green) expressed the fluorescent protein (red) within 48 hours. **(H)** Length of

the *Atoh1/nEGFP* HC stripe was used to quantify the extent of HC differentiation in control virus versus *Lin28b* virus-treated cultures. The grey box indicates the estimated time-point at which the lentiviral-driven *Lin28b* overexpression reached a biologically relevant level. Data expressed as mean \pm SEM (n = 4, *p<0.05).

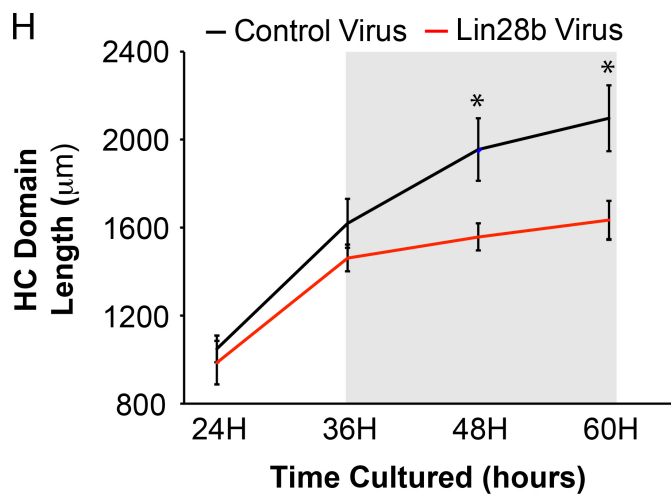
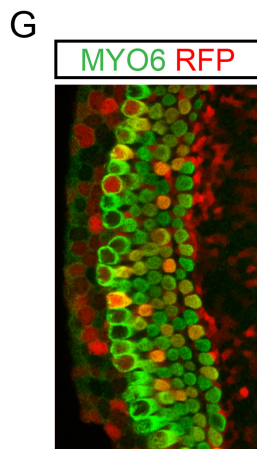
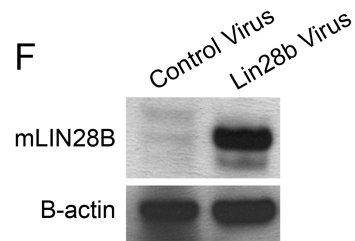
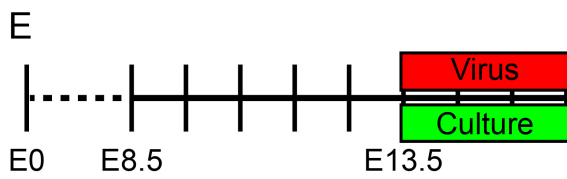
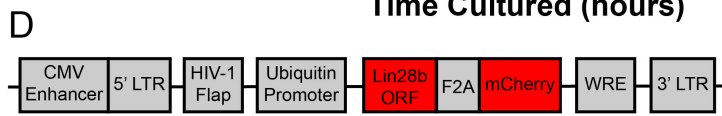
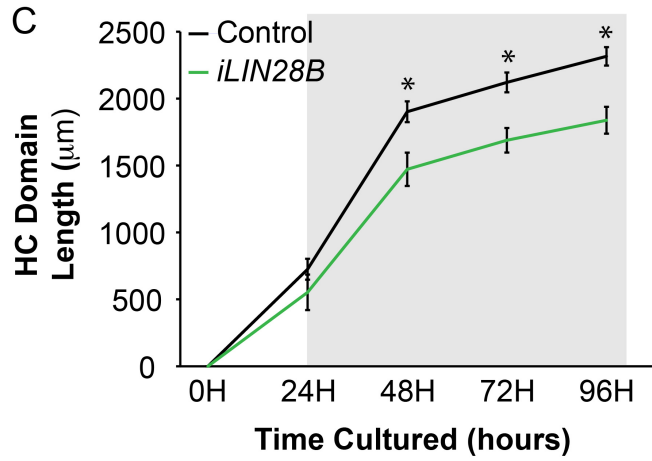
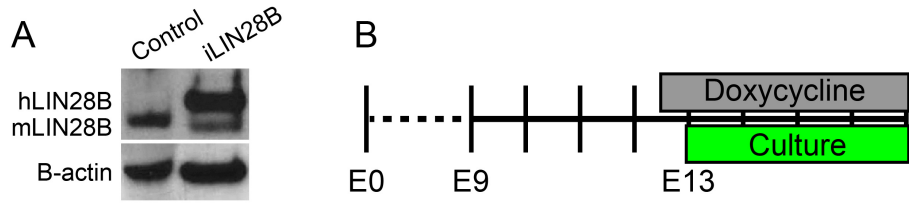


Figure 2.6: *LIN28B* overexpression delays progenitor cell cycle withdrawal and causes mis-patterning of the auditory sensory epithelium. (A-L) EdU incorporation (red) in HCs (MYO7a, blue) and SCs (SOX2, green) was analyzed at 18.5 following a single EdU pulse at E13.5. Shown are whole mount preparations of basal, mid, and apical cochlear segments from control and *Pax2-iLIN28B* inner ears. Yellow asterisks mark ectopic IHCs and dashes indicate missing OHCs. Scale bar, 50 μ m. **(M-O)** Quantification of HC-specific EdU incorporation in E18.5 control (grey) and *iLIN28B* (red) cochlear tissue following a single EdU pulse at E12.5 (M), a single EdU pulse at E13.5 (N), or once daily EdU pulses from E14.5 through E17.5 (O). Data expressed as mean \pm SEM (n = 2, *p<0.05). **(P, Q)** Cross-sections of E18.5 control and *Pax2-iLIN28B* cochleae. EdU (red) was given once daily from E14.5 through E17.5. HCs are marked by MYO7A (white) and SC subtypes are marked by P27 (green) and SOX2 (blue) immuno-staining. Scale bar, 50 μ m. Asterisk (Q) marks an ectopic SC disrupting the bi-layered patterning of the cochlear epithelia in an *iLIN28B* cochlea. **(R)** Quantification of HC and SC subtypes per cochlear cross-section in control (grey) and *iLIN28B* (red) cochleae. Data expressed as mean \pm SEM (n = 3 animals per group (5 cross sections per animal), *p<0.05). **(S)** RT-qPCR expression analysis of *let-7* target genes associated with growth and proliferation in E14.5 control (grey) and *iLIN28B* (red) cochlear epithelia. Data expressed as mean \pm SEM (n = 3, *p<0.05). Abbreviations: i – phalangeal cell, p – pillar cell, d – Deiter’s cell, h – Hensen’s cell.

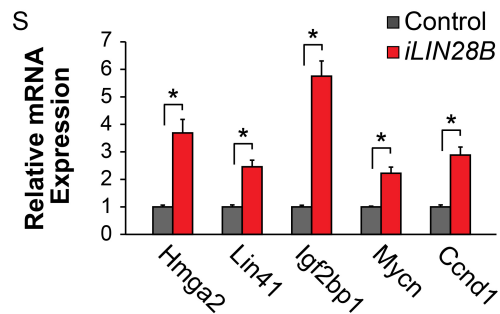
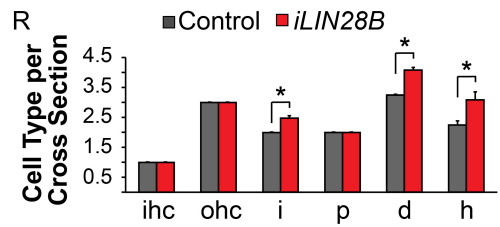
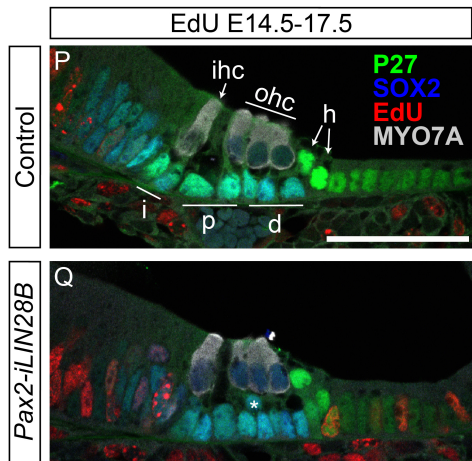
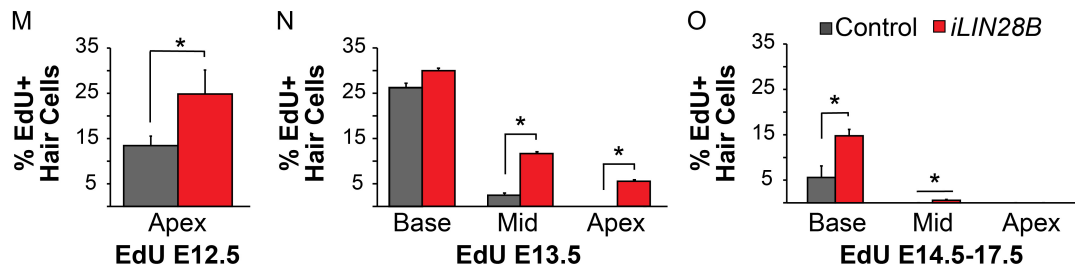
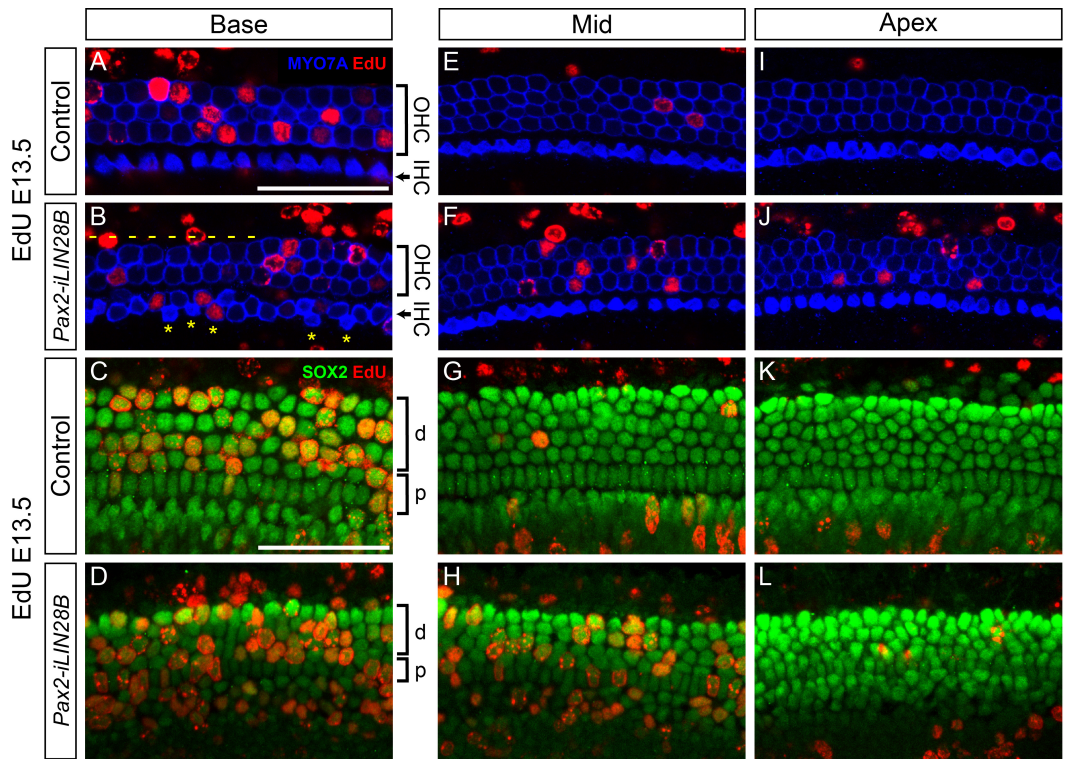


Figure 2.7: *LIN28B* overexpression delays progenitor cell cycle withdrawal and causes mis-patterning of the auditory sensory epithelium. (A-B) Cross-sections of E15.5 control and *Pax2-iLIN28B* cochleae. A single EdU pulse was given 3 hours prior to collecting. No EdU incorporation (red) was observed within the sensory domain (p27/Kip1, green) of control and *iLIN28B* cochleae. Scale bar, 50 μ m. **(C)** Length measurements of E18.5 control (grey) and *Pax2-iLIN28B* (red) cochlear ducts. Data expressed as mean \pm SEM (n = 14, n.s. – not significant) **(D-E)** Quantification of IHC (D) and OHC (E) density within control (grey) and *Pax2-iLIN28B* cochlear epithelia. Data expressed as mean \pm SEM (n = 5, *p<0.04). **(F)** Quantification of ectopic IHCs within the base, mid, and apex of control (grey) and *Pax2-iLIN28B* (red) cochlear epithelia. Data expressed as mean \pm SEM (n = 5, p<0.05). **(G)** Quantification of missing OHCs within the base, mid, and apex of control (grey) and *Pax2-iLIN28B* (red) cochlear epithelia. Data expressed as mean \pm SEM (n = 5, p<0.03). **(H-I)** Cross-sections through the mid-basal turn of E18.5 control and *Pax2-iLIN28B* cochlea. HCs are marked by *Atoh1/nEGFP* expression (green) and SCs are marked by S100 (red) and SOX2 (blue) immuno-staining. Scale bar, 50 μ m.

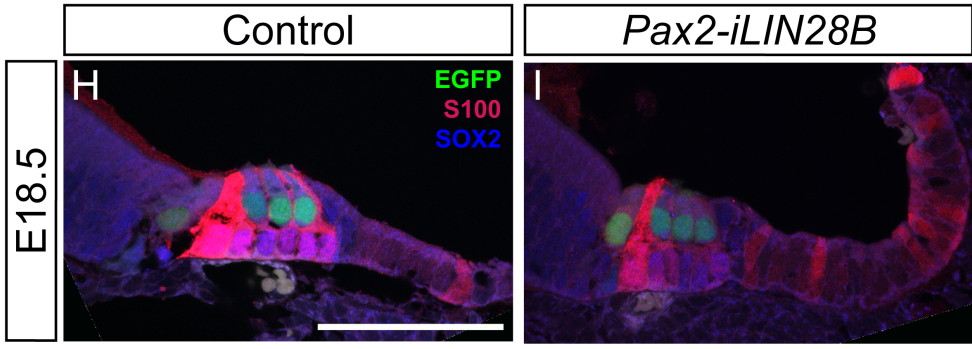
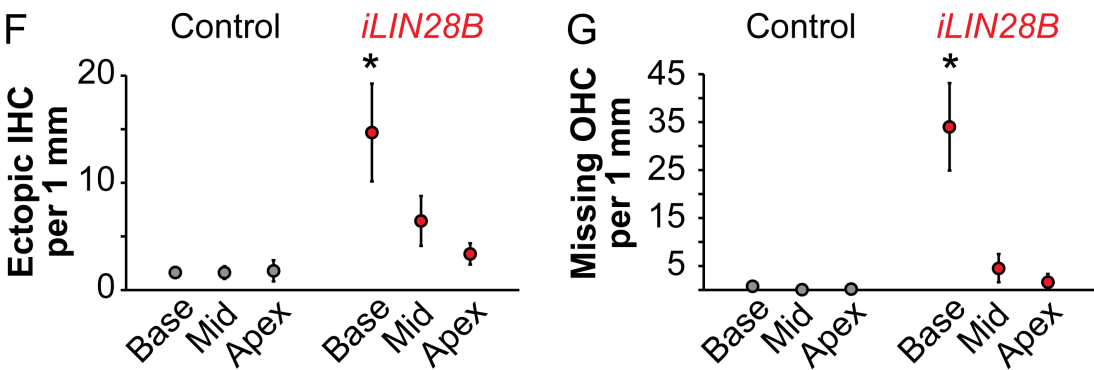
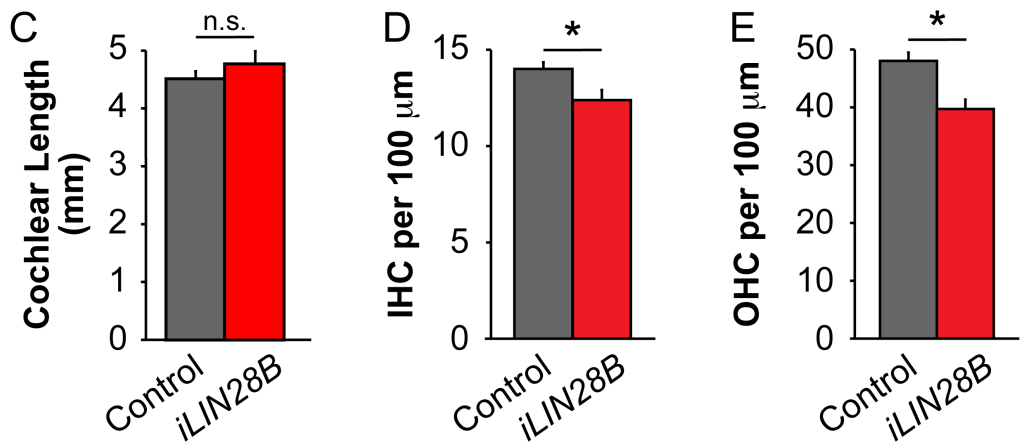
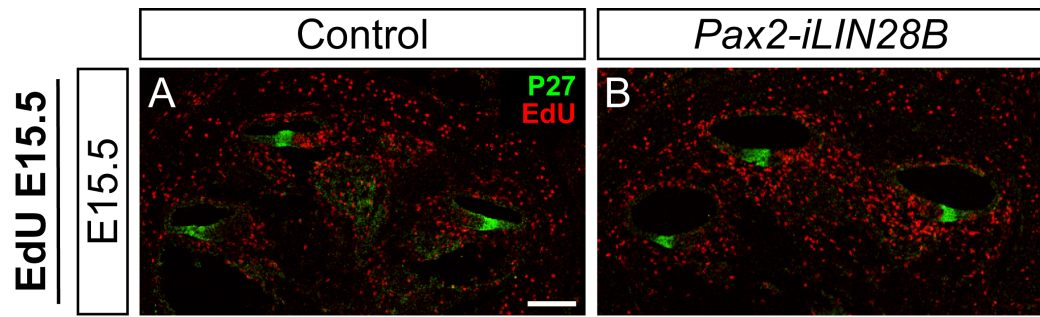


Figure 2.8: *Let-7* overexpression accelerates progenitor cell cycle withdrawal. (A) Schematic of the *iLet-7g* construct, which expresses a LIN28A/B-resistant form of *let-7g* driven by a tetracycline inducible promoter (*tetO*) within the *Coll1A1* locus (Zhu et al., 2011a). **(B)** RT-qPCR analysis showing that mature *let-7g* is specifically overexpressed within the cochlear epithelium of *iLet-7g* transgenic mice after doxycycline treatment. **(C-E)** *Let-7* targets are downregulated at the transcript or protein level following *iLet-7* overexpression **(C-D)** LIN28B protein levels in E13.5 control and *iLet-7* cochlear epithelia. Data expressed as mean \pm SEM (n = 2, *p<0.05). **(E)** Relative *Lin28b* and *Hmga2* transcript expression within E13.5 control (grey) and *iLet-7* (green) cochlear epithelia. Data expressed as mean \pm SEM (n = 3, *p<0.05). **(F-H')** Schematic and analysis of EdU pulse chase experiment. **(G-H')** Cross-sections of E14.5 control and *Pax2 iLet-7* cochleae. A single EdU pulse was given at E13.5 and EdU incorporation (green) within SOX2+ (red) prosensory progenitor cells was analyzed after 24 hours. High power images of the basal turn are shown in ('). Scale bar, 50 μ m. **(I)** Quantification of EdU incorporation (G-H'). Data expressed as mean \pm SEM (n = 2, *p<0.05).

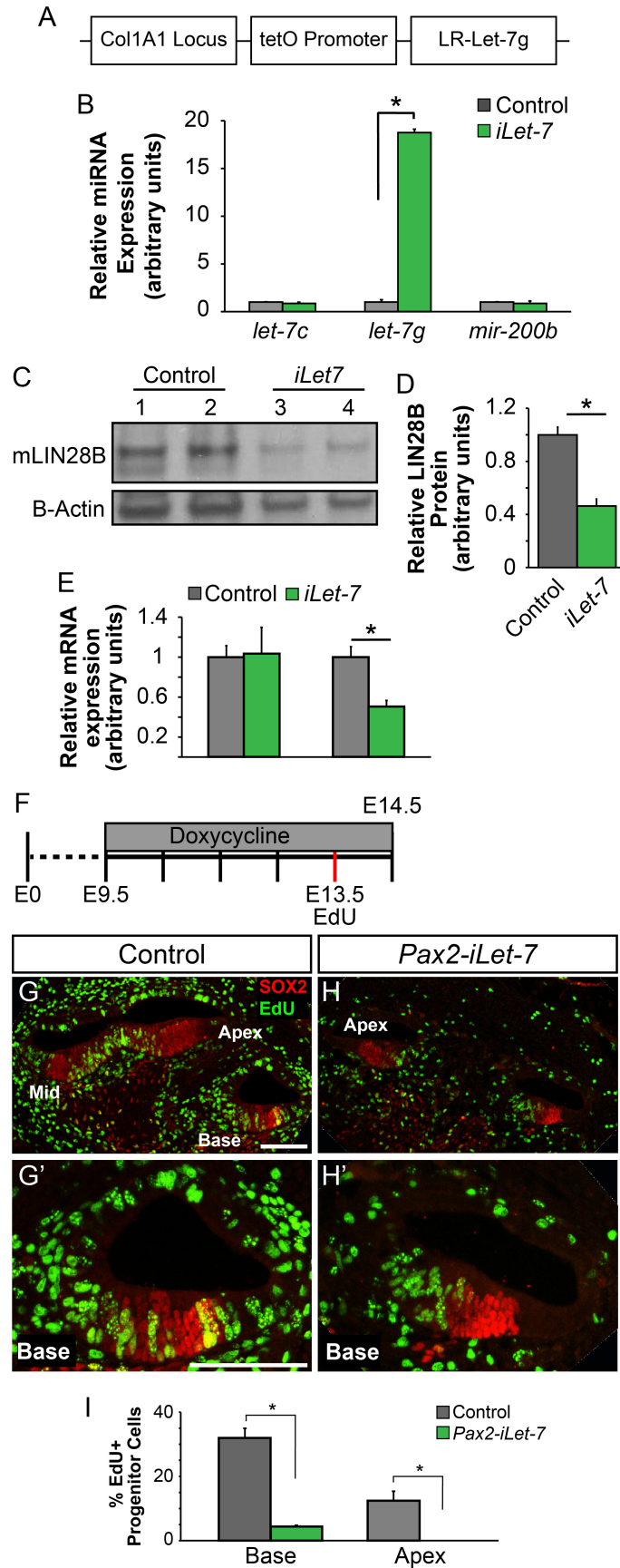
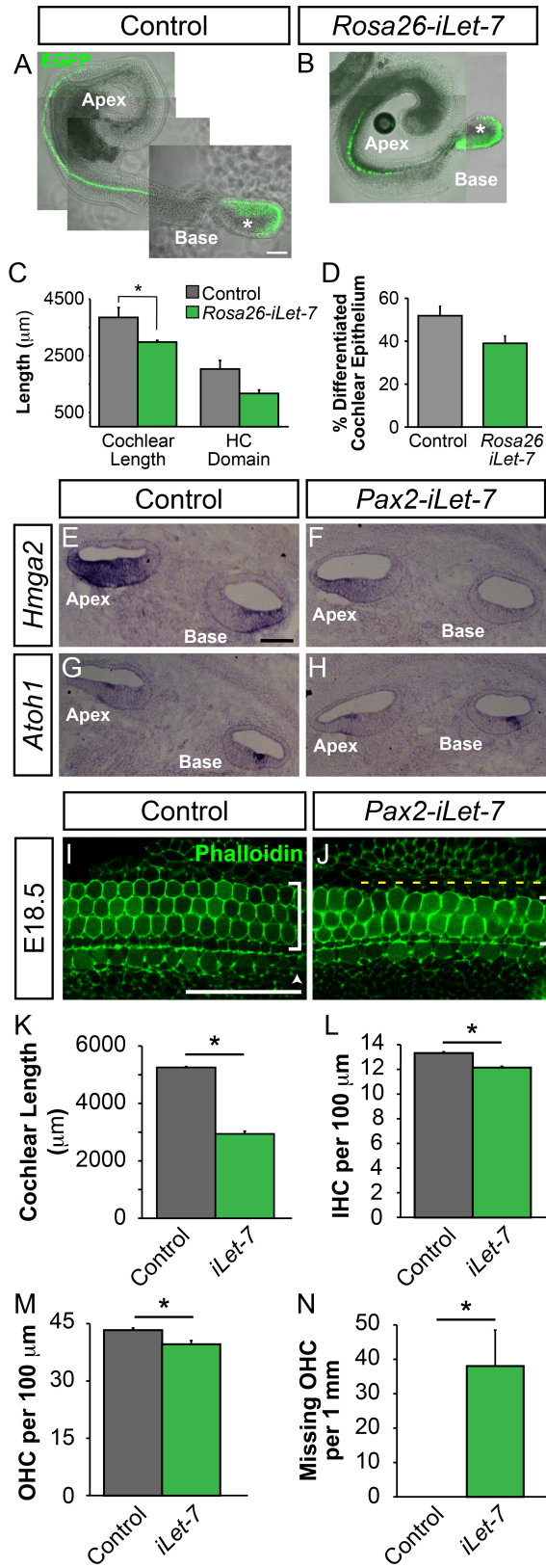


Figure 2.9: *Let-7* overexpression does not accelerate progenitor differentiation. (A-B) Bright field and green fluorescence image overlays of acutely isolated E14.5 control and *Rosa26 iLet-7* cochlear ducts. *Atoh1/nEGFP* reporter (EGFP, green) marks nascent HCs. Asterisks denote EGFP expression within HCs of the vestibular sacculus. Scale bar, 200 μ m. **(C-D)** Analysis of E14.5 control and *iLet-7* cochlear ducts shown in A-B. Data expressed as mean \pm SEM (n = 4, *p<0.05). **(E-H)** ISH based analysis of *Hmga2* (E, F) and *Atoh1* (G, H) expression in E14.5 Pax2 *iLet-7* and control cochlear tissue. Scale bar, 50 μ m. **(I, J)** HC phenotype in E18.5 control and Pax2 *iLet-7* cochlear whole mounts. HCs are marked by phalloidin (green). Shown is the basal turn. Arrowheads indicate IHC domain, brackets indicate OHC domain, and yellow dashes indicate missing OHCs. Scale bar, 50 μ m. **(K-N)** Quantification of cochlear duct length (K) HC density (L, M) and missing OHCs (N) in E18.5 *iLet-7* (green) and control (grey) cochlear epithelia. Data expressed as mean \pm SEM (n = 3, *p<0.05).



Chapter 3

Manipulation of the *Lin28b/let-7* axis modulates the capacity for supporting cell-to-hair cell conversion

INTRODUCTION

Unlike sensory cells of the olfactory and lingual epithelia, which undergo constant turnover throughout life, sensory cells of the mammalian auditory epithelium are only produced during embryonic development. The adult auditory epithelium is remarkably quiescent and lacks the ability to regenerate damaged HCs. Consequently, in mammals the effects of ototoxic injury (e.g. traumatic noise exposure and treatment with certain antibiotics or chemotherapeutics) are irreversible and lead to sensorineural hearing loss. Remarkably, this quiescence is not universal throughout the vertebrate lineage. Many species, including cartilaginous fish, reptiles, amphibians, and birds, are able to regenerate HCs, both as a part of normal cell maintenance and in response to trauma (Groves, 2010; Groves et al., 2013).

In non-mammalian vertebrates, HC loss triggers the de-differentiation of nearby SCs, which are able to replace lost HCs through two distinct mechanisms. First, SCs can trans-differentiate into HCs without re-entering the cell cycle. These SCs down-regulate their SC-specific genetic program and up-regulate HC-specific genes to directly switch their fate (Cafaro et al., 2007; Roberson et al., 2004; Stone and Cotanche, 2007). Several days after injury, HC regeneration switches to a mitotic process. De-differentiated SCs re-enter the cell cycle, generating precursors that give rise to both HCs and SCs (Corwin and Cotanche, 1988; Ryals and Rubel, 1988; Stone and Cotanche, 2007). It is not known why mammalian SCs lack the capacity to de-differentiate and regenerate HCs; however, this loss is generally associated with the epithelial specializations required for high frequency hearing (e.g. the development of distinct HC and SC subtypes and the resulting morphological complexity) (Groves, 2010).

Intriguingly, recent studies suggest that under certain permissive conditions mammalian SCs can function as progenitors and give rise to HCs. For instance, cultured SCs, purified from the early postnatal mouse cochleae, are able to generate Atoh1+ HCs through both mitotic and non-mitotic mechanisms. In these experiments, regenerative capacity was tightly correlated with the ability to down-regulate expression of the cell cycle dependent kinase inhibitor p27^{Kip1}. However, this capacity quickly declined over the first postnatal week and the ability for SCs to generate new HCs was completely lost by the second week of life (White et al., 2006).

Disruption of the Notch signaling pathway has also been found to stimulate mammalian HC regeneration. During embryonic development, activation of the Notch signaling cascade within a subset of prosensory progenitors restricts these cells to a SC fate (Brooker et al., 2006; Kiernan et al., 2005a; Lanford et al., 1999). However, differentiated SCs retain the capacity to become HCs, and pharmacological inhibition of Notch signaling results in the generation of new HCs primarily through direct trans-differentiation (Doetzlhofer et al., 2009; Korrapati et al., 2013a; Mizutari et al., 2013a; Yamamoto et al., 2006). There is also an age-dependent decline in the ability for Notch inhibition to stimulate SC-to-HC conversion, and in the adult cochlea only apically located SCs respond to Notch inhibition to infrequently generate HCs (Mizutari et al., 2013a).

It is not known why older mammalian SCs lose the capacity to generate HCs, but this association between juvenility and tissue repair is a common phenomena that is widespread across many species (Poss, 2010). Recently, two studies have suggested that *Lin28a/b* re-expression can counteract the age-related decline in cellular regeneration. In

both cases, *let-7* repression was necessary to mediate this effect, although *let-7* repression alone was not sufficient to enhance tissue repair (Shyh-Chang et al., 2013; Yuan et al., 2012). Intriguingly, *let-7* miRNAs are highly expressed in the adult newt inner ear, and become significantly downregulated during HC regeneration (Tsonis et al., 2007). Is *let-7* downregulation essential for SC de-differentiation and does the *Lin28b/let-7* axis mediate the regenerative capacity of the postnatal inner ear? To test this we overexpressed *LIN28B* or *let-7* and measured the capacity for HC generation in the absence of Notch signaling. We found that *LIN28B* overexpression significantly enhanced SC conversion, while *let-7* overexpression significantly impaired it. Future cochlear regeneration therapies will require a strict balance of SC de-differentiation, proliferation, and HC generation to successfully recapitulate a functional auditory epithelium. Our results indicate that manipulation of the *Lin28b/let-7* axis could help to achieve this equilibrium.

RESULTS

***LIN28B* re-expression promotes SC conversion in the absence of Notch signaling.**

To determine whether *LIN28B* re-expression might enhance SC plasticity, *LIN28B* was re-expressed in the late embryonic cochlea and the ability of SCs to generate new HCs in the absence of Notch signaling was analyzed in early postnatal (P2) cochlear explant cultures (Fig. 3.1 A). To block Notch signaling, explants were treated with the γ -secretase inhibitor DAPT, which broadly inhibits γ -secretase activity preventing cleavage of the Notch intracellular domain (NICD). Our analysis was limited to the cochlear mid-base where early postnatal SCs only infrequently convert to HCs in response to Notch inhibition (Doetzlhofer et al., 2009). In contrast to early embryonic *LIN28B* induction, late embryonic *LIN28B* induction did not alter the number or organization of HCs and SCs (Fig. 3.1 B-E; Control 50.8 ± 1.5 HCs/100 μ m and 55.1 ± 1.1 outer SCs/100 μ m, *iLIN28B* 51.5 ± 1.0 HCs/100 μ m and 54.9 ± 1.2 outer SCs/100 μ m, n = 2 per group). No difference in the number of HCs was observed in untreated control and *LIN28B* overexpressing cochlear explants after 3 days in culture (Fig. 3.1 F, G, L). Treatment with the γ -secretase inhibitor DAPT for 3 days significantly increased the number of MYO7A and *Atoh1/nEGFP* positive HCs in both control and *iLIN28B* explants (Fig. 3.1 H-L); however, *LIN28B* overexpressing explants generated significantly more new HCs than controls (Fig. 3.1 L, M). Interestingly, these newly generated HCs largely lacked EdU incorporation, suggesting that they originated from post-mitotic cells. Taken together, our findings suggest that *LIN28B* re-expression increased the frequency of direct SC-to-HC conversion in response to γ -secretase inhibition.

***Let-7* overexpression antagonizes SC conversion in the absence of Notch signaling.**

We next set out to determine whether *let-7* downregulation was necessary for SC-to-HC conversion. *Let-7* overexpression was induced in the late embryonic cochlea (E17.5) and HC generation in the absence of γ -secretase activity was measured in early postnatal (P2) cochlear explant cultures (Fig. 3.2 A). This time we limited our analysis to the cochlear mid-apex where early postnatal SCs readily convert to HCs when Notch signaling is inhibited (Doetzlhofer et al., 2009). *Let-7* overexpression in the late embryonic cochlea did not alter the number or organization of HCs and SCs (Fig. 3.2 B-E; Control 58.4 ± 1.9 HCs/100 μ m and 60.2 ± 1.1 outer SCs/100 μ m, *iLet-7* 56.1 ± 1.4 HCs/100 μ m and 57.5 ± 1.6 outer SCs/100 μ m, n = 2 per group) and no difference in the number of HCs was observed in untreated control and *let-7* overexpressing cochlear explants after 3 days in culture (Fig. 3.2 F, G, J). Strikingly, we found that *let-7* overexpression significantly decreased the number of MYO7A and *Atoh1/nEGFP* positive HCs that were generated following DAPT treatment (Fig. 3.2 H-K). While control explant cultures had a 96% increase in HCs following Notch inhibition, *iLet-7* cultures had only a 30% increase in HCs (Fig. 3.2 K; n = 4 Control, 5 *iLet-7*, p < 0.005). Thus, our findings suggest that *let-7* downregulation is necessary for SC-to-HC conversion and that *let-7* overexpression significantly antagonizes this process.

DISCUSSION

HC loss is among the leading causes of human deafness, since in contrast to non-mammalian vertebrates mammals are unable to regenerate damaged HCs. Thus, uncovering mechanisms that promote HC regeneration/repair within the mammalian inner ear remains a major focus within the auditory research community. For non-mammalian vertebrates, SCs are the main source of post-embryonic HC production and HC replenishment after trauma (Burns and Corwin, 2013). Strikingly, mammalian SCs can generate HCs under certain permissive conditions, such as Notch inhibition or Wnt over-stimulation, but this ability rapidly declines during the first week of life (Chai et al., 2012; Korrapati et al., 2013b; Mizutani et al., 2013b; Shi et al., 2013).

Here, we show that LIN28B re-activation in the early postnatal murine cochlea enhances the generation of new HCs in response to Notch inhibition, whereas *let-7* overexpression represses this ability. The vast majority of newly generated HCs in our LIN28B paradigm were generated by a non-mitotic process, suggesting that this increase in newly generated HCs was due to an increased number of SCs that converted into HCs in response to Notch inhibition. How does LIN28B re-expression alter the response of SCs? A recent study showed that LIN28A re-activation in adult mice boosts tissue repair by reprogramming cellular metabolism (Shyh-Chang et al., 2013) and it is possible that enhancement of oxidative SC metabolism had a positive effect on the ability of SCs to switch cell fate and convert into HCs. Alternatively, it is possible that LIN28B re-expression altered the differentiation state of SCs. For instance, in zebrafish, *Lin28* becomes reactivated in Müller glia after damage and promotes Müller glia de-differentiation and subsequent retina regeneration, at least in part by decreasing *let-7*

miRNA levels (Ramachandran et al., 2010). Indeed, *let-7* downregulation was found to be necessary but not sufficient to promote cellular regeneration in multiple models of murine tissue repair (Shyh-Chang et al., 2013) and *let-7* miRNAs become significantly downregulated in the adult newt inner ear during HC regeneration (Tsonis et al., 2007). Similarly, we found that maintained *let-7* expression significantly antagonized SC-to-HC conversion in the absence of Notch signaling, suggesting that *let-7* downregulation is necessary for cochlear SC de-differentiation in the murine cochlea.

We have found that *let-7* miRNAs are rapidly upregulated during differentiation of the murine cochlear epithelium and are highly expressed in early postnatal HCs and SCs. Could the *let-7* miRNAs contribute to the developmental decline in SC regenerative capacity? Previous findings suggest that *let-7* expression increases during maturation of the postnatal cochlea (Weston et al., 2006), although further experiments are needed to link this expression to the decline in regenerative capacity. Our preliminary data suggests that LIN28B overexpression, which significantly represses *let-7* expression, can enhance SC-to-HC conversion in the absence of Notch signaling during the second postnatal week of life. Future experiments will address how long this effect persists and whether SC-to-HC conversion can be stimulated *in vivo*.

MATERIALS AND METHODS

Mouse Breeding and Genotyping: For details on transgenic lines and genotyping see Chapter 2. To induce *iLIN28B* expression, doxycycline (dox) was delivered to time-mated females via ad libitum access to feed containing 2 grams of doxycycline per kilogram feed (Bioserv #F3893) starting at E15.5 and continuing until harvesting. To induce *iLet-7* expression, dox treatment was begun at E17.5. Embryonic development was considered as E0.5 on the day a mating plug was observed. Littermates expressing only the *M2-rtTA* transgene were used as controls.

Hair cell generation Assay: P2 cochlear surface preparations were cultured on SPI black membranes (SPI Supplies, Structure Probe) in DMEM-F12 (Life Technologies) containing 1x N2 supplement (Life Technologies), 5 ng/mL EGF (Sigma), 2.5 ng/mL FGF (Sigma), 100 U/mL penicillin (Sigma) and 10 μ g/mL doxycycline (Sigma). Experimental cultures were treated with 10 μ M DAPT (γ -secretase inhibitor IX, N-[N-(3,5-Difluorophenacetyl-L-alanyl)]-S-phenylglycine *t*-Butyl Ester, Calbiochem-EMD Biosciences) to block Notch signaling. Control cultures received DMSO (0.04%). Media was refreshed once at 24h and cultures were fixed at 72h. To monitor proliferation, explants were grown in the presence of 3 μ M EdU. For HC quantification, cochlear explant cultures were sub-divided in to four parts: apex (0 - 1500 μ M); mid apex (1500 - 3000 μ M); mid base (3000 - 4500 μ M); base (4500-5500). A sampling (4 per region) of high-power confocal z-stack images were taken through the HC and SC layers within these regions and HC density and proliferation were manually quantified using Imaris software (Bitplane) and ImageJ. HCs were identified by *MYO7A* and *Atoh1/nEGFP* co-expression (See Chapter 2 for details of immunostaining protocol).

Figure 3.1: *LIN28B* re-expression promotes supporting cell conversion in the absence of Notch signaling. (A) Schematic of HC proliferation assay. *LIN28B* overexpression was induced at E15.5 and *iLIN28B* and control cochlear explants were cultured in the presence of DAPT or DMSO starting at P2. SC-to-HC conversion was quantified after 3 DIV. **(B-E)** Late embryonic induction (E15.5) of the *iLIN28B* transgene does not impact HC or SC patterning and number. Shown are acutely isolated cochlea whole mounts from P2 control and Rosa26 *iLIN28B* animals. HCs are marked by *Atoh1/nEGFP* (green, B, C) and MYO7A (red, B, C) and SCs are marked by SOX2 (blue, D, E) Scale bar, 50 μm . **(F-K)** *LIN28B* overexpression promotes SC-to-HC conversion in the absence of Notch signaling. Shown are mid-basal segments of P2 control and *iLIN28B* cochlear explants after 3 days of DMSO (F, G) or DAPT (H-K) treatment. HCs are marked by *Atoh1/nEGFP* (green) and MYO7A (red) and SCs are marked by SOX2 (blue). Scale bar, 50 μm . **(L, M)** Quantification of F-K. Data expressed as mean \pm SEM (n = 3, *p<0.03).

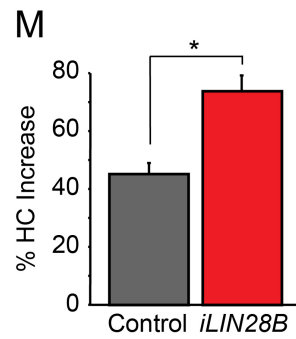
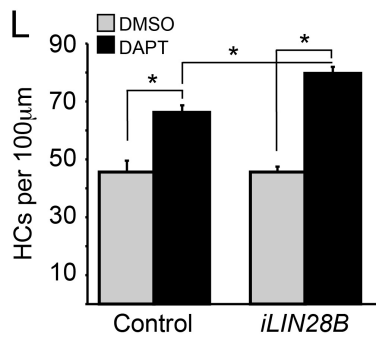
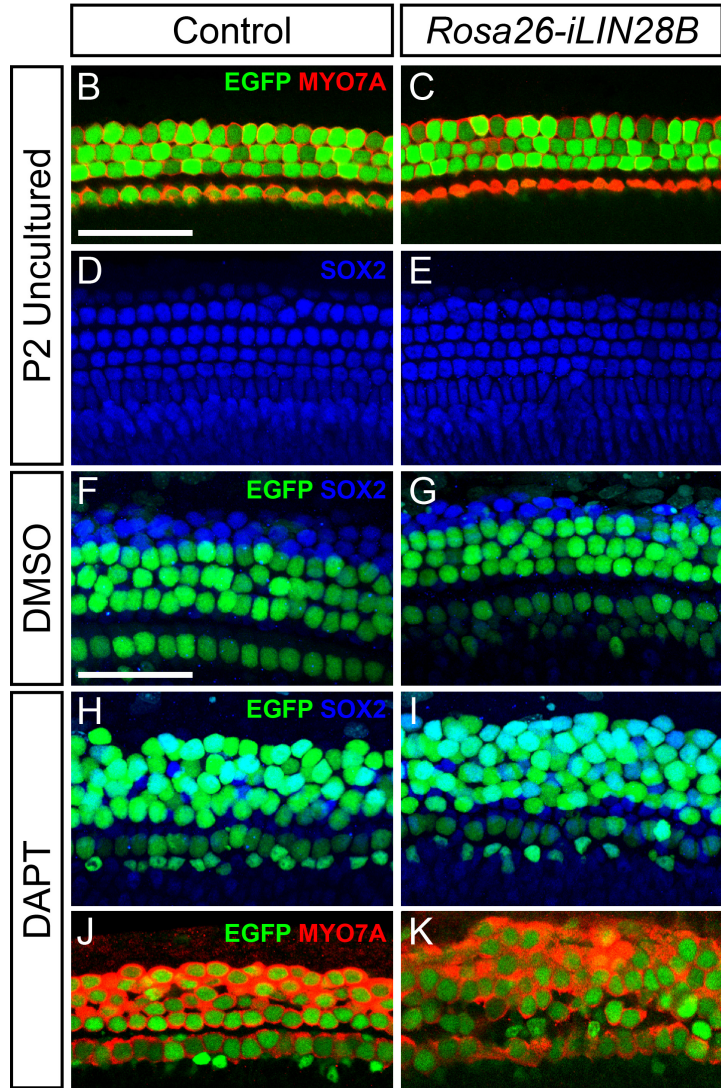
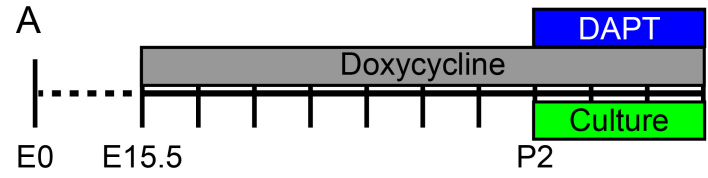
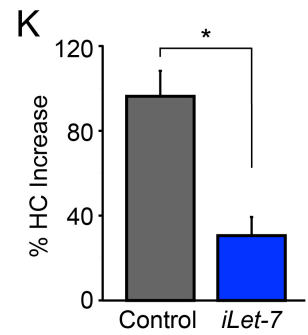
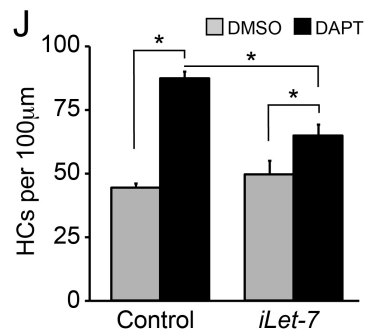
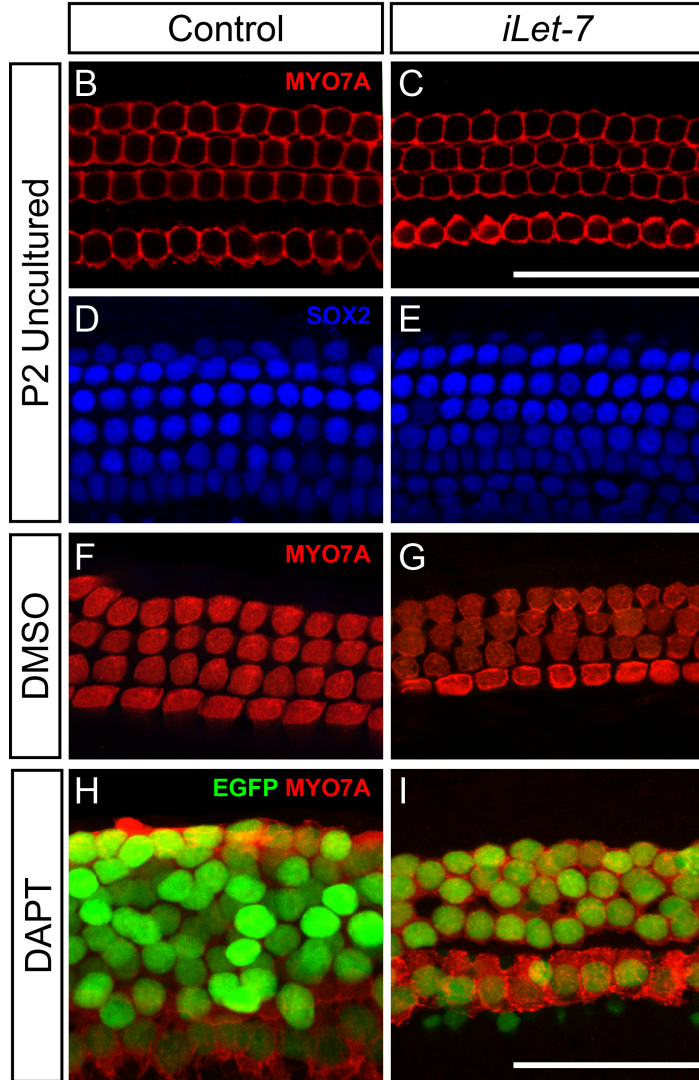
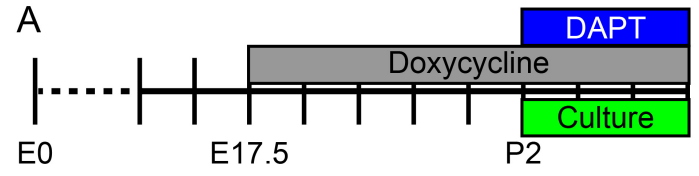


Figure 3.2: *Let-7* overexpression antagonizes supporting cell conversion in the absence of Notch signaling. (A) Schematic of HC proliferation assay. *Let-7* overexpression was induced at E17.5 and *iLet-7* and control cochlear explants were cultured in the presence of DAPT or DMSO starting at P2. SC-to-HC conversion was quantified after 3 DIV. (B-E) Late embryonic induction (E17.5) of the *iLet-7* transgene does not impact HC or SC patterning and number. Shown are acutely isolated cochlea whole mounts from P2 control and *iLet-7* animals. HCs are marked by MYO7A (red, B, C) and SCs are marked by SOX2 (blue, D, E) Scale bar, 50 μ m. (F-I) *Let-7* overexpression significantly antagonizes SC-to-HC conversion in the absence of Notch signaling. Shown are mid-apical segments of P2 control and *iLet-7* cochlear explants after 3 days of DMSO (F, G) or DAPT (H, I) treatment. HCs are marked by *Atoh1/nEGFP* (green) and MYO7A (red). Scale bar, 50 μ m. (J, K) Quantification of F-I. Data expressed as mean \pm SEM (n = 4-5 per group, *p \leq 0.02).



APPENDIX A:

Identification of LIN28B's mRNA targets in the differentiating cochlear epithelium

Several recent genome wide studies have revealed that LIN28A and LIN28B can directly alter the protein abundance of their mRNA targets through transcript stabilization and/or modulation of translational efficiency (Cho et al., 2012; Graf et al., 2013; Hafner et al., 2013; Peng et al., 2011; Wilbert et al., 2012). In order to identify these potential targets in the differentiating cochlea, we chose to characterize the gene expression profile of *Pax2-iLIN28B* overexpressing cochlear epithelia versus non-transgenic littermate controls. Because LIN28B is an RNA-binding protein, we reasoned that at least some of its effects would be reflected at the transcript level.

Our microarray study revealed a number of interesting transcript changes in response to LIN28B overexpression (Tables 1 and 2). While several *let-7* target genes appeared on this list, there were also a number of genes lacking putative *let-7* binding sites that may be direct targets of LIN28B. Among these genes are several morphogens and morphogen effectors, transcription factors, and RNA binding proteins. Functional analysis of gene pathways suggests that these altered transcripts are linked to many key processes including cellular assembly, protein synthesis, metabolism, and cell survival, among others (Table 3). qRT-PCR validation of our microarray hits is still underway, but so far many of the transcript changes appear to be upheld (Fig. A.1). In the future, we plan to use immunoprecipitation followed by qRT-PCR to determine whether LIN28B directly interacts with any of our candidate mRNAs.

EXPERIMENTAL DESIGN

Microarray Analysis: Timed pregnant females were administered dox feed (2 grams of doxycycline per kilogram feed) beginning at E11.5 and cochlea epithelia were obtained from E15.5 *Pax2-iLIN28B* (*iLIN28B* tg/+; *rtTA-EGFP* tg/+; *Pax2-Cre* tg/+) and non-transgenic control (*rtTA-EGFP* tg/+; *Pax2-Cre* tg/+) littermates. Total RNA was extracted using the miRNEasy Micro Kit (Qiagen) and submitted to the JHMI High Throughput Biology Deep Sequencing & Microarray Core (www.microarray.jhmi.edu) for profiling. Microarray experiments were performed on three biological replicate RNA samples for each condition (*Pax2-iLIN28B* versus control). Total RNA was labeled using Ambion® Expression WT kit (Life Technologies). Labeled RNA was hybridized onto GeneChip® Mouse Exon 1.0 ST Arrays (Affymetrix) and chips were scanned and analyzed according to manufactures instructions. GeneChip Expression Affymetrix CEL files were extracted and their data normalized with the Partek GS 6.6 platform (Partek Inc.) Partek's extended meta-probe set was used with RMA normalization to create quantile-normalized log₂ transcript signal values, which were used in subsequent ANOVA analyses. Reported here are transcripts that were more than 3 standard deviations up or down regulated with at least 12 total probes per gene. p-values ≤ 0.07 were considered significant.

Quantitative PCR Validation: Timed pregnant females were administered dox feed beginning at E8.5 and cochlea epithelia were obtained from E14.5 *Rosa26-iLIN28B* (*iLIN28B* tg/+; *M2-rtTA* tg/+) and non-transgenic control (*M2-rtTA* tg/+) littermates. Total RNA was extracted using the miRNEasy Micro Kit (Qiagen) and cDNA was reverse transcribed using the iScript cDNA synthesis kit (Bio-Rad). SYBR Green based

qPCR was performed using Fast SYBR® Green Master Mix reagent (Applied Biosystems, Life Technologies) and gene-specific primers. The ribosomal gene *Rpl19* was used as an endogenous reference gene. Relative gene expression was analyzed using the $\Delta\Delta$ CT method (Schmittgen and Livak, 2008).

Gene	Forward Primer	Reverse Primer
Rpl19	GGT CTG GTT GGA TCC CAA TG	CCC GGG AAT GGA CAG TCA
Igf2bp1	GGA GCA GAC CAG GCA AGC TA	GGG CAT GGT TCT CCA GTT GA
Trim10	GGC TCC TGA CGG ATA TCA GAA G	CGG GTT TCC GGC ACT TT
Shisa7	GATGTAGTGTCGCAGAGCGG	CTTGGGGCTGTTGACGTTGT
Fst	GAA AAC CTA CCG CAA CGA ATG	TCC GGC TGC TCT TTG CAT
Camk4	TGT TAA AGA AAA CAG TGG ACA AGA AGA	GGT GTG AGA GAC GCA GGA GAA
Npy	AGGTAACAAGCGAATGGGGC	GATGTAGTGTCGCAGAGCGG
Fabp7	GGA AGG TGG CAA AGT GGT GAT	TGG AAA TTG ATC TCT GTG TTC TTG A

Table 1: Transcripts upregulated by more than 3 standard deviations

<i>SD iLIN28B vs. Control Log2(FC)</i>	<i>Unique Gene Symbol (updated)</i>	<i>Gene AccID</i>	<i>iLIN28B vs. Cont (p-val)</i>	<i>Mean iLIN28B</i>	<i>Mean Control</i>	<i>iLIN28B vs. Cont paired (ratio)</i>
> +6σ	Penk	NM_001002927	0.004	8.62	7.41	2.31
+6σ	Igf2bp1	NM_009951	0.0001	9.94	9.01	1.90
+6σ	Trim10	NM_011280	0.026	7.57	6.70	1.82
+6σ	Zfp808	NM_001039239	0.013	8.24	7.49	1.69
+6σ	Shisa7	NM_172737	0.039	7.42	6.84	1.50
+6σ	Slc4a1	NM_011403	0.061	8.89	8.35	1.45
+6σ	Fst	NM_008046	0.008	9.21	8.70	1.43
+6σ	5730507C01Rik	BC150925	0.022	8.75	8.24	1.43
+6σ	Foxp2	NM_053242	0.002	7.71	7.22	1.40

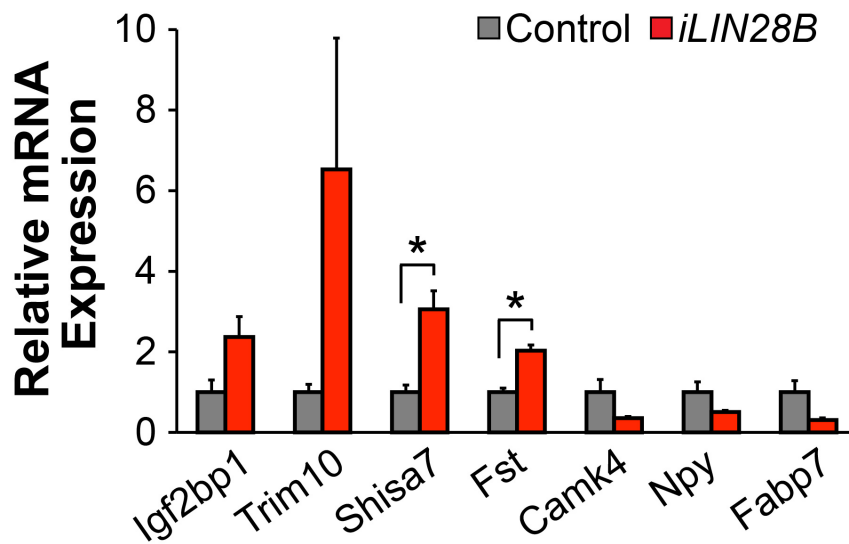
Table 2: Transcripts downregulated by more than 3 standard deviations

<i>SD iLIN28B vs. Control Log2(FC)</i>	<i>Unique Gene Symbol (updated)</i>	<i>Gene AccID</i>	<i>iLIN28B vs. Cont (p-val)</i>	<i>Mean iLIN28B</i>	<i>Mean Control</i>	<i>iLIN28B vs. Cont paired (ratio)</i>
-6σ	Cd300lh	NM_199201	0.013	8.58	9.58	0.50
-6σ	Gm11711	NM_001101657	0.010	8.55	9.51	0.51
-6σ	Spp1	NM_009263	0.032	6.41	7.28	0.55
-6σ	Cdhr1	NM_130878	0.069	6.63	7.44	0.57
-6σ	Gm11711	NM_001101657	0.006	8.53	9.35	0.57
-6σ	Nhlh1	NM_010916	0.050	6.53	7.31	0.58
-6σ	Camk4	NM_009793	0.051	7.11	7.85	0.60
-6σ	Npy	NM_023456	0.032	9.05	9.73	0.62
-6σ	Calb1	NM_009788	0.022	7.44	8.11	0.63
-6σ	Gpr64	NM_178712	0.060	7.87	8.52	0.64
-6σ	Fabp7	NM_021272	0.027	8.69	9.34	0.64
-6σ	Islr2	NM_001161536	0.008	6.54	7.17	0.64
-6σ	Kcnp4	NM_030265	0.003	5.47	6.06	0.67
-6σ	Slc44a5	NM_001081263	0.004	6.54	7.10	0.67
-6σ	Necab1	NM_178617	0.047	6.70	7.25	0.68
-6σ	Maob	NM_172778	0.008	7.39	7.94	0.68
-6σ	Kcnh5	NM_172805	0.001	6.13	6.65	0.70
-6σ	Cckar	NM_009827	0.066	6.68	7.17	0.71

Table 3: Gene pathway categories and functional annotations

<i>Categories</i>	<i>Diseases or Functions Annotation</i>	<i>p-Value</i>
Cellular Assembly and Organization, Cellular Function and Maintenance, Nervous System Development and Function	Quantity of axons	2.10E-04
Neurological Disease, Psychological Disorders	Tauopathy	5.56E-04
Endocrine System Disorders, Gastrointestinal Disease, Metabolic Disease	Diabetes mellitus	7.91E-04
Protein Synthesis	Synthesis of protein	1.37E-03
Metabolic Disease, Neurological Disease, Psychological Disorders	Alzheimer's disease	1.44E-03
Nervous System Development and Function, Tissue Development	Accumulation of neurons	1.45E-03
Lipid Metabolism, Small Molecule Biochemistry	Redistribution of glycolipid	1.52E-03
Cell Morphology, Cellular Assembly and Organization, Nervous System Development and Function	Size of axons	1.52E-03
Cell Death and Survival, Nervous System Development and Function	Survival of sensory neurons	1.79E-03
Cell Morphology, Cellular Assembly and Organization, Cellular Development, Cellular Function and Maintenance, Nervous System Development and Function, Tissue Development	Axonogenesis	1.81E-03

Figure A.1: qRT-PCR validation of the *iLIN28B* microarray. Gene hits from the *iLIN28B* microarray were validated using SYBR Green-based qRT-PCR with gene specific primers in E14.5 control (grey) and *iLIN28B* (red) cochlear epithelia. Data expressed as mean \pm SEM (n = 4, *p<0.05).



REFERENCES:

Ambros, V., Horvitz, H.R., 1984. Heterochronic mutants of the nematode *Caenorhabditis elegans*. *Science* 226, 409-416.

Avraham, K.B., Hasson, T., Steel, K.P., Kingsley, D.M., Russell, L.B., Mooseker, M.S., Copeland, N.G., Jenkins, N.A., 1995. The mouse Snell's waltzer deafness gene encodes an unconventional myosin required for structural integrity of inner ear hair cells. *Nature genetics* 11, 369-375.

Balzer, E., Heine, C., Jiang, Q., Lee, V.M., Moss, E.G., 2010. LIN28 alters cell fate succession and acts independently of the let-7 microRNA during neurogenesis in vitro. *Development* 137, 891-900.

Benito-Gonzalez, A., Doetzlhofer, A., 2014. Hey1 and Hey2 control the spatial and temporal pattern of mammalian auditory hair cell differentiation downstream of Hedgehog signaling. *The Journal of neuroscience : the official journal of the Society for Neuroscience* 34, 12865-12876.

Bermingham, N.A., Hassan, B.A., Price, S.D., Vollrath, M.A., Ben-Arie, N., Eatock, R.A., Bellen, H.J., Lysakowski, A., Zoghbi, H.Y., 1999. Math1: an essential gene for the generation of inner ear hair cells. *Science* 284, 1837-1841.

Bok, J., Zenczak, C., Hwang, C.H., Wu, D.K., 2013. Auditory ganglion source of Sonic hedgehog regulates timing of cell cycle exit and differentiation of mammalian cochlear hair cells. *Proceedings of the National Academy of Sciences of the United States of America* 110, 13869-13874.

Brooker, R., Hozumi, K., Lewis, J., 2006. Notch ligands with contrasting functions: Jagged1 and Delta1 in the mouse inner ear. *Development* 133, 1277-1286.

Buechner, J., Tomte, E., Haug, B.H., Henriksen, J.R., Lokke, C., Flaegstad, T., Einvik, C., 2011. Tumour-suppressor microRNAs let-7 and mir-101 target the proto-oncogene MYCN and inhibit cell proliferation in MYCN-amplified neuroblastoma. *British journal of cancer* 105, 296-303.

Burns, J.C., Corwin, J.T., 2013. A historical to present-day account of efforts to answer the question: "what puts the brakes on mammalian hair cell regeneration?". *Hearing research* 297, 52-67.

Cafaro, J., Lee, G.S., Stone, J.S., 2007. Atoh1 expression defines activated progenitors and differentiating hair cells during avian hair cell regeneration. *Developmental dynamics : an official publication of the American Association of Anatomists* 236, 156-170.

Cepko, C., 2014. Intrinsically different retinal progenitor cells produce specific types of progeny. *Nature reviews. Neuroscience* 15, 615-627.

- Chai, R., Kuo, B., Wang, T., Liaw, E.J., Xia, A., Jan, T.A., Liu, Z., Taketo, M.M., Oghalai, J.S., Nusse, R., Zuo, J., Cheng, A.G., 2012. Wnt signaling induces proliferation of sensory precursors in the postnatal mouse cochlea. *Proceedings of the National Academy of Sciences of the United States of America* 109, 8167-8172.
- Chen, P., Johnson, J.E., Zoghbi, H.Y., Segil, N., 2002. The role of Math1 in inner ear development: Uncoupling the establishment of the sensory primordium from hair cell fate determination. *Development* 129, 2495-2505.
- Chen, P., Segil, N., 1999. p27(Kip1) links cell proliferation to morphogenesis in the developing organ of Corti. *Development (Cambridge, England)* 126, 1581-1590.
- Cho, J., Chang, H., Kwon, S.C., Kim, B., Kim, Y., Choe, J., Ha, M., Kim, Y.K., Kim, V.N., 2012. LIN28A is a suppressor of ER-associated translation in embryonic stem cells. *Cell* 151, 765-777.
- Corwin, J.T., Cotanche, D.A., 1988. Regeneration of sensory hair cells after acoustic trauma. *Science* 240, 1772-1774.
- Costa, M.R., Muller, U., 2014. Specification of excitatory neurons in the developing cerebral cortex: progenitor diversity and environmental influences. *Frontiers in cellular neuroscience* 8, 449.
- Dabdoub, A., Puligilla, C., Jones, J.M., Fritsch, B., Cheah, K.S., Pevny, L.H., Kelley, M.W., 2008. Sox2 signaling in prosensory domain specification and subsequent hair cell differentiation in the developing cochlea. *Proceedings of the National Academy of Sciences of the United States of America* 105, 18396-18401.
- Doetzlhofer, A., Basch, M.L., Ohyama, T., Gessler, M., Groves, A.K., Segil, N., 2009. Hey2 regulation by FGF provides a Notch-independent mechanism for maintaining pillar cell fate in the organ of Corti. *Developmental cell* 16, 58-69.
- Dominguez-Frutos, E., Lopez-Hernandez, I., Vendrell, V., Neves, J., Gallozzi, M., Gutsche, K., Quintana, L., Sharpe, J., Knoepfler, P.S., Eisenman, R.N., Trumpp, A., Giraldez, F., Schimmang, T., 2011. N-myc controls proliferation, morphogenesis, and patterning of the inner ear. *The Journal of neuroscience : the official journal of the Society for Neuroscience* 31, 7178-7189.
- Driver, E.C., Pryor, S.P., Hill, P., Turner, J., Ruther, U., Biesecker, L.G., Griffith, A.J., Kelley, M.W., 2008. Hedgehog signaling regulates sensory cell formation and auditory function in mice and humans. *The Journal of neuroscience : the official journal of the Society for Neuroscience* 28, 7350-7358.
- Ecsedi, M., Grosshans, H., 2013. LIN-41/TRIM71: emancipation of a miRNA target. *Genes & development* 27, 581-589.

- Graf, R., Munschauer, M., Mastrobuoni, G., Mayr, F., Heinemann, U., Kempa, S., Rajewsky, N., Landthaler, M., 2013. Identification of LIN28B-bound mRNAs reveals features of target recognition and regulation. *RNA biology* 10.
- Groves, A.K., 2010. The challenge of hair cell regeneration. *Experimental biology and medicine* 235, 434-446.
- Groves, A.K., Zhang, K.D., Fekete, D.M., 2013. The genetics of hair cell development and regeneration. *Annual review of neuroscience* 36, 361-381.
- Guo, Y., Chen, Y., Ito, H., Watanabe, A., Ge, X., Kodama, T., Aburatani, H., 2006. Identification and characterization of lin-28 homolog B (LIN28B) in human hepatocellular carcinoma. *Gene* 384, 51-61.
- Hafner, M., Max, K.E., Bandaru, P., Morozov, P., Gerstberger, S., Brown, M., Molina, H., Tuschl, T., 2013. Identification of mRNAs bound and regulated by human LIN28 proteins and molecular requirements for RNA recognition. *RNA* 19, 613-626.
- Hasson, T., Gillespie, P.G., Garcia, J.A., MacDonald, R.B., Zhao, Y., Yee, A.G., Mooseker, M.S., Corey, D.P., 1997. Unconventional myosins in inner-ear sensory epithelia. *The Journal of cell biology* 137, 1287-1307.
- Heo, I., Joo, C., Cho, J., Ha, M., Han, J., Kim, V.N., 2008. Lin28 mediates the terminal uridylation of let-7 precursor MicroRNA. *Molecular cell* 32, 276-284.
- Huang, Y., 2012. A mirror of two faces: Lin28 as a master regulator of both miRNA and mRNA. *Wiley interdisciplinary reviews. RNA* 3, 483-494.
- Johnson, S.M., Grosshans, H., Shingara, J., Byrom, M., Jarvis, R., Cheng, A., Labourier, E., Reinert, K.L., Brown, D., Slack, F.J., 2005. RAS is regulated by the let-7 microRNA family. *Cell* 120, 635-647.
- Kelley, M.W., 2006. Regulation of cell fate in the sensory epithelia of the inner ear. *Nature reviews. Neuroscience* 7, 837-849.
- Kiernan, A.E., Cordes, R., Kopan, R., Gossler, A., Gridley, T., 2005a. The Notch ligands DLL1 and JAG2 act synergistically to regulate hair cell development in the mammalian inner ear. *Development* 132, 4353-4362.
- Kiernan, A.E., Pelling, A.L., Leung, K.K., Tang, A.S., Bell, D.M., Tease, C., Lovell-Badge, R., Steel, K.P., Cheah, K.S., 2005b. Sox2 is required for sensory organ development in the mammalian inner ear. *Nature* 434, 1031-1035.
- Klump, H., Schiedlmeier, B., Vogt, B., Ryan, M., Ostertag, W., Baum, C., 2001. Retroviral vector-mediated expression of HoxB4 in hematopoietic cells using a novel coexpression strategy. *Gene therapy* 8, 811-817.

Knoepfler, P.S., Cheng, P.F., Eisenman, R.N., 2002. N-myc is essential during neurogenesis for the rapid expansion of progenitor cell populations and the inhibition of neuronal differentiation. *Genes & development* 16, 2699-2712.

Kopecky, B., Fritzsche, B., 2012. The myc road to hearing restoration. *Cells* 1, 667-698.

Kopecky, B., Santi, P., Johnson, S., Schmitz, H., Fritzsche, B., 2011. Conditional Deletion of N-Myc Disrupts Neurosensory and Non-Sensory Development of the Ear. *Dev Dynam* 240, 1373-1390.

Korrapati, S., Roux, I., Glowatzki, E., Doetzlhofer, A., 2013. Notch signaling limits supporting cell plasticity in the hair cell-damaged early postnatal murine cochlea. *PLoS one* 8, e73276.

La Torre, A., Georgi, S., Reh, T.A., 2013. Conserved microRNA pathway regulates developmental timing of retinal neurogenesis. *Proceedings of the National Academy of Sciences of the United States of America* 110, E2362-2370.

Lagos-Quintana, M., Rauhut, R., Yalcin, A., Meyer, J., Lendeckel, W., Tuschl, T., 2002. Identification of tissue-specific microRNAs from mouse. *Current biology : CB* 12, 735-739.

Laine, H., Sulg, M., Kirjavainen, A., Pirvola, U., 2010. Cell cycle regulation in the inner ear sensory epithelia: Role of cyclin D1 and cyclin-dependent kinase inhibitors. *Developmental biology* 337, 134-146.

Lanford, P.J., Lan, Y., Jiang, R., Lindsell, C., Weinmaster, G., Gridley, T., Kelley, M.W., 1999. Notch signalling pathway mediates hair cell development in mammalian cochlea. *Nature genetics* 21, 289-292.

Lee, Y.S., Dutta, A., 2007. The tumor suppressor microRNA let-7 represses the HMGA2 oncogene. *Genes & development* 21, 1025-1030.

Lee, Y.S., Liu, F., Segil, N., 2006. A morphogenetic wave of p27Kip1 transcription directs cell cycle exit during organ of Corti development. *Development* 133, 2817-2826.

Lin, Y.C., Hsieh, L.C., Kuo, M.W., Yu, J., Kuo, H.H., Lo, W.L., Lin, R.J., Yu, A.L., Li, W.H., 2007. Human TRIM71 and its nematode homologue are targets of let-7 MicroRNA and its zebrafish orthologue is essential for development. *Molecular biology and evolution* 24, 2525-2534.

Liu, Z., Owen, T., Zhang, L., Zuo, J., 2010. Dynamic expression pattern of Sonic hedgehog in developing cochlear spiral ganglion neurons. *Developmental dynamics : an official publication of the American Association of Anatomists* 239, 1674-1683.

Livesey, F.J., Cepko, C.L., 2001. Vertebrate neural cell-fate determination: lessons from the retina. *Nature reviews. Neuroscience* 2, 109-118.

Lois, C., Hong, E.J., Pease, S., Brown, E.J., Baltimore, D., 2002. Germline transmission and tissue-specific expression of transgenes delivered by lentiviral vectors. *Science* 295, 868-872.

Lumpkin, E.A., Collisson, T., Parab, P., Moer-Abdalla, A., Haeberle, H., Chen, P., Doetzlhofer, A., White, P., Groves, A., Segil, N., Johnson, J.E., 2003. Math1-driven GFP expression in the developing nervous system of transgenic mice. *Gene Expr Patterns* 3, 389-395.

Mayr, C., Hemann, M.T., Bartel, D.P., 2007. Disrupting the pairing between let-7 and Hmga2 enhances oncogenic transformation. *Science* 315, 1576-1579.

McConnell, S.K., Kaznowski, C.E., 1991. Cell cycle dependence of laminar determination in developing neocortex. *Science* 254, 282-285.

Mizutari, K., Fujioka, M., Hosoya, M., Bramhall, N., Okano, H.J., Okano, H., Edge, A.S., 2013. Notch inhibition induces cochlear hair cell regeneration and recovery of hearing after acoustic trauma. *Neuron* 77, 58-69.

Molenaar, J.J., Domingo-Fernandez, R., Ebus, M.E., Lindner, S., Koster, J., Drabek, K., Mestdagh, P., van Sluis, P., Valentijn, L.J., van Nes, J., Broekmans, M., Haneveld, F., Volckmann, R., Bray, I., Heukamp, L., Sprussel, A., Thor, T., Kieckbusch, K., Klein-Hitpass, L., Fischer, M., Vandesompele, J., Schramm, A., van Noesel, M.M., Varesio, L., Speleman, F., Eggert, A., Stallings, R.L., Caron, H.N., Versteeg, R., Schulte, J.H., 2012. LIN28B induces neuroblastoma and enhances MYCN levels via let-7 suppression. *Nature genetics* 44, 1199-1206.

Moss, E.G., 2007. Heterochronic genes and the nature of developmental time. *Current biology* : CB 17, R425-434.

Moss, E.G., Tang, L., 2003. Conservation of the heterochronic regulator Lin-28, its developmental expression and microRNA complementary sites. *Developmental biology* 258, 432-442.

Newman, M.A., Thomson, J.M., Hammond, S.M., 2008. Lin-28 interaction with the Let-7 precursor loop mediates regulated microRNA processing. *RNA* 14, 1539-1549.

Nimmo, R.A., Slack, F.J., 2009. An elegant miRror: microRNAs in stem cells, developmental timing and cancer. *Chromosoma* 118, 405-418.

Nishino, J., Kim, I., Chada, K., Morrison, S.J., 2008. Hmga2 promotes neural stem cell self-renewal in young but not old mice by reducing p16Ink4a and p19Arf Expression. *Cell* 135, 227-239.

Nishino, J., Kim, S., Zhu, Y., Zhu, H., Morrison, S.J., 2013. A network of heterochronic genes including Imp1 regulates temporal changes in stem cell properties. *eLife* 2.

Nowak, J.S., Choudhury, N.R., de Lima Alves, F., Rappsilber, J., Michlewski, G., 2014. Lin28a regulates neuronal differentiation and controls miR-9 production. *Nature communications* 5, 3687.

Ohyama, T., Groves, A.K., 2004. Generation of Pax2-Cre mice by modification of a Pax2 bacterial artificial chromosome. *Genesis* 38, 195-199.

Ohyama, T., Groves, A.K., Martin, K., 2007. The first steps towards hearing: mechanisms of otic placode induction. *The International journal of developmental biology* 51, 463-472.

Okano, T., Xuan, S., Kelley, M.W., 2011. Insulin-like growth factor signaling regulates the timing of sensory cell differentiation in the mouse cochlea. *The Journal of neuroscience : the official journal of the Society for Neuroscience* 31, 18104-18118.

Peng, S., Chen, L.L., Lei, X.X., Yang, L., Lin, H., Carmichael, G.G., Huang, Y., 2011. Genome-wide studies reveal that Lin28 enhances the translation of genes important for growth and survival of human embryonic stem cells. *Stem cells* 29, 496-504.

Poleskaya, A., Cuvellier, S., Naguibneva, I., Duquet, A., Moss, E.G., Harel-Bellan, A., 2007. Lin-28 binds IGF-2 mRNA and participates in skeletal myogenesis by increasing translation efficiency. *Genes & development* 21, 1125-1138.

Poss, K.D., 2010. Advances in understanding tissue regenerative capacity and mechanisms in animals. *Nature reviews. Genetics* 11, 710-722.

Puligilla, C., Kelley, M.W., 2009. Building the world's best hearing aid; regulation of cell fate in the cochlea. *Current opinion in genetics & development* 19, 368-373.

Raft, S., Groves, A.K., 2014. Segregating neural and mechanosensory fates in the developing ear: patterning, signaling, and transcriptional control. *Cell and tissue research*.

Ramachandran, R., Fausett, B.V., Goldman, D., 2010. *Ascl1a* regulates Muller glia dedifferentiation and retinal regeneration through a Lin-28-dependent, let-7 microRNA signalling pathway. *Nature cell biology* 12, 1101-1107.

Rehfeld, F., Rohde, A.M., Nguyen, D.T., Wulczyn, F.G., 2015. Lin28 and let-7: ancient milestones on the road from pluripotency to neurogenesis. *Cell and tissue research* 359, 145-160.

Reinhart, B.J., Slack, F.J., Basson, M., Pasquinelli, A.E., Bettinger, J.C., Rougvie, A.E., Horvitz, H.R., Ruvkun, G., 2000. The 21-nucleotide let-7 RNA regulates developmental timing in *Caenorhabditis elegans*. *Nature* 403, 901-906.

Roberson, D.W., Alosi, J.A., Cotanche, D.A., 2004. Direct transdifferentiation gives rise to the earliest new hair cells in regenerating avian auditory epithelium. *Journal of neuroscience research* 78, 461-471.

- Ruben, R.J., 1967. Development of the inner ear of the mouse: a radioautographic study of terminal mitoses. *Acta oto-laryngologica*, Suppl 220:221-244.
- Ryals, B.M., Rubel, E.W., 1988. Hair cell regeneration after acoustic trauma in adult Coturnix quail. *Science* 240, 1774-1776.
- Rybak, A., Fuchs, H., Smirnova, L., Brandt, C., Pohl, E.E., Nitsch, R., Wulczyn, F.G., 2008. A feedback loop comprising lin-28 and let-7 controls pre-let-7 maturation during neural stem-cell commitment. *Nature cell biology* 10, 987-993.
- Sacheli, R., Nguyen, L., Borgs, L., Vandenbosch, R., Bodson, M., Lefebvre, P., Malgrange, B., 2009. Expression patterns of miR-96, miR-182 and miR-183 in the development inner ear. *Gene Expr Patterns* 9, 364-370.
- Schimmang, T., Pirvola, U., 2013. Coupling the cell cycle to development and regeneration of the inner ear. *Seminars in cell & developmental biology* 24, 507-513.
- Schmittgen, T.D., Livak, K.J., 2008. Analyzing real-time PCR data by the comparative C(T) method. *Nature protocols* 3, 1101-1108.
- Schulman, B.R., Esquela-Kerscher, A., Slack, F.J., 2005. Reciprocal expression of lin-41 and the microRNAs let-7 and mir-125 during mouse embryogenesis. *Developmental dynamics : an official publication of the American Association of Anatomists* 234, 1046-1054.
- Schulman, B.R.M., Liang, X.P., Stahlhut, C., DelConte, C., Stefani, G., Slack, F.J., 2008. The let-7 microRNA target gene, Mlin41/Trim71 is required for mouse embryonic survival and neural tube closure. *Cell cycle* 7, 3935-3942.
- Schwamborn, J.C., Berezikov, E., Knoblich, J.A., 2009. The TRIM-NHL protein TRIM32 activates microRNAs and prevents self-renewal in mouse neural progenitors. *Cell* 136, 913-925.
- Shenoy, A., Blelloch, R.H., 2014. Regulation of microRNA function in somatic stem cell proliferation and differentiation. *Nature reviews. Molecular cell biology* 15, 565-576.
- Sher, A.E., 1971. Embryonic and Postnatal-Development of Inner-Ear of Mouse. *Acta Oto-Laryngol*, 1-&.
- Shi, F.X., Hua, L.X., Edge, A.S.B., 2013. Generation of hair cells in neonatal mice by beta-catenin overexpression in Lgr5-positive cochlear progenitors. *Proceedings of the National Academy of Sciences of the United States of America* 110, 13851-13856.
- Shyh-Chang, N., Daley, G.Q., 2013a. Lin28: primal regulator of growth and metabolism in stem cells. *Cell stem cell* 12, 395-406.

Shyh-Chang, N., Zhu, H., Yvanka de Soysa, T., Shinoda, G., Seligson, M.T., Tsanov, K.M., Nguyen, L., Asara, J.M., Cantley, L.C., Daley, G.Q., 2013b. Lin28 enhances tissue repair by reprogramming cellular metabolism. *Cell* 155, 778-792.

Son, E.J., Ma, J.H., Ankamreddy, H., Shin, J.O., Choi, J.Y., Wu, D.K., Bok, J., 2015. Conserved role of Sonic Hedgehog in tonotopic organization of the avian basilar papilla and mammalian cochlea. *Proceedings of the National Academy of Sciences of the United States of America* 112, 3746-3751.

Son, E.J., Wu, L., Yoon, H., Kim, S., Choi, J.Y., Bok, J., 2012. Developmental gene expression profiling along the tonotopic axis of the mouse cochlea. *PloS one* 7, e40735.

Stone, J.S., Cotanche, D.A., 2007. Hair cell regeneration in the avian auditory epithelium. *The International journal of developmental biology* 51, 633-647.

Tateya, T., Imayoshi, I., Tateya, I., Hamaguchi, K., Torii, H., Ito, J., Kageyama, R., 2013. Hedgehog signaling regulates prosensory cell properties during the basal-to-apical wave of hair cell differentiation in the mammalian cochlea. *Development* 140, 3848-3857.

Thornton, J.E., Gregory, R.I., 2012. How does Lin28 let-7 control development and disease? *Trends in cell biology*.

Tsonis, P.A., Call, M.K., Grogg, M.W., Sartor, M.A., Taylor, R.R., Forge, A., Fyffe, R., Goldenberg, R., Cowper-Sal-lari, R., Tomlinson, C.R., 2007. MicroRNAs and regeneration: Let-7 members as potential regulators of dedifferentiation in lens and inner ear hair cell regeneration of the adult newt. *Biochemical and biophysical research communications* 362, 940-945.

Urbach, A., Yermalovich, A., Zhang, J., Spina, C.S., Zhu, H., Perez-Atayde, A.R., Shukrun, R., Charlton, J., Sebire, N., Mifsud, W., Dekel, B., Pritchard-Jones, K., Daley, G.Q., 2014. Lin28 sustains early renal progenitors and induces Wilms tumor. *Genes & development* 28, 971-982.

Viswanathan, S.R., Daley, G.Q., Gregory, R.I., 2008. Selective blockade of microRNA processing by Lin28. *Science* 320, 97-100.

Viswanathan, S.R., Powers, J.T., Einhorn, W., Hoshida, Y., Ng, T.L., Toffanin, S., O'Sullivan, M., Lu, J., Phillips, L.A., Lockhart, V.L., Shah, S.P., Tanwar, P.S., Mermel, C.H., Beroukhim, R., Azam, M., Teixeira, J., Meyerson, M., Hughes, T.P., Llovet, J.M., Radich, J., Mullighan, C.G., Golub, T.R., Sorensen, P.H., Daley, G.Q., 2009. Lin28 promotes transformation and is associated with advanced human malignancies. *Nature genetics* 41, 843-848.

Weston, M.D., Pierce, M.L., Rocha-Sanchez, S., Beisel, K.W., Soukup, G.A., 2006. MicroRNA gene expression in the mouse inner ear. *Brain research* 1111, 95-104.

- White, P.M., Doetzlhofer, A., Lee, Y.S., Groves, A.K., Segil, N., 2006. Mammalian cochlear supporting cells can divide and trans-differentiate into hair cells. *Nature* 441, 984-987.
- Wilbert, M.L., Huelga, S.C., Kapeli, K., Stark, T.J., Liang, T.Y., Chen, S.X., Yan, B.Y., Nathanson, J.L., Hutt, K.R., Lovci, M.T., Kazan, H., Vu, A.Q., Massirer, K.B., Morris, Q., Hoon, S., Yeo, G.W., 2012. LIN28 binds messenger RNAs at GGAGA motifs and regulates splicing factor abundance. *Molecular cell* 48, 195-206.
- Woods, C., Montcouquiol, M., Kelley, M.W., 2004. Math1 regulates development of the sensory epithelium in the mammalian cochlea. *Nature neuroscience* 7, 1310-1318.
- Wu, L., Belasco, J.G., 2005. Micro-RNA regulation of the mammalian lin-28 gene during neuronal differentiation of embryonal carcinoma cells. *Molecular and cellular biology* 25, 9198-9208.
- Wulczyn, F.G., Smirnova, L., Rybak, A., Brandt, C., Kwidzinski, E., Ninnemann, O., Strehle, M., Seiler, A., Schumacher, S., Nitsch, R., 2007. Post-transcriptional regulation of the let-7 microRNA during neural cell specification. *Faseb J* 21, 415-426.
- Xu, B., Zhang, K., Huang, Y., 2009. Lin28 modulates cell growth and associates with a subset of cell cycle regulator mRNAs in mouse embryonic stem cells. *RNA* 15, 357-361.
- Yamamoto, N., Tanigaki, K., Tsuji, M., Yabe, D., Ito, J., Honjo, T., 2006. Inhibition of Notch/RBP-J signaling induces hair cell formation in neonate mouse cochleas. *J Mol Med* 84, 37-45.
- Yuan, J., Nguyen, C.K., Liu, X.H., Kanellopoulou, C., Muljo, S.A., 2012. Lin28b Reprograms Adult Bone Marrow Hematopoietic Progenitors to Mediate Fetal-Like Lymphopoiesis. *Science* 335, 1195-1200.
- Zhao, C., Sun, G., Li, S., Lang, M.F., Yang, S., Li, W., Shi, Y., 2010. MicroRNA let-7b regulates neural stem cell proliferation and differentiation by targeting nuclear receptor TLX signaling. *Proceedings of the National Academy of Sciences of the United States of America* 107, 1876-1881.
- Zhao, C., Sun, G., Ye, P., Li, S., Shi, Y., 2013. MicroRNA let-7d regulates the TLX/microRNA-9 cascade to control neural cell fate and neurogenesis. *Scientific reports* 3, 1329.
- Zheng, J.L., Gao, W.Q., 2000. Overexpression of Math1 induces robust production of extra hair cells in postnatal rat inner ears. *Nature neuroscience* 3, 580-586.
- Zhou, X., Benson, K.F., Ashar, H.R., Chada, K., 1995. Mutation responsible for the mouse pygmy phenotype in the developmentally regulated factor HMGI-C. *Nature* 376, 771-774.

Zhu, H., Shyh-Chang, N., Segre, A.V., Shinoda, G., Shah, S.P., Einhorn, W.S., Takeuchi, A., Engreitz, J.M., Hagan, J.P., Kharas, M.G., Urbach, A., Thornton, J.E., Triboulet, R., Gregory, R.I., Consortium, D., Investigators, M., Altshuler, D., Daley, G.Q., 2011. The Lin28/let-7 axis regulates glucose metabolism. *Cell* 147, 81-94.

Erin Jennifer Golden

855 N Wolfe Street Baltimore, MD 21205
egolden2@jhmi.edu | (443) 287-4198

Education

Johns Hopkins University School of Medicine **Baltimore, MD**
PhD, Neuroscience 2015
Dissertation: The *LIN28B/let-7* axis regulates developmental timing in the mammalian cochlear epithelium

Franklin & Marshall College **Lancaster, PA**
Bachelor of Arts 2006
Special Studies: Physiological and Sociological Influences on Behavior

Grants and Awards

Pre-Doctoral Individual National Research Service Award (F31) 2012-2014
National Institute of Deafness and Other Communication Disorders, NIH

Graduate Research Fellowship Program, Honorable Mention 2010
National Science Foundation

Post-Baccalaureate Intramural Research Training Award 2006-2008
National Institute on Aging, NIH

Hackman Summer Research Scholarship 2005
Franklin & Marshall College

Research Experience

Johns Hopkins University School of Medicine **Baltimore, MD**
PhD Candidate; Advisor: Angelika Doetzlhofer 2008-2015
Understanding the role of the *Lin28b/let-7* axis in cochlear development

- Characterized the novel expression of the *Lin28b/let-7* axis in the differentiating cochlea
- Investigated the effects of disrupting this axis using mouse transgenics
- Uncovered a novel mechanism regulating the temporal precision of cochlear development

National Institute on Aging, NIH**Baltimore, MD**

Post-Baccalaureate Fellow; Advisor: Mark P. Mattson

2006-2008

Examining the neuroendocrine system in health and disease

- Investigated the use of a type II diabetes medication for the treatment of Huntington's disease
- Characterized the involvement of glucagon-like peptide 1 (GLP-1) in sweet taste perception
- Uncovered link between circulating BDNF and indices of metabolic and cardiovascular disease

Franklin & Marshall College**Lancaster, PA**

Hackman Research Fellow; Advisor: Michal Penn

2005

Characterizing the effects of psychological trauma on mental and moral wellbeing

- Compared the development of young people from India, Kenya, and the United States in correlation with exposure to psychological trauma
- Collaborated with the Pennsylvania Department of Public Health to investigate salmonella outbreaks in the state over the past one hundred years.

Publications**Articles**

Golden EJ, Benito-Gonzalez A, Doetzlhofer A. 2015. *Lin28b* regulates developmental timing in the mammalian cochlea. In revision for *PNAS*

Martin B, Chadwick W, Cong W, Pantaleo N, Daimon CM, **Golden E**, Becker K, Wood WH, Carlson OD, Egan JM, Maudsley S. 2012. Euglycemic agents can ameliorate metabolic and hypothalamic dysfunction in the N171-82Q model of huntington's disease. Under review at *Journal of Biological Chemistry*

Golden E, Emiliano A, Maudsley S, Windham BG, Carlson OD, Egan JM, Ferrucci L, Martin B, Mattson MP. 2010. Circulating brain-derived neurotrophic factor and indices of metabolic and cardiovascular health: data from the Baltimore Longitudinal Study of Aging. *PLoS ONE*. 5(4):e10099

Stranahan AM, Lee K, Martin B, Maudsely S, **Golden E**, Cutler RG, Mattson MP. 2009. Voluntary exercise and caloric restriction enhance hippocampal dendritic spine density and BDNF in diabetic mice. *Hippocampus*. 19(10):951-61

Martin B, Pearson M, Brenneman R, **Golden E**, Wood W, Prabhu V, Becker KG, Mattson MP, Maudsley S. 2009. Gonadal transcriptome alterations in response to dietary energy intake: sensing the reproductive environment. *PLoS ONE*. 4(1):e4146

Martin B, Brenneman R, **Golden E**, Walent T, Becker KG, Prabhu VV, Wood W, Ladenheim B, Cadet JL, Maudsley S. 2009. Growth factor signals in neural cells: coherent patterns of interaction control multiple levels of molecular and phenotypic responses. *J Biol Chem*. 284(4):2493-511

Martin B, **Golden E**, Carlson OD, Pistell P, Zhou J, Kim W, Frank BP, Thomas S, Chadwick WA, Greig NH, Bates GP, Sathasivam K, Bernier M, Maudsley S, Mattson MP, Egan JM. 2009. Exendin-4 improves glycemic control, ameliorates brain and pancreatic pathologies, and extends survival in a mouse model of Huntington's disease. *Diabetes*. 58(2):318-28

Martin B, Pearson M, Brenneman R, **Golden E**, Keselman A, Iyun T, Carlson O, Egan JM, Becker KG, Wood W, Vinayakumar P, de Cabo R, Maudsley S, Mattson MP. 2008. Conserved and differential effects of dietary energy intake on the hippocampal transcriptomes of females and males. *PLoS ONE*. 3(6):e2398

Shin YK, Martin B, **Golden E**, Dotson CD, Maudsley S, Kim W, Jang HJ, Mattson MP, Drucker DJ, Egan JM, Munger SD. 2008. Modulation of taste sensitivity by GLP-1 signaling. *Journal of Neurochemistry*. 106(1):455-63.

Carlson O, Martin B, Stote KS, **Golden E**, Maudsley S, Najjar SS, Ferrucci L, Ingram DK, Longo DL, Rumpler WV, Baer DJ, Egan JM, Mattson MP. 2007. Impact of reduced meal frequency without caloric restriction on glucose regulation in healthy, normal weight middle-aged men and women. *Metabolism*. 56(12):1729-34.

Martin B, Pearson M, Kebejian L, **Golden E**, Keselman A, Bender M, Carlson O, Egan JM, Ladenheim B, Cadet JL, Becker KG, Wood W, Duffy K, Vinayakumar P, Maudsley S, Mattson MP. 2007. Sex-dependent metabolic, neuroendocrine and cognitive responses to dietary energy restriction and excess. *Endocrinology*. 148(9):4318-33.

Reviews

Golden E, Cong WN, Pantaleo N, White CM, Maudsley S, Martin B. 2010. Ghrelin and metabolic syndrome: mechanisms of disease and therapeutics. *CNS & Neurological Disorders – Drug Targets*. 9(5):557-63

Martin B, **Golden E**, Egan JM, Mattson MP, Maudsley S. 2008. Reduced energy intake: the secret to a long and healthy life? *IBS Journal of Science*. 2(2):35-39

Martin B, **Golden E**, Egan JM, Mattson MP, Maudsley S. 2008. Caloric restriction: impact upon pituitary function and reproduction. *Ageing Research Reviews*. 7(3):209-24

Martin B, **Golden E**, Keselman A, Stone MD, Mattson MP, Egan JM, Maudsley S. 2008. Therapeutic perspectives for the treatment of huntington's disease: treating the whole body. *Histology and Histopathology*. 23(2):237-50.

Teaching Experience

2013 Teaching Assistant, Great Discoveries in Neuroscience, JHU
2011 Teaching Assistant, Nervous System & Special Senses, JHU SOM
2010 Teaching Assistant, Neuroscience & Cognition II, JHU SOM
2006 Teaching Assistant, Introduction to Neuroscience, Franklin & Marshall
2005 Teaching Assistant, Physiology & Development, Franklin & Marshall

Meetings, Courses, & Presentations

2015 ARO Midwinter Meeting, Baltimore, MD – Invited Talk
2014 ARO Midwinter Meeting, San Diego, CA – Invited Talk
2013 ARO Midwinter Meeting, Baltimore, MD – Poster
2013 Keystone Meeting on Noncoding RNAs in Cancer & Development
Vancouver, BC – Poster
2012 ARO Midwinter Meeting, San Diego, CA – Poster
2011 Society for Neuroscience Annual Meeting, Washington, DC – Invited Talk
2011 MBL Biology of the Inner Ear Summer Course, Woods Hole, MA
2011 ARO Midwinter Meeting, Baltimore, MD - Poster
2008 NIA Postbaccalaureate Research Festival, Baltimore, MD – Poster
2008 NIA Annual Scientific Retreat, Baltimore, MD – Poster
2007 Huntington's Disease Society for America Annual Coalition Meeting,
Wakefield, MA – Poster
2007 NIA Annual Scientific Retreat, Baltimore, MD – Poster
2007 Society for Neuroscience Annual Meeting, San Diego, CA – Poster
2005 Franklin & Marshall Fall Research Festival, Lancaster, PA – Invited Talk

Memberships in Professional Societies

2007-present Society for Neuroscience (SNF)
2008-present American Association for the Advancement of Science (AAAS)
2011-present Association for Research in Otolaryngology (ARO)

University Service

2008-2014 Leadership Initiative for the Environment (LIFE), President
2009-2011 Neuroscience Department Retreat Planning Committee
2009-2010 Neuroscience Department Alternative Scientific Career Seminars
2009-2013 Neuroscience Department Student-Faculty Lunch Seminars
2011-2013 Take Back the Tap Sustainability Initiative
2011-2013 Johns Hopkins Sustainability Office Student Advisory Council